AN EXTENDED LEAST SQUARES METHOD TO SEPARATE THE INCIDENT AND REFLECTED WAVE FIELDS FOR LONG-CRESTED AND SHORT-CRESTED WAVES

A Dissertation

by

YUANZHE ZHI

Submitted to the Office of Graduate and Professional Studies of
Texas A&M University
in partial fulfillment of the requirements for the degree of

DOCTOR OF PHILOSOPHY

Chair of Committee,	Robert Randall
Co-Chair of Committee,	Moo-Hyun Kim
Committee Members,	Kuang-An Chang
	Alejandro Orsi
Head of Department,	Sharath Girimaji

May 2018

Major Subject: Ocean Engineering

Copyright 2018 Yuanzhe Zhi

ABSTRACT

An extended least square method for reflection analysis that separates long-crested or short-crested wave fields into the incident and reflected components from the measured wave surface elevations and from other wave parameters is presented. This method uses the least squares technique by minimizing the squared errors between the measured and the estimated wave heights. This method applies linear wave theory including the linear dispersion relationship and the transfer functions translating the surface wave elevations and other wave parameters. The wave parameters are measured simultaneously from several positions, and the wave probe measurements from three or an arbitrary number of the positions are selected for reflection analysis.

A probe spacing algorithm is described that determines the total number of the wave probes and their positions between the wave maker and the reflecting structure and selects three probes from the pre-arranged probe array for reflection analysis. The algorithm automates the arrangement of wave probes for a wave basin test involving several wave conditions featuring the wave period and water depth, and the corresponding wavelength varies according to these conditions.

New software, named REFANA (reflection analysis), has been written that conducts the reflection analysis using the extended least square method and determines the number of probes and their positions and selects three of them for the reflection analysis. The incident wave heights determined by REFANA approximate the input incident wave heights. The reflection coefficients computed by REFANA agree well with REFLS, a commercial software for

reflection analysis. Moreover, probe positions can be arranged automatically using REFANA, which also minimizes the total number of required wave probes.

Experimental measurements of wave reflection on two different breakwaters are conducted in the laboratory, and the reflection coefficients are evaluated using the software REFANA. The results from REFANA are compared to the REFLS commercial software. Also, an empirical function is developed to estimate reflection coefficient in front of breakwaters. The empirical function is a two sigmoid-curve (s-shaped) function, such as logistic function and error function, in terms of the surf similarity number. The empirical function with proper coefficients can approximate the reflection coefficient for a rough, sloped, and permeable breakwater.

DEDICATION

This dissertation is dedicated to my son Jonathan Zhi, my wife Xiaojun (June) Wu, my parents Dr. Jianyong Li and Jingjie Zhi, and my academic adviser Dr. Robert Randall.

ACKNOWLEDGEMENTS

The author is grateful to Professor Robert E. Randall, academic supervisor; and Professor Moo-Hyun Kim, co-chair of graduate advisory committee; as well as Professor Kuang-An Chang and Professor Alejandro H. Orsi, graduate advisory committee members.

The author also wishes to express his appreciation to Mr. Johnnie P. Reed, Technical Lab Coordinator of Ocean Engineering, who was of great assistance in setting electronic apparatus for experiments, and to Mr. Kirk Martin, TEES Research Engineer, whose expertise in LabVIEW improved the data acquisition system and facilitated the wave data collections.

Appreciation is also extended to my fellow graduate students, including Mr. Ryan Burke, Mr. Ashwin Gadgil, and Mr. Bohdon Wowtschuk, and to student workers, Ms. Madeline Brisson, Ms. Mckenzie Griffith, Ms. Martina Garcia, and Ms. Hannah Huezo, whose participation provided great help in the experimental modeling test. Appreciation also goes to Ms. Altaf Taqi, who allowed me to participate in her laboratory modeling tests gave the author a chance to study spectrum analysis for directional waves.

Finally, the author wishes to his great appreciation and gratitude to his mother, Jingjie Zhi, and his father, Jianyong Li, for their encouragement and to his wife, Xiaojun Wu, for her patience and love and to his son, Jonathan Zhi, as the biggest motivation.

CONTRIBUTORS AND FUNDING SOURCES

This work was supported by a dissertation committee consisting of Professor Robert Randall, advisor, Professor Moo-Hyun Kim, co-advisor, Professor Kuang-An Chang of the Department of Ocean Engineering, and Professor Alejandro H. Orsi of the Department of Oceanography.

The sources of funding for this research were the Center for Dredging Studies, Haynes Coastal Engineering Laboratory, and Bauer Professorship in Dredging Engineering. The modeling tests were sponsored by SmithGroup JJR under supervision of Mr. Jack Cox and Ms. Margaret Boshek and the tests were conducted in Haynes Coastal Engineering Laboratory. The capacitance wave gauges and other electronic instruments were prepared by Mr. Johnnie P. Reed, Technical Lab Coordinator of Ocean Engineering. Data acquisition using Helios, a LabView based software was conducted by Mr. Kirk Martin, TEES Research Engineer.

Graduate students, Mr. Ryan Burke, Mr. Ashwin Gadgil, and Mr. Bohdon Wowtschuk, and student workers, Ms. Madeline Brisson, Ms. Mckenzie Griffith, Ms. Martina Garcia, and Ms. Hannah Huezo, provided assistance during the physical model tests.

All other work, including the photographs and the figures, conducted for the dissertation was completed by the student independently.

NOMENCLATURE

δ_m	Wave steepness
ELSM	Extended least squares method
$\varepsilon_{n,p}$	Error between the measured and the estimated wave for the n^{th} Fourier component at probe p
f_n	Wave frequency
$F_{n,p}$	n^{th} Fourier coefficient of the measured wave at probe p
F_{In}	n^{th} Fourier coefficient of the estimated incident wave
F_{Rn}	n^{th} Fourier coefficient of the estimated reflected wave
φ	Angle between probe pair orientation and wave direction
ϕ	Velocity potential
g	Gravitational acceleration
G	Goodness function
$G(f,\theta)$	Direction distribution function
$\gamma_{n,p}$	Phase shift due to reflection for the n^{th} Fourier component at probe p
h	Water depth
H	Wave height
$H_{n,p}$	Transfer function for measured wave for the n^{th} Fourier component at probe p
$H_{In,p}$	Transfer function for estimated incident wave for the n^{th} Fourier component at probe p

$H_{In,p}$	Transfer function for estimated reflected wave for the n^{th} Fourier component at probe p
η	Surface elevation
i	Imaginary number $i = \sqrt{-1}$
k_n	Wave number for the n^{th} Fourier component, $k_n = 2\pi/\lambda_n$
K_R	Reflection coefficient
LSM	Least squares method
λ_p	Wavelength corresponding to the peak frequency f_p
ω_n	Circular frequency $\omega_n = 2\pi f_n$
p	Pressure
p	Probe position $p = 1,2, \dots, P$
θ	Wave direction
θ	Averaged slope of breakwater
θ_d	Slope of breakwater beneath the berm
θ_u	Slope of breakwater above the berm
SWL	Still water level
t_m	The m^{th} temporal step for time series
T	Wave period or duration of recording
ψ	Angle between x-axis and probe pair orientation
u	Particle velocity along the x-axis
u_t	Particle acceleration along the x-axis
v	Particle velocity along the y-axis

v_t	Particle acceleration along the y-axis
w	Particle velocity along the z-axis
w_t	Particle acceleration along the z-axis
$W_{n,p}$	Weighting coefficient for the n^{th} Fourier component at probe p
ξ	Surf similarity number (Irribarren number)

TABLE OF CONTENTS

Page

LIST OF FIGURES

Page

LIST OF TABLES

Page

CHAPTER I

INTRODUCTION AND LITERATURE REVIEW

Introduction

The measured surface elevations and the corresponding flow fields in front of a physical model in a laboratory water wave basin test are altered by the interference of incident waves generated by the wave maker and reflected waves from model and the basin boundaries. The wave reflections are also inevitable in a harbor basin, which can cause excessive wave elevations that jeopardize the entry and docking of the ships, increase scouring and beach erosion, and destabilize the costal structures. Since the levels of reflections are quantified by the reflection coefficients, which is a ratio of the incident and the reflected wave heights, a reflection analysis method for separating incident and reflected waves and obtaining reflection coefficients from the co-existing wave field is necessary.

A review of the methods for reflection analysis is presented chronologically. Based on the assumption that the profile of water surface elevation is a summation of many sinusoidal signals, a least squares method minimizing the squares of errors between the measured and estimated waves using three wave probes proposed by Mansard and Funke (1980) is widely used in reflection analysis for both regular and irregular waves. The least squares method employs the measurements from three wave probes positioned parallel to the wave propagation direction and at specified probe positions are required according to the specific wavelength to eliminate the impact of singularities and to enhance accuracy and versatility in wider bandwidths. However, a basin model test may consist of multiple wave conditions featuring the water depth and wave period with their corresponding wavelengths, and more wave probes may be required. A probe

spacing algorithm automatically arranges the wave probe array and selects three of them for reflection analysis for a specific wavelength is efficient for a basin model test having multiple wave conditions.

The measurements for estimating the wave spectra that is for practicing reflection analysis may employs the other wave parameters, such as pressure and particle velocity, instead of surface elevation, which is according to the instruments used for observation. Also, the waves may propagate obliquely. An extended least squares method (ELSM) conducting reflection analysis for the obliquely propagated waves by using surface elevation and the other wave parameters expressed as the product of surface elevation and the corresponding transfer function are necessary. The transfer function translating wave parameters from expression of surface elevation are based on linear wave theory. The reflection from the laboratory basin boundary such as rock beach for reflection absorbing is inevitable that contaminants the wave field in front of the model. Removal of the reflections from basin boundary when using ELSM is also necessary.

The real ocean is three-dimensional and to simulate the real sea, many laboratories are equipped with wave makers being able to generate multidirectional or short-crest waves. The multidirectional waves are considered as the superposition of composite waves with variable amplitudes, frequencies, phases, and directions. The spectrum of the reflection coefficients is accordingly a function of both frequency and wave direction. The methods for measuring and estimating directional spectrum is reviewed, which are more complicated than measurements of long-crested wave, and a simple method using ELSM estimating the incident and reflected spectra and the spectrum of reflection coefficients is useful.

Objectives

The objectives for this dissertation are listed as follows:

1. Developing an extended least square method (ELSM) for reflection analysis using measurements of surface elevation and other wave parameters from an arbitrary number of probes for both normal and oblique waves.
2. Developing a probe spacing algorithm that automates the arrangement of the wave probes, estimates the space between the wave maker and model, and selects three of the probes for reflection analysis for a laboratory basin test consisting of multiple wave conditions.
3. Developing a software REFANA consisting of reflection analysis method for normal and oblique waves and incorporating probe spacing algorithm
4. Conducting a breakwater project in Haynes Coastal Engineering Laboratory (Randall, et al. 2016) and using its data for reflection analysis. The reflection coefficients computed by REFANA are also compared to REFLS of GEDAP (Miles and Funke 1990), a commercial software.
5. Empirical equation for estimating reflection coefficients in front of a sloped, rough, and permeable breakwater is developed, which is based on the experimental data for a rubble mounded breakwater.

Literature Review

Methods for reflection analysis are generally classified according to the application of linear or higher order wave theories, and usage of frequency or time domain. Most of the existing reflection analysis methods are frequency domain methods using small amplitude wave theory. Isaacson (1991) reviews and simplifies several methods to analyze wave reflection for linear regular nonbreaking waves. Hughes (1993) discusses methods of reflection analysis for non-breaking waves in a comprehensive manner including methods using linear waves theory and some early works employing higher order wave theory. Yu (2010) reviews and introduces several reflection analysis methods for irregular waves, he uses the reflection coefficient spectrum and the expression of bulk reflection coefficient. A recent review by Varghese et al. (2016) discusses techniques for estimation reflection characteristics in front of coastal structures.

The envelope of co-existing wave profiles features uniform extremes, the incident and reflected wave heights, and the corresponding reflection coefficient are obtained by measuring these extremes by using one wave probe slowly moving parallel to the wave propagation direction for one fourth of wave length, or applying two wave probes at the node and anti-node. This is the node-and-anti-node method that is presented by Dean and Dalrymple (1991), and Hughes (1993). The incident and reflected wave heights are the summation and subtraction of extremes of surface elevations, respectively, and the coefficient of reflection is the ratio of reflected wave height over the incident wave height. The node and anti-node method is for regular waves only, and knowing the positions of the node and anti-node a-priori is required for reliability.

The two-point method presented by Thornton and Calhoun (1972), and Goda and Suzuki (1976) is for both regular and irregular waves. This method employs two wave probes at fixed

positions to measure wave heights from both probes and the phase shifts between the two probes. The measured wave profiles with known amplitudes and phase differences are equated to theoretical wave profiles consisting of the incident and reflected parts with corresponding amplitudes to be determined, and the trigonometric manipulation gives expressions of incident and reflected amplitude spectra in terms of the spectra of measured amplitudes and phase differences. Spectral densities for incident and reflected waves are then computed. The incident and reflected wave heights are computed as four times the zeroth moment of their spectra. Spectrum of reflection coefficients are then the ratio of amplitude spectra of the reflected wave over incident wave.

Mansard and Funk (1980) showed that the 2-point method has limitations, such as limited frequency range, critical gauge positions causing singularity, and sensitivity to errors. A least square method minimizes the squares of errors between measured and theoretical signals. The errors are assumed to be caused by nonlinear wave interaction, signal noise, etc. and are represented as a noise term in the expression of the theoretical wave profile. The least squares method overcomes the limitations of the two-point method, which was initially proposed by Mansard and Funke (1980) for irregular waves, and the application of this method on monochromatic waves was discussed by Isaacson (1991). Wave heights are measured from three probes aligned parallel to the wave propagation direction, and two groups of phase shifts among these probes with certain distances apart are also measured. Incident and reflected spectral densities and wave heights, spectrum of reflection coefficients, and averaged reflection coefficient are obtained and represent the same as for two-point method. The least square method overcomes limitations of limited frequency range and sensitivities to error, but the limitation of

critical probe spacing that causes singularity remains, which is cumbersome and labor intensive for analyzing waves with conditions of multiple wavelengths.

Isaacson (1991) proposed a reflection analysis method for linear regular waves via measuring wave heights from three probes. This method avoids measurements of phases and the computing of phase shifts for regular wave only. Isaacson (1991) and Hughes (1993) both indicated that this method gives better accuracy compared with two-point and least square methods. Isaacson (1991) also extended his three-probe method for oblique reflection by avoiding alignment of wave gauges parallel to the axis normal to wave maker.

Other reflection analysis methods involving measurements of particle velocities are the vertical array method and co-located velocities method. The former method employs vertically distributed wave gauge and velocity gauge measuring surface elevation and horizontal particle velocity, respectively, at the same location, which was proposed by Guza, et al. (1984) for long wave and was modified by Hughes (1993) with the introduction of a time lag (τ) between two probes. The latter method measures both horizontal and vertical particle velocities Hughes (1993). The principle of these methods is equating measured values in terms of Fourier components to theoretical values. Hughes (1993) showed that methods of vertical and co-located arrays using the linear assumptions twice on both heights and particle velocities is relatively inaccurate compared with the least square method involving linear theory only once.

Frigaard and Brorsen (1995) presented a time-domain method employing digital filters to separate incident and reflected waves in real time. The measurements of wave elevations come from the two probes parallel to the propagation direction of the waves. This method gives coefficients of reflection in the form of a time series rather than a spectrum.

There is always nonlinear phenomenon for waves in basin tests. The waves may be generated using linear wave theory, however the effects from basin bottom or side walls always cause nonlinearity, and reflection analysis employing the assumption of linear dispersion relation accordingly introduces inevitable errors. Mansard, et al. (1985) presented a non-linear reflection analysis technique using a nonlinear least squares technique that treats waves as a linear fundamental wave, a bounded second harmonic component, and free harmonic component, separately. Mansard, et al. (1985) concluded that this method is more accurate than other linear reflection techniques.

Based on two-point and least square methods, Lin and Huang (2004) proposed a technique separating incident and reflected higher harmonic waves using four wave gauges. This method distinguishes and isolates the free and locked modes in the higher harmonics. This method is used in software WAVELAB (2016).

To measure and estimate the directional spectra, Barber (1961) applied two-dimensional direct Fourier transform method to transform the cross-covariance function; Longuet-Higgins et al. (1963) presented a parameterizing method expanding directional spectrum into a Fourier series; Capon (1968) proposed a method using the maximum likelihood method (MLM) to estimate the directional spectrum; Panicker, et al. (1974) presented the “locked phase method” and “random phase method” to estimate directional spectra using measurements from wave-gauge arrays; Isobe and Kondo (1984) presented the modified maximum likelihood method (MMLM) to estimate the directional spectrum in a co-existing wave field including both indent and reflected wave field.

CHAPTER II

LINEAR WATER WAVE THEORY AND BASIN LIMITATION

A Review of Linear Water Wave Theory

Governing equation and boundary conditions

Considering a two-dimensional x-z plane and assuming that the fluid motion is irrotational and the water is incompressible, the velocity potential exists and satisfies the continuity, which is expressed as a divergence of gradient deriving the governing equation - Laplace equation. The governing equation in two-dimensional form is presented in Equation 1.

$$\nabla^2\phi = \frac{\partial^2\phi}{\partial x^2} + \frac{\partial^2\phi}{\partial z^2} = 0 \qquad 1$$

where: ϕ is velocity potential and the velocities u and w in terms of velocity potential are presented in Equation 2

$$u = \frac{\partial\phi}{\partial x}, \qquad w = \frac{\partial\phi}{\partial z} \qquad 2$$

The kinematic boundary conditions characterizing no penetrations or separations on boundaries, shall be maintained on both bottom and free surface. Mathematically, it is expressed (Equation 3) such that the total derivative of the boundary is zero for either an impermeable bottom or to move with free surface.

$$\frac{df}{dt} = \frac{\partial f}{\partial t} + u\frac{\partial f}{\partial x} + w\frac{\partial f}{\partial z} = 0 \qquad 3$$

The expressions of boundaries $f(x, z, t) = 0$, such as bottom and free surface are expressed in Equations 4

and 5, respectively.

$$f(x,z) = z + h(x) = 0 \quad (4)$$

$$f(x,z,t) = z - \eta(x,t) = 0 \quad (5)$$

Substituting the expressions of the bottom and free surface boundaries into kinematic boundary condition to obtain the bottom boundary condition and kinematic free surface boundary condition expressed in Equations 6 and 7, respectively.

$$w + u\frac{dh}{dx} = 0, \qquad z = -h(x) \quad (6)$$

$$w - \frac{\partial \eta}{\partial t} - u\frac{\partial \eta}{\partial x} = 0, \qquad z = \eta(x,t) \quad (7)$$

The dynamic free surface boundary condition presented in Equation 8 should be held to support the variation of pressure across the interface, which can be obtained by substituting two-dimensional irrotationality condition into Euler equation that is a governing equation of motion.

$$-\frac{\partial \phi}{\partial t} + \frac{1}{2}(u^2 + w^2) + gz = C(t), \qquad z = \eta(x,t) \quad (8)$$

The lateral boundary conditions are held since the waves are periodic both spatially and temporally. The spatial and temporal lateral boundary conditions are presented in the Equations 9 and 10, respectively.

$$\phi(x,t) = (x,y,t) \quad (9)$$

$$\phi(x,t) = (x,t+T) \quad (10)$$

Linearized governing equation and boundary conditions

Taylor series expansion is usually used to linearize governing equation and boundary conditions, which transfer boundary conditions from free surface $z = \eta$ to still water level $z = 0$ by expansion and then retaining linear terms of parameters η, u, and w only. The definition of Taylor series expansion is expressed in Equation 11.

$$f(x,z,t)|_{z=\eta} = f(x,z,t)|_{z=0} + (\eta - 0)\frac{\partial f}{\partial z}\Big|_{z=0} + \cdots \qquad 11$$

Substituting kinematic free surface boundary condition, i.e. Equation 7, into Equation 11, and categorizing the terms according to their orders to have:

$$\left(w - \frac{\partial \eta}{\partial t} - u\frac{\partial \eta}{\partial x}\right)_{z=\eta} = \left(w - \frac{\partial \eta}{\partial t} - u\frac{\partial \eta}{\partial x}\right)_{z=0} + \eta\frac{\partial}{\partial z}\left(w - \frac{\partial \eta}{\partial t} - u\frac{\partial \eta}{\partial x}\right)_{z=0} + \cdots$$

$$\left(w - \frac{\partial \eta}{\partial t}\right)_{z=0} - \left[u\frac{\partial \eta}{\partial x} - \eta\left(\frac{\partial w}{\partial z} - \frac{\partial^2 \eta}{\partial t \partial z} - \frac{\partial u}{\partial z}\frac{\partial \eta}{\partial x} - u\frac{\partial^2 \eta}{\partial x \partial z}\right)\right]_{z=0} + \cdots = 0$$

Canceling all higher order terms to obtain linearized kinematic free surface boundary condition.

$$w = \frac{\partial \eta}{\partial t}\Big|_{z=0}, \qquad or\ \frac{\partial \phi}{\partial z}\Big|_{z=0} = \frac{\partial \eta}{\partial t}$$

Substituting dynamic free surface boundary condition, i.e. Equation 8, into Equation 11, and categorizing the terms according to their orders to have:

$$\left(-\frac{\partial \phi}{\partial t} + \frac{u^2 + w^2}{2} + g\eta\right)_{z=\eta}$$

$$= \left(-\frac{\partial \phi}{\partial t} + \frac{u^2 + w^2}{2} + g\eta\right)_{z=0} + \eta\frac{\partial}{\partial z}\left(-\frac{\partial \phi}{\partial t} + \frac{u^2 + w^2}{2} + g\eta\right)_{z=0} + \cdots$$

$$\left(-\frac{\partial \phi}{\partial t} + g\eta\right)_{z=0} + \left[\frac{u^2 + w^2}{2} + \eta\frac{\partial}{\partial z}\left(-\frac{\partial \phi}{\partial t} + \frac{u^2 + w^2}{2} + g\eta\right)\right]_{z=0} + \cdots = C(t)$$

Canceling all higher order terms to obtain linearized dynamic free surface boundary condition. Also, notice that $C(t) = 0$ since η has zero spatial and temporal mean.

$$\left(-\frac{\partial \phi}{\partial t} + g\eta\right)_{z=0} = C(t), \qquad or\ \eta = \frac{1}{g}\frac{\partial \phi}{\partial t}\Big|_{z=0} + \frac{1}{g}C(t)$$

Accordingly, the governing equation and the linearized boundary conditions are tabulated in Table 1.

Table 1. Governing equation and linearized boundary conditions

Description	Expression
Governing Equation G.O.V.	$\nabla^2\phi = 0$
Bottom Boundary Condition (horizontal) B.B.C.	$\frac{\partial\phi}{\partial z} = 0, \qquad z = -h$
Kinematic Free Surface Boundary Condition K.F.S.B.C.	$\frac{\partial\phi}{\partial z} = \frac{\partial\eta}{\partial t}, \qquad z = 0$
Dynamic Free Surface Boundary Condition D.F.S.B.C.	$\eta = \frac{1}{g}\frac{\partial\phi}{\partial t}, \qquad z = 0$
Lateral Boundary Condition L.B.C.	$\phi(x,t) = (x+\lambda,t)$ $\phi(x,t) = (x,t+T)$

Solution of velocity potential and dispersion relationship

The governing equation is a partial differential equation (PDE), which is solved by first applying method of separation of variables separating the equation into a product of the functions of each variable and then by substituting the boundary conditions.

let:

$$\phi(x,z,t) = X(x)Z(z)T(t)$$

Substituting into governing equation to governing equation to have:

$$\frac{1}{X(x)}\frac{d^2X(x)}{dx^2} + \frac{1}{Z(z)}\frac{d^2Z(z)}{dz^2} = 0$$

The equation can be held only when each term equal to the same constant, i.e. α, while with reversed signs, which yield a pair of ordinary differential equation (ODE), such as:

$$\frac{d^2X(x)}{dx^2} + \alpha X(x) = 0$$

$$\frac{d^2Z(z)}{dz^2} - \alpha Z(z) = 0$$

Constant α shall be positive, because the periodicity in $X(x)$ requires positive α, which could be mathematically proved using energy method to prove that α is non-negative, and then to prove α is non-zero using proof by contradiction. Using the solution of positive α for the ODE pair to obtain a general solution for velocity potential that is presented in Equation 12.

$$\phi = \left(A\cos\sqrt{\alpha}x + B\sin\sqrt{\alpha}x\right)\cdot\left(Ce^{\sqrt{\alpha}z} + De^{-\sqrt{\alpha}z}\right)\cdot T(t) \quad 12$$

Substituting bottom boundary condition into $\partial\phi/\partial z = 0,\ on\ z = -h$ and letting $C = De^{2\sqrt{\alpha}h}$. Then, substituting lateral boundary condition to satisfy the periodicity, which requires that $\sqrt{\alpha}\lambda = 2\pi$, and obtained the velocity potential in Equation 13.

$$\phi = \cosh k(z+h)\,[K_1(t)\cos kx + K_2(t)\sin kx] \quad 13$$

Where:

$$K_1(t) = 2A\left[\cos\left(\sqrt{\alpha}x\right)\right]De^{\sqrt{\alpha}h}T(t)$$

$$K_2(t) = 2B\left[\sin\left(\sqrt{\alpha}x\right)\right]De^{\sqrt{\alpha}h}T(t)$$

Substituting velocity potential (Equation 13) into dynamic free surface boundary condition, and using sine or cosine function (Equation 14) with amplitude of half of wave height for the expression of surface elevation on the left side of the equation.

$$\eta(x,t) = \frac{H}{2}\sin(kx - \omega t)$$

$$\eta(x,t) = \frac{H}{2}\cos(kx - \omega t) \quad 14$$

To get the expression of the derivatives of $K_1(t)$ and $K_2(t)$. Integrating them with respective to t, and substituting them into Equation 13 to obtain the velocity potential that is presented in Equations 15.

$$\phi = \frac{H}{2}\frac{g}{\omega}\frac{\cosh[k(h+z)]}{\cosh kh}\cos(kx-\omega t)$$
$$\phi = -\frac{H}{2}\frac{g}{\omega}\frac{\cosh[k(h+z)]}{\cosh kh}\sin(kx-\omega t) \quad (15)$$

Substituting the velocity potential into kinematic free surface boundary condition to yield the dispersion relationship, presented in Equation 16.

$$\omega^2 = gk\tanh kh \quad (16)$$

Wave properties and transfer functions

Considering an oblique wave with wave direction θ, the velocity potential for the oblique wave in polar form may be written as Equation 17.

$$\phi = -i\frac{H}{2}\frac{g}{\omega}\frac{\cosh[k(h+z)]}{\cosh kh}e^{-i[k(x\cos\theta + y\sin\theta)-\omega t]} \quad (17)$$

The corresponding surface elevations for the oblique wave is presented in Equation 18, which is obtained by substituting the velocity potential into dynamic free surface boundary condition at still water level (z = 0).

$$\eta = \frac{1}{g}\frac{\partial\phi}{\partial t}\Big|_{z=0} = \frac{H}{2}e^{-i[k(x\cos\theta + y\sin\theta)-\omega t]} \quad (18)$$

The particle velocities are presented in Equation 19.

$$u = -\frac{\partial \phi}{\partial x} = \frac{H}{2}\omega \frac{\cosh[k(h+z)]}{\sinh kh} \cos\theta \, e^{-i[k(x\cos\theta + y\sin\theta) - \omega t]}$$

$$v = -\frac{\partial \phi}{\partial y} = \frac{H}{2}\omega \frac{\cosh[k(h+z)]}{\sinh kh} \sin\theta \, e^{-i[k(x\cos\theta + y\sin\theta) - \omega t]} \qquad 19$$

$$w = -\frac{\partial \phi}{\partial z} = -i\frac{H}{2}\omega \frac{\sinh[k(h+z)]}{\sinh kh} e^{-i[k(x\cos\theta + y\sin\theta) - \omega t]}$$

The particle accelerations are presented in Equation 20.

$$u_t = \frac{\partial u}{\partial t} = i\frac{H}{2}\omega^2 \frac{\cosh[k(h+z)]}{\sinh kh} \cos\theta \, e^{-i[k(x\cos\theta + y\sin\theta) - \omega t]}$$

$$v_t = \frac{\partial v}{\partial t} = i\frac{H}{2}\omega^2 \frac{\cosh[k(h+z)]}{\sinh kh} \sin\theta \, e^{-i[k(x\cos\theta + y\sin\theta) - \omega t]} \qquad 20$$

$$w_t = \frac{\partial w}{\partial t} = \frac{H}{2}\omega^2 \frac{\sinh[k(h+z)]}{\sinh kh} e^{-i[k(x\cos\theta + y\sin\theta) - \omega t]}$$

The pressure under progressive wave are presented in Equation 21.

$$\begin{aligned} p &= -\rho g z + \rho \frac{\partial \phi}{\partial t} \\ &= -\rho g z + \rho g \frac{H}{2} \frac{\cosh[k(h+z)]}{\cosh kh} e^{-i[k(x\cos\theta + y\sin\theta) - \omega t]} \end{aligned} \qquad 21$$

The transfer equations equating the surface elevation and other wave parameters, such as the particle velocities, the particle accelerations, and the pressure under a progressive wave are tabulated in Table 2.

Table 2. Transfer functions.

Wave Parameter	Symbol	Transfer Function
Surface elevation	η	1
Particle velocity (x)	u	$\omega \frac{\cosh[k(h+z)]}{\sinh kh} \cos\theta$
Particle velocity (y)	v	$\omega \frac{\cosh[k(h+z)]}{\sinh kh} \sin\theta$
Particle velocity (z)	w	$-i\omega \frac{\sinh[k(h+z)]}{\sinh kh}$
Particle acceleration (x)	u_t	$i\omega^2 \frac{\cosh[k(h+z)]}{\sinh kh} \cos\theta$
Particle acceleration (y)	v_t	$i\omega^2 \frac{\cosh[k(h+z)]}{\sinh kh} \sin\theta$
Particle acceleration (z)	w_t	$\omega^2 \frac{\sinh[k(h+z)]}{\sinh kh}$
Pressure ($p + \rho g z$)	$\tilde{p}$	$\rho g \frac{\cosh[k(h+z)]}{\cosh kh}$

Wave Generator Breaking Wave Design Curves for Haynes Coastal Engineering Laboratory

This section introduces the wave generator breaking wave design curves for 3-D shallow water wave basin in Haynes Coastal Engineering Laboratory. The design curves are bounded by both breaking criteria and wave generator capacity that is based on the height-to-stroke ratio, which are plotted and represented as maximum wave heights versus wave periods under specific water depths. The dispersion relationship, breaking criteria, and height-to-stroke ratio are introduced successively for convenience of demonstrating wave breaking criteria. The design curves offer an

theoretical estimation for the wave height capability of maximum non-breaking wave that can be generated in the 3-D shallow water basin in Haynes Coastal Engineering Laboratory.

Wavelengths iteration

Wavelength λ or wave number k is initially specified for wave classifications that are then used as indices for the selection of the breaking criteria. The shallow, intermediate, and deep-water waves can be defined and tabulated as represented in Table 3.

Table 3. Classification of waves according to water depth.

Wave Type	Classified By k		Classified By λ
Shallow	$kh < \pi/10$	or	$h/\lambda < 1/20$
Intermediate	$\pi/10 < kh < \pi$	or	$1/20 < h/\lambda < 1/2$
Deep	$kh > \pi$	or	$h/\lambda < 1/20$

The corresponding wave length and wave number under the specified water depth and wave period can be numerically iterated from dispersion relationship using Equation 16. Since the circular frequency can be defined as $\sigma = 2\pi/T$ and the relationship between wave number and wave length is$k = 2\pi/\lambda$, the formula for iteration can be derived from dispersion relationship and represented as Equation 22.

$$\lambda = \frac{gT^2}{2\pi}\tanh\left(\frac{2\pi h}{\lambda}\right) \qquad 22$$

The initial guess for numerical iteration, which is derived from the approximation of dispersion relationship that was initially proposed by Eckhart (1952) and was later altered by

Fenton and McKee (1990) for minimizing errors in wave length estimation for both short and long waves, can be represented as Equation 23.

$$\lambda = \frac{gT^2}{2\pi}\left\{\tanh\left[\left(\frac{4\pi^2 h}{gT^2}\right)^{3/4}\right]\right\}^{2/3} \qquad 23$$

The wave number is accordingly computed by using the relationship between wave number and wave length, i.e. $k = 2\pi/\lambda$. The wave lengths for wave periods varying up to 10 s and water depth varying between 0.1 m and 1 m with 0.1 m incremental depth are represented in Figure 1.

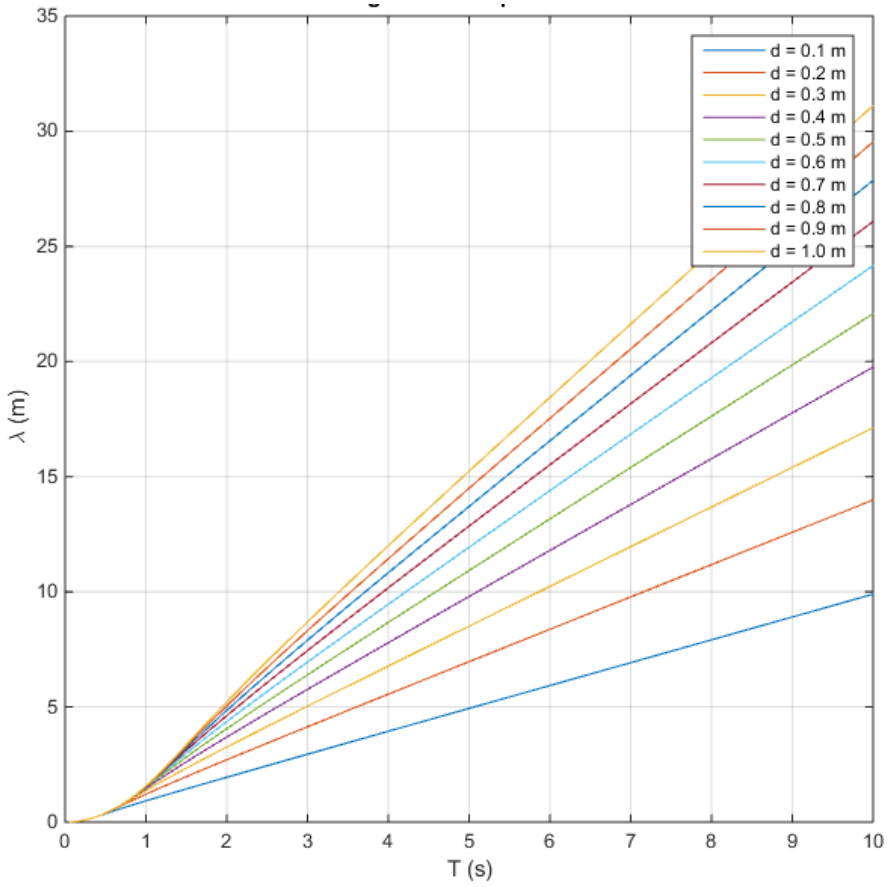

Figure 1. Wavelength from dispersion relation.

Breaking criteria

Breaking criteria are generally represented as either limiting steepness δ_m that is a ratio of wave height versus wave length or breaking index κ that is a ratio of wave height versus water depth (Equation 24), the latter criteria is usually used for shallow-water wave. These criteria are presented in Table 4.

$$\delta_m = \left(\frac{H}{\lambda}\right)_b$$
$$\kappa = \left(\frac{H}{h}\right)_b \quad (24)$$

Table 4. Break criteria.

Method	Equation	Applicability
Michell (1893)	$\delta_{mo} = \frac{1}{7}$	Deep-water wave Plane bottom
Miche (1944)	$\delta_m = \frac{1}{7}\tanh\left(\frac{2\pi h}{\lambda}\right)$	General form Plane bottom
	$\kappa = 0.89$	Shallow-water wave Plane bottom
Goda (1970)	$\kappa = 0.17\frac{\lambda_o}{h_b}\left[1 - e^{-\left(\frac{1.5\pi h_b}{\lambda_o}\right)}\right]$	General form Plane bottom
Kamphuis (1991)	$\delta_{ms} = 0.095\tanh\left(\frac{2\pi h_b}{\lambda_{pb}}\right)$	General form Significant wave height Peak period wavelength
	$\kappa_s = 0.56$	Shallow-water wave Significant wave height Peak period wavelength
Kamphuis (2000)	$\kappa = 0.78$	Shallow-water wave Flat bottom

Wave generator capacity

The wave generator capacity is based upon the height-to-stroke ratio (H/S), which is for estimating the heights of waves that are generated by knowing the wave number k (or wave length λ), water depth h, and wave board stroke S. The first-order height-to-stroke ratio (S. A. Hughes 1993) for piston typed wave generator is represented in Equation 25.

$$\frac{H}{S} = \frac{2[\cosh(2kh) - 1]}{\sinh(2kh) + 2kh} \qquad 25$$

For water depths varying up to 1 m with 0.1 m incremental water depth and wave period varying up to 10 s, the corresponding maximum wave height that can be generated under the maximum stroke amplitude 0.988 m is plotted and represented in Figure 2.

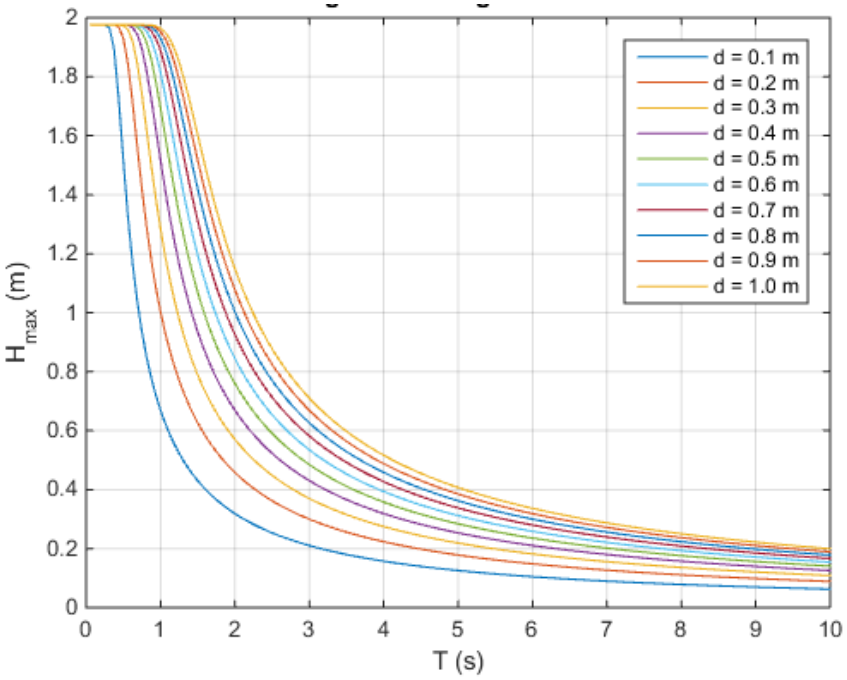

Figure 2. Wave height from height-to-stroke ratio.

Wave height capacity

The wave height capacity for a shallow water wave basin in Haynes Laboratory is estimated and plotted as an envelope of the breaking criteria and first-order height-to-stroke ratio. This design curve is for estimation of maximum non-breaking wave under maximum paddle stroke. The design curves presenting the non-breaking waves are bounded by Goda (1970) breaking criteria presented in Figure 3.

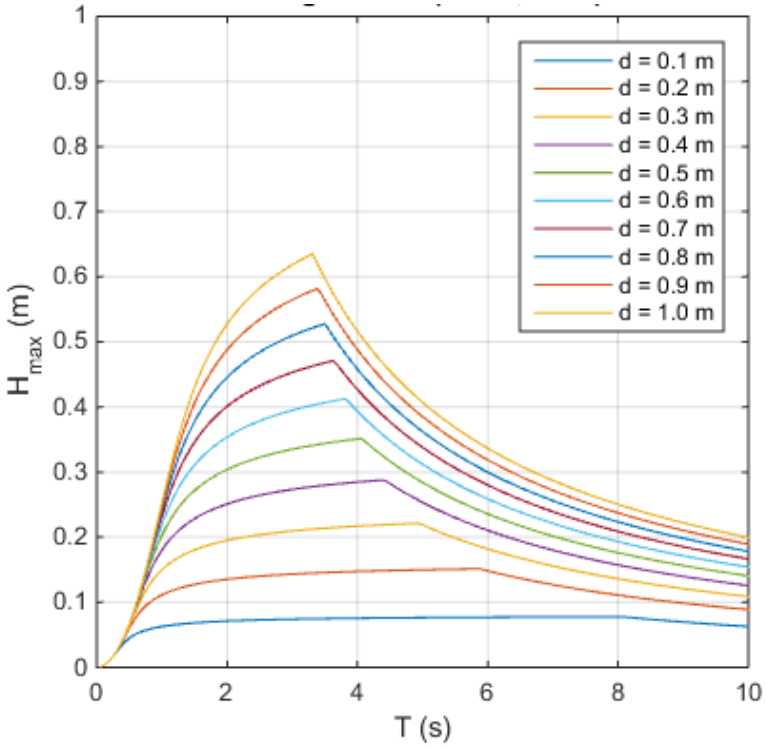

Figure 3. Design curve for 3-D wave basin in Haynes Coastal Engineering Laboratory.

CHAPTER III

REFLECTION ANALYSIS USING EXTENDED LEAST SQUARES METHOD

Assumption and Coordinate System

Airy wave theory (often referred to as linear wave theory) is used and a fully developed wave filed in front of a reflected structure is linearly superposed by incident wave trains moving toward the structure and their reflected wave trains moving away from the structure, which generate a co-existing wave field. Both incident and reflected wave fields are assumed to be linearly superposed by wave trains from different directions and the wave of each direction is assumed to be linearly superposed by infinite number of wavelets with variable amplitudes, frequencies, and initial phases. For long-crest wave, the wave directions to constitute the surface profile are at a uniform value. In physical modeling experiment, reflection from basin's side walls may be assumed to be negligible with properly placed effective absorption material.

Cartesian coordinate is used with x-axis being perpendicular to the toe of reflected structure and orienting positively away from the structure and with y-axis being orthogonal to x-axis and orienting to the left of the positive x-axis. The coordinate system is presented in Figure 4. Angle θ is the incident wave angle, i.e. $\theta_I = \theta$, it is made by the x axis turning counter-clock-wisely to the incident wave crest orthogonal (orientation of the incident wave component) and, which ranges from 0 to π counter clockwise from the positive x-axis.

Accordingly, to have the relationship between the incident and reflected wave angles, which are presented in Equation 26 in term of angle theta θ.

$$\theta_I = \theta$$
$$\theta_R = \pi - \theta \qquad (26)$$

The corresponding sine and cosine functions are presented in Equation 27.

$$\sin\theta_I = \sin\theta\,, \qquad \cos\theta_I = \cos\theta$$
$$\sin\theta_R = \sin\theta\,, \qquad \cos\theta_R = -\cos\theta \qquad (27)$$

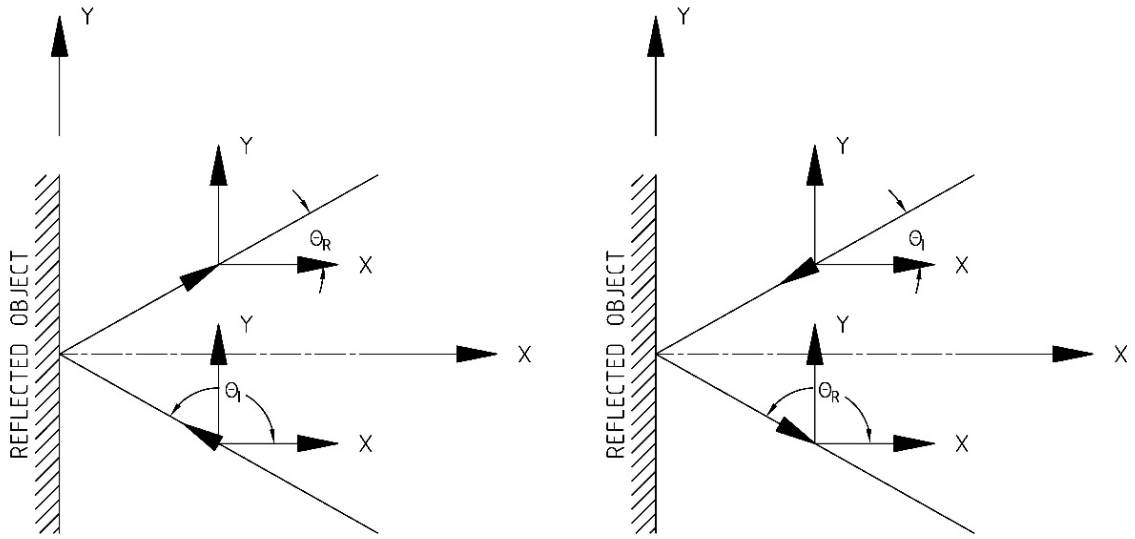

Figure 4. Coordinate system for incident and reflected wave system.

For long-crest wave, the reflection analysis is usually conducted using least squares method by minimizing the square errors between the spectra of observed and estimated surface elevations. This method was proposed by Mansard and Funke (1980), and the author presents an extended version applied on both normal and oblique waves.

Reflection Analysis for Long-Crest Normal or Oblique Wave Using Lest Squares Method

Time series of surface elevation

The observed surface elevation at a fixed point (probe p) can be presented as superposition of many sinusoid waves, and the trigonometric form of the surface elevation is the real part of polar form of that can be presented in Equation 28.

$$\left(\eta_{m,p}\right)_M = \sum_{n=1}^{N} F_{n,p} e^{i\omega_n t_m} \tag{28}$$

Where: $\left(\eta_{m,p}\right)_M = \eta_p(t_m)$ is the observed time series of surface elevation; t_m is cumulative time with $t_m = m\Delta t$, and Δt is time incremental; $F_{n,p}$ is the measured Fourier components of frequency ω_n at probe p; ω_n is circular frequency defined as $\omega_n = 2\pi f_n = 2\pi n/T$; $\alpha_{n,p}$ is the initial phase of frequency ω_n.Let T be the total record duration, the time incremental is defined as $T = N\Delta t$, and accordingly $t_m = mT/N$.

The estimated surface elevation may be presented as superposition of incident wave and reflected wave, and each wave is assumed to be the superposition of many sinusoidal waves, the polar form of which is presented in Equation 29.

$$\begin{aligned}\left(\eta_{m,p}\right)_E = &\sum_{n=1}^{N} F_{In} e^{i(-k_n x_p \cos\theta_I - k_n y_p \sin\theta_I + \omega_n t_m)} \\ &+ \sum_{n=1}^{N} F_{Rn} e^{i(-k_n x_p \cos\theta_R - k_n y_p \sin\theta_R + \omega_n t_m)}\end{aligned} \tag{29}$$

Where: $\left(\eta_{m,p}\right)_E = \eta_p\left(x_p, y_p, t_m\right)$ is the estimated time series of surface elevation; F_{In} and F_{Rn} are the incident and reflected Fourier components of frequency ω_n; k_n is wave number and related with circular frequency by dispersion relationship; $\left(x_p, y_p\right)$ is the position of probe p

relative to the first probe; θ is incident wave angle; θ_R is the reflected wave angle having relationship with incident wave angle as $\theta_R = \pi - \theta$. The estimated surface elevation in the wave field constituted by the incident and reflected waves can be re-written and presented in Equation 30.

$$\left(\eta_{m,p}\right)_E = \sum_{n=1}^{N} H_{In,p} F_{In} e^{i(-k_n x_p \cos\theta - k_n y_p \sin\theta + \omega_n t_m)} + \sum_{n=1}^{N} H_{Rn,p} F_{Rn} e^{i(k_n x_p \cos\theta - k_n y_p \sin\theta + \omega_n t_m)} \quad (30)$$

Fourier transform of time series of surface elevation

The discrete Fourier transformation is defined and presented in Equation 31.

$$F(\omega_n) = \sum_{m=1}^{N} \eta_m e^{-i\omega_n t_m} \quad (31)$$

Where: $F(\omega_n) = F_n$ is the amplitude spectrum of surface elevation. Substitute Equations 28 into Equation 31 to get the amplitude spectrum of measured wave as presented in Equation 32.

$$\mathcal{F}\left\{\left(\eta_{m,p}\right)_M\right\} = F_{n,p} \quad (32)$$

Substitute Equations 30. into Equation 31 to get the amplitude spectrum of estimated wave as presented in Equation 33.

$$\mathcal{F}\left\{\left(\eta_{m,p}\right)_E\right\} = F_{In} e^{ik_n(-x_p \cos\theta - y_p \sin\theta)} + F_{Rn} e^{ik_n(x_p \cos\theta - y_p \sin\theta)} \quad (33)$$

LSM to separate incident and reflected waves for obliquely long-crest wave

Using three wave gauges placed parallel to the reflected structure orthogonal or parallel to x-axis, the sum of squares of errors is accordingly presented as Equation 34.

$$\sum_{p=1}^{3}\left(\varepsilon_{n,p}\right)^2 = \sum_{p=1}^{3}\left[F_{In}e^{ik_n\left(-x_p\cos\theta - y_p\sin\theta\right)} + F_{Rn}e^{ik_n\left(x_p\cos\theta - y_p\sin\theta\right)} - F_{n,p}\right]^2 \quad (34)$$

Where: $\epsilon_{n,p}$ is the error between the observed and estimated amplitude spectra.

The minimum square value is assumed to be achieved the partial derivative of sum of squares of $\varepsilon_{n,p}$ with respective to both $F_{I,n}$ and $F_{R,n}$ are zero, such that presented in Equation 35.

$$\frac{\partial\left[\sum_{p=1}^{3}\left(\varepsilon_{n,p}\right)^2\right]}{\partial F_{In}} = \frac{\partial\left[\sum_{p=1}^{3}\left(\varepsilon_{n,p}\right)^2\right]}{\partial F_{Rn}} = 0 \quad (35)$$

To get an equation pair, such that

$$\sum_{p=1}^{3}\left[F_{In}e^{ik_n\left(-x_p\cos\theta - y_p\sin\theta\right)} + F_{Rn}e^{ik_n\left(x_p\cos\theta - y_p\sin\theta\right)} - F_{n,p}\right]e^{ik_n\left(-x_p\cos\theta - y_p\sin\theta\right)} = 0$$

$$\sum_{p=1}^{3}\left[F_{In}e^{ik_n\left(-x_p\cos\theta - y_p\sin\theta\right)} + F_{Rn}e^{ik_n\left(x_p\cos\theta - y_p\sin\theta\right)} - F_{n,p}\right]e^{ik_n\left(x_p\cos\theta - y_p\sin\theta\right)} = 0$$

Rearranging the above equation pair to obtain Equation 36:

$$\begin{aligned} F_{In}\left(\sum_{p=1}^{3}e^{i2k_n\left(-x_p\cos\theta - y_p\sin\theta\right)}\right) + 3F_{Rn} &= \sum_{p=1}^{3}F_{n,p}e^{ik_n\left(-x_p\cos\theta - y_p\sin\theta\right)} \\ F_{Rn}\left(\sum_{p=1}^{3}e^{i2k_n\left(x_p\cos\theta - y_p\sin\theta\right)}\right) + 3F_{In} &= \sum_{p=1}^{3}F_{n,p}e^{ik_n\left(x_p\cos\theta - y_p\sin\theta\right)} \end{aligned} \quad (36)$$

Solving Equation 36 to obtain F_{In} and F_{Rn} presented in Equation 37.

$$F_{In} = \frac{O_2 O_3 - 3O_4}{O_1 O_2 - 9}$$
$$F_{Rn} = \frac{O_1 O_4 - 3O_3}{O_1 O_2 - 9} \quad (37)$$

The spectrum of reflection coefficients is presented in Equation 38 as a ratio of F_{Rn} over F_{In}, such that

$$K_R = \frac{F_{Rn}}{F_{In}} = \frac{O_1 O_4 - 3O_3}{O_2 O_3 - 3O_4} \quad (38)$$

Notice that when the wave direction normal to the reflected structure, the angle $\theta = 0$. The parameters in Equation 37 and Equation 38 are presented in Equation 39.

$$O_1 = \sum_{p=1}^{3} e^{-i2k_n x_p \cos\theta}$$
$$O_2 = \sum_{p=1}^{3} e^{i2k_n x_p \cos\theta}$$
$$O_3 = \sum_{p=1}^{3} F_{p,n} e^{-ik_n x_p \cos\theta} \quad (39)$$
$$O_4 = \sum_{p=1}^{3} F_{p,n} e^{ik_n x_p \cos\theta}$$

Reflection Analysis for Long-Crest Normal or Oblique Wave Using Extended Lest Squares Method (ELSM)

The measurements used for reflection analysis can be other wave parameters that are expressed as a product of surface elevation and transfer function $H_{n,p}$ presented in Table 2 relating the surface elevation and corresponding wave parameter. Also, to practice the reflection analysis using an arbitary number of probes, Zelt and Skejebreia (1992) introduced the weighted

sum of the squares of the errors for each wave gauge with non-uniform weighting coefficient $W_{n,p}$.

Time series of a wave parameter

The observed wave variable at a fixed point (probe p) is assumed to be superposition of many sinusoid waves that is a product of surface elevation (Equation 28) and the corresponding transfer function according to the types of measurements, and its polar form can be presented in Equation 40.

$$f_p(t_m) = \sum_{n=1}^{N} H_{n,p} F_{n,p} e^{i\omega_n t_m} \tag{40}$$

Where: $\left(f_{m,p}\right)_M = f_p(t_m)$ is the observed time series of wave parameter; $H_{n,p} = H_{n,p}(\omega_n, \theta)$ is transfer function (Table 2) relating the wave parameter and surface elevation and $H_{n,p} = 1$ when the wave parameter is surface elevation.

The estimated surface elevation may be presented as superposition of incident wave and reflected wave, and each wave is assumed to be the superposition of many sinusoidal waves that are the products of surface elevation (Equation 30) and the corresponding transfer function, the polar form of which is presented in Equation 41.

$$\begin{aligned} f_p\left(x_p, y_p, t_m\right) = & \sum_{n=1}^{N} H_{In,p} F_{In} e^{i\left(-k_n x_p \cos\theta - k_n y_p \sin\theta + \omega_n t_m\right)} \\ & + \sum_{n=1}^{N} H_{Rn,p} F_{Rn} e^{i\left(k_n x_p \cos\theta - k_n y_p \sin\theta + \omega_n t_m\right)} \end{aligned} \tag{41}$$

Where: $\left(f_{m,p}\right)_E = f_p\left(x_p, y_p, t_m\right)$ is the estimated time series of wave parameter; $H_{In,p} = H_{n,p}(\omega_n, \theta)$ and $H_{Rn,p} = H_{n,p}(\omega_n, \theta_R)$ are transfer functions for incident and reflected waves, respectively, and notice that $H_{In,p} = H_{Rn,p} = 1$ for surface elevations.

Fourier Transform of time series of wave parameter

Using Fourier transform on time series by substituting Equations 40 and 41 into Equation 31 to have the amplitude spectra of measured and estimated wave variables presented in the Equations 42 and 43, respectively.

$$\mathcal{F}\left\{\left(f_{m,p}\right)_M\right\} = H_{n,p}F_{n,p} \tag{42}$$

$$\mathcal{F}\left\{\left(f_{m,p}\right)_E\right\} = H_{In,p}F_{In}e^{ik_n(-x_p\cos\theta - y_p\sin\theta)} + H_{Rn,p}F_{Rn}e^{ik_n(x_p\cos\theta - y_p\sin\theta)} \tag{43}$$

ELSM to separate incident and reflected waves for obliquely long-crest wave

Probes measuring wave parameters are placed parallel to the reflected structure orthogonal or parallel to x-axis, the error $\varepsilon_{n,p}$ between the observed and estimated waves is accordingly presented as Equation 44.

$$\varepsilon_{n,p} = H_{In,p}F_{In}e^{ik_n(-x_p\cos\theta - y_p\sin\theta)} + H_{Rn,p}F_{Rn}e^{ik_n(x_p\cos\theta - y_p\sin\theta)} - H_{n,p}F_{n,p} \tag{44}$$

In order to practice the reflection analysis using any number of gauges, Zelt and Skejebreia (1992) introduced the weighted sum of the squares of the errors for each wave gauge with either uniform or non-uniform weighting $W_{n,p}$, which is presented in Equation 45, as

$$E_n = \sum_{p=1}^{P} W_{n,p}\varepsilon_{n,p}\varepsilon_{n,p}^* \tag{45}$$

Where: $W_{n,p}$ is the weighting coefficient for wave gauge p at frequency ω_n, which equals to unity for uniform weighting coefficient, the principle of selecting the weighting coefficient will be discussed later.

Since the minimum of the weighed sum of squares of errors occurs when E_n is stationary that holds the criteria, such that in Equation 46 as.

$$\frac{\partial E_n}{\partial F_{In}} = \frac{\partial E_n}{\partial F_{Rn}} = 0 \tag{46}$$

To further obtain a pair of Equation 47.

$$\begin{gathered}\sum_{p=1}^{P} W_{n,p} H_{In,p} \varepsilon_{n,p} e^{ik_n(-x_p \cos\theta - y_p \sin\theta)} = 0 \\ \sum_{p=1}^{P} W_{n,p} H_{Rn,p} \varepsilon_{n,p} e^{ik_n(x_p \cos\theta - y_p \sin\theta)} = 0\end{gathered} \tag{47}$$

Substituting Equation 44 into Equation 47 to get an Equation pair.

$$\sum_{p=1}^{P} W_{n,p} H_{In,p} \left(H_{In,p} F_{In} e^{ik_n(-x_p \cos\theta - y_p \sin\theta)} + H_{Rn,p} F_{Rn} e^{ik_n(x_p \cos\theta - y_p \sin\theta)} - H_{n,p} F_{n,p}\right) e^{ik_n(-x_p \cos\theta - y_p \sin\theta)} = 0$$

$$\sum_{p=1}^{P} W_{n,p} H_{Rn,p} \left(H_{In,p} F_{In} e^{ik_n(-x_p \cos\theta - y_p \sin\theta)} + H_{Rn,p} F_{Rn} e^{ik_n(x_p \cos\theta - y_p \sin\theta)} - H_{n,p} F_{n,p}\right) e^{ik_n(-x_p \cos\theta - y_p \sin\theta)} = 0$$

And rearranging the above equation pair to obtain Equation 48:

$$F_{In}\left[\sum_{p=1}^{P} W_{n,p}H_{In,p}H_{In,p}e^{i2k_n(-x_p\cos\theta - y_p\sin\theta)}\right]$$

$$+ F_{Rn}\left(\sum_{p=1}^{P} W_{n,p}H_{In,p}H_{Rn,p}e^{-i2k_n y_p\sin\theta}\right)$$

$$= \sum_{p=1}^{P} W_{n,p}H_{In,p}H_{n,p}F_{n,p}e^{ik_n(-x_p\cos\theta - y_p\sin\theta)}$$

48

$$F_{In}\left(\sum_{p=1}^{P} W_{n,p}H_{In,p}H_{Rn,p}e^{-i2k_n y_p\sin\theta}\right)$$

$$+ F_{Rn}\left[\sum_{p=1}^{P} W_{n,p}H_{Rn,p}H_{Rn,p}e^{i2k_n(x_p\cos\theta - y_p\sin\theta)}\right]$$

$$= \sum_{p=1}^{P} W_{n,p}H_{Rn,p}H_{n,p}F_{n,p}e^{ik_n(x_p\cos\theta - y_p\sin\theta)}$$

Parameterizing the equation by letting:

$$O_1 = \sum_{p=1}^{P} W_{n,p}H_{In,p}H_{In,p}e^{i2k_n(-x_p\cos\theta - y_p\sin\theta)}$$

$$O_2 = \sum_{p=1}^{P} W_{n,p}H_{Rn,p}H_{Rn,p}e^{i2k_n(x_p\cos\theta - y_p\sin\theta)}$$

$$O_3 = \sum_{p=1}^{P} W_{n,p}H_{In,p}H_{n,p}F_{n,p}e^{ik_n(-x_p\cos\theta - y_p\sin\theta)}$$

$$O_4 = \sum_{p=1}^{P} W_{n,p}H_{Rn,p}H_{n,p}F_{n,p}e^{ik_n(x_p\cos\theta - y_p\sin\theta)}$$

And rewriting the Equation 48 into the Equation 42 to have Equation 49.

$$F_{In}O_1 + F_{Rn}\left(\sum_{p=1}^{P} W_{n,p}H_{In,p}H_{Rn,p}e^{-i2k_n y_p \sin\theta}\right) = O_3$$

$$F_{In}\left(\sum_{p=1}^{P} W_{n,p}H_{In,p}H_{Rn,p}e^{-i2k_n y_p \sin\theta}\right) + F_{Rn}O_2 = O_4 \qquad 49$$

Solving Equation 49 and presenting F_{In} and F_{Rn} in terms of $F_{n,p}$. The expression of F_{In} and F_{Rn} are expressed in the Equations 50 and 51, respectively.

$$F_{In} = \frac{O_2O_3 - \left(\sum_{p=1}^{P} W_{n,p}H_{In,p}H_{Rn,p}e^{-i2k_n y_p \sin\theta}\right)O_4}{O_1O_2 - \left(\sum_{p=1}^{P} W_{n,p}H_{In,p}H_{Rn,p}e^{-i2k_n y_p \sin\theta}\right)^2} \qquad 50$$

$$F_{Rn} = \frac{O_1O_4 - \left(\sum_{p=1}^{P} W_{n,p}H_{In,p}H_{Rn,p}e^{-i2k_n y_p \sin\theta}\right)O_3}{O_1O_2 - \left(\sum_{p=1}^{P} W_{n,p}H_{In,p}H_{Rn,p}e^{-i2k_n y_p \sin\theta}\right)^2} \qquad 51$$

The corresponding spectrum of reflection coefficients is presented in Equation 52 as a ratio of F_{Rn} over F_{In}, i.e. $K_R = F_{Rn}/F_{In}$.

$$K_R = \left|\frac{O_1O_4 - \left(\sum_{p=1}^{P} W_{n,p}H_{In,p}H_{Rn,p}e^{-i2k_n y_p \sin\theta}\right)O_3}{O_2O_3 - \left(\sum_{p=1}^{P} W_{n,p}H_{In,p}H_{Rn,p}e^{-i2k_n y_p \sin\theta}\right)O_4}\right| \qquad 52$$

Notice that this expression become the conventional least square method when using uniformed weighting coefficients, i.e. $W_{n,p} \to 1$, and using measurements of surface elevations, i.e. $H_{n,p} = H_{In,p} = H_{Rn,p} \to 1$, from three probes, i.e. $P = 3$. The solution using an arbitrary number of wave probes (Zelt and Sejelbreia 1992) is also a special solution for this general expression by using $W_{n,p}$, using measurements of surface elevations with transfer functions equaling to unity, and by using $P = P$.

Removal of The Reflection from Laboratory Basin Boundary

The reflection from laboratory basin boundary is inevitable that interferes the co-existing wave field in front of a model. However, the reflection coefficient of the basin boundary is usually given in priori, which can be either computed using reflection analysis before the model test or estimated by multiplying a proper reflection coefficient to the input incident wave spectra. Let the amplitude spectrum of the basin boundary as F_{RRn}, the estimated time series of surface elevation can be presented in Equation 53.

$$\begin{aligned} f_p(x_p, y_p, t_m) = & \sum_{n=1}^{N} H_{In,p} F_{In} e^{i(-k_n x_p \cos\theta - k_n y_p \sin\theta + \omega_n t_m)} \\ & + \sum_{n=1}^{N} H_{Rn,p} F_{Rn} e^{i(k_n x_p \cos\theta - k_n y_p \sin\theta + \omega_n t_m)} \\ & + \sum_{n=1}^{N} H_{Rn,p} F_{RRn} e^{i(k_n x_p \cos\theta - k_n y_p \sin\theta + \omega_n t_m)} \end{aligned} \quad 53$$

Using Fourier transformation (Equation 31) to obtain the amplitude spectrum of estimated wave as presented in Equation 54.

$$\begin{aligned} \mathcal{F}\left\{(\eta_{m,p})_E\right\} = & H_{In,p} F_{In} e^{i(-k_n x_p \cos\theta - k_n y_p \sin\theta + \omega_n t_m)} \\ & + H_{Rn,p} F_{Rn} e^{i(k_n x_p \cos\theta - k_n y_p \sin\theta + \omega_n t_m)} \\ & + H_{Rn,p} F_{RRn} e^{i(k_n x_p \cos\theta - k_n y_p \sin\theta + \omega_n t_m)} \end{aligned} \quad 54$$

The squares of errors between the measured wave (Equation 32) and the estimated wave is presented in Equation 55.

$$\sum_{p=1}^{3}\left(\varepsilon_{n,p}\right)^2 = \sum_{p=1}^{3}\Big[H_{In,p}F_{In}e^{i\left(-k_n x_p \cos\theta - k_n y_p \sin\theta + \omega_n t_m\right)} + H_{Rn,p}F_{Rn}e^{i\left(k_n x_p \cos\theta - k_n y_p \sin\theta + \omega_n t_m\right)} + H_{Rn,p}F_{RRn}e^{i\left(k_n x_p \cos\theta - k_n y_p \sin\theta + \omega_n t_m\right)} - F_{n,p}\Big]^2 \quad (55)$$

Using the extended least squares error method (Equation 35), to get a pair of Equation 56.

$$F_{In}\left[\sum_{p=1}^{P} W_{n,p}H_{In,p}H_{In,p}e^{i2k_n\left(-x_p \cos\theta - y_p \sin\theta\right)}\right] + \left(F_{Rn} + F_{RRn}\right)\left(\sum_{p=1}^{P} W_{n,p}H_{In,p}H_{Rn,p}e^{-i2k_n y_p \sin\theta}\right) = \sum_{p=1}^{P} W_{n,p}H_{In,p}H_{n,p}F_{n,p}e^{ik_n\left(-x_p \cos\theta - y_p \sin\theta\right)} \quad (56)$$

$$F_{In}\left(\sum_{p=1}^{P} W_{n,p}H_{In,p}H_{Rn,p}e^{-i2k_n y_p \sin\theta}\right) + \left(F_{Rn} + F_{RRn}\right)\left[\sum_{p=1}^{P} W_{n,p}H_{Rn,p}H_{Rn,p}e^{i2k_n\left(x_p \cos\theta - y_p \sin\theta\right)}\right] = \sum_{p=1}^{P} W_{n,p}H_{Rn,p}H_{n,p}F_{n,p}e^{ik_n\left(x_p \cos\theta - y_p \sin\theta\right)}$$

Parameterizing Equation 56 using Equation 39 to have Equation 57

$$F_{In}O_1 + (F_{Rn} + F_{RRn})\left(\sum_{p=1}^{P} W_{n,p}H_{In,p}H_{Rn,p}e^{-i2k_n y_p \sin\theta}\right) = O_3$$

$$F_{In}\left(\sum_{p=1}^{P} W_{n,p}H_{In,p}H_{Rn,p}e^{-i2k_n y_p \sin\theta}\right) + (F_{Rn} + F_{RRn})O_2 = O_4 \quad (57)$$

Solving Equation 57 to obtain the expressions of the incident and reflected spectra with removal of the reflection from laboratory boundary, that are presented in Equation 58.

$$F_{In} = \frac{O_2O_3 - \left(\sum_{p=1}^{P} W_{n,p}H_{In,p}H_{Rn,p}e^{-i2k_n y_p \sin\theta}\right)O_4}{O_1O_2 - \left(\sum_{p=1}^{P} W_{n,p}H_{In,p}H_{Rn,p}e^{-i2k_n y_p \sin\theta}\right)^2}$$

$$F_{Rn} = \frac{O_1O_4 - \left(\sum_{p=1}^{P} W_{n,p}H_{In,p}H_{Rn,p}e^{-i2k_n y_p \sin\theta}\right)O_3}{O_1O_2 - \left(\sum_{p=1}^{P} W_{n,p}H_{In,p}H_{Rn,p}e^{-i2k_n y_p \sin\theta}\right)^2} - F_{RRn} \quad (58)$$

The spectrum of the reflection coefficients considering the reflection from basin boundary is according computed as the ration of F_{Rn} over F_{In}, which is presented in Equation 59.

$$K_{Rn} = \left|\frac{O_1O_4 - \left(\sum_{p=1}^{P} W_{n,p}H_{In,p}H_{Rn,p}e^{-i2k_n y_p \sin\theta}\right)O_3}{O_2O_3 - \left(\sum_{p=1}^{P} W_{n,p}H_{In,p}H_{Rn,p}e^{-i2k_n y_p \sin\theta}\right)O_4} - \frac{F_{RRn}\left[O_1O_2 - \left(\sum_{p=1}^{P} W_{n,p}H_{In,p}H_{Rn,p}e^{-i2k_n y_p \sin\theta}\right)^2\right]}{O_2O_3 - \left(\sum_{p=1}^{P} W_{n,p}H_{In,p}H_{Rn,p}e^{-i2k_n y_p \sin\theta}\right)O_4}\right| \quad (59)$$

Reflection analysis for Short-Crest Waves Using Extended Least Squares Method

The short-crest wave is considered as superposition of many sinusoid waves featuring different not only the amplitudes, frequencies, and initial phases, but also different directions θ_j. Accordingly, measurement of a directional spectrum requires more probes, rather than obtaining spectrum of long-crest by measuring the surface elevation at a fixed position. The wave energy accordingly distributed across both along frequency ω_n and direction θ_j, and to have the

relationship between an energy density spectrum and its directional spectrum, such that in Equation 60.

$$S(\omega) = \int_{-\pi}^{\pi} S(\omega, \theta)\, d\theta \tag{60}$$

Using the relationship between the energy density spectrum and the frequency spectrum, which is presented in Equation 61.

$$S(f_n) = \frac{|F(f_n)|^2}{2f_o}$$
$$S(\omega_n) = (2\pi)^2 \frac{|F(\omega_n)|^2}{2\omega_o} \tag{61}$$

Where:

$$nf_o = f_n$$
$$n\omega_o = \omega_n$$
$$\omega = 2\pi f$$

Accordingly, to have the relationships presented in Equation 62.

$$F_p(\omega) = \int_{-\pi}^{\pi} F_p(\omega, \theta)\, d\theta$$
$$F_I(\omega) = \int_{-\pi}^{\pi} F_I(\omega, \theta)\, d\theta \tag{62}$$
$$F_R(\omega) = \int_{-\pi}^{\pi} F_R(\omega, \theta)\, d\theta$$

Reflection analysis for short-crest wave is presented by firstly using least squares method or the extended least squares method presented in the previous sections in this chapter to compute $F_I(\omega)$ and $F_R(\omega)$ and both are in term of $F_p(\omega)$. Then either using parameterize method

to estimate $F_p(\omega, \theta_n)$ and obtain the directional spectra $F_I(\omega, \theta_n)$ and $F_R(\omega, \theta_n)$, or using the form of directional spectrum in terms of directional distribution function. The reflection coefficients are accordingly a ratio of $F_R(\omega, \theta_n)$ over $F_I(\omega, \theta_n)$, which is a directional spectrum, i.e. $K_R(\omega, \theta_n)$. The transfer functions are also directional spectra.

Time series of wave parameter for short-crest wave

The time series of measured wave in terms of measurement from the first probe is presented in Equation 63.

$$\left(f_{m,k,p}\right)_M = \sum_{n}^{N}\sum_{j}^{M} H_{n,j,p}F_{n,j,p}\, e^{i(\omega_n t_m + \theta_j l_k)} \tag{63}$$

The time series of estimated wave is a superposition of incident and reflected wave, which is presented in Equation 64.

$$\begin{aligned}&\left(f_{m,k,p}\right)_E \\ &= \sum_{n}^{N}\sum_{j}^{M} H^I_{n,j,p}F^I_{n,j,p} e^{i(-k_n x_p \cos\theta_j - k_n y_p \sin\theta_j + \omega_n t_m + \theta_j l_k)} \\ &+ \sum_{n}^{N}\sum_{j}^{M} H^R_{n,j,p}F^R_{n,j,p} e^{i(k_n x_p \cos\theta_j - k_n y_p \sin\theta_j + \omega_n t_m + \theta_j l_k)}\end{aligned} \tag{64}$$

Where: l_k is the orientation of probe array.

Results of the short-crested wave

Using two-dimensional Fourier transformation that:

$$F\left(\omega_n, \theta_j\right) = \sum_{m}^{N}\sum_{k}^{M} f(t_m, l_k)\, e^{-i(\omega_n t_m + \theta_j l_k)}$$

Using the Equations 50, 51, and 52 to obtain $F^I_{n,j,p}$, $F^R_{n,j,p}$, and K_R, respectively. We notice that these spectra are functions of frequency ω when the incident wave propagates along a unity-direction, i.e. $F_I = F_I(\omega_n)$, $F_R = F_R(\omega_n)$, and $K_R = K_R(\omega_n)$, however, when the composite waves are multi-directional, these values become a function of both frequency ω and direction θ, that is to say, directional spectrum, i.e. $F_I = F_I(\omega_n, \theta_j)$, $F_R = F_R(\omega_n, \theta_j)$, and $K_R = K_R(\omega_n, \theta_j)$. The Fourier components of the incident $F^I_{n,j,p}$ and the reflected $F^R_{n,j,p}$ wave are presented in Equation 67. The reflection coefficient for directional wave is presented in Equation 66.

$$F^I_{n,j,p} = \frac{O_2 O_3 - \left(\sum_{p=1}^{P} W_{n,p} H^I_{n,j,p} H^R_{n,j,p} e^{-i2k_n y_p \sin\theta_j}\right) O_4}{O_1 O_2 - \left(\sum_{p=1}^{P} W_{n,p} H^I_{n,j,p} H^R_{n,j,p} e^{-i2k_n y_p \sin\theta_j}\right)^2}$$

$$F^R_{n,j,p} = \frac{O_1 O_4 - \left(\sum_{p=1}^{P} W_{n,p} H^I_{n,j,p} H^R_{n,j,p} e^{-i2k_n y_p \sin\theta_j}\right) O_3}{O_1 O_2 - \left(\sum_{p=1}^{P} W_{n,p} H^I_{n,j,p} H^R_{n,j,p} e^{-i2k_n y_p \sin\theta_j}\right)^2} \quad 65$$

$$K_R(\omega_n, \theta_n) = \frac{O_1 O_4 - \left(\sum_{p=1}^{P} W_{n,p} H^I_{n,j,p} H^R_{n,j,p} e^{-i2k_n y_p \sin\theta_j}\right) O_3}{O_2 O_3 - \left(\sum_{p=1}^{P} W_{n,p} H^I_{n,j,p} H^R_{n,j,p} e^{-i2k_n y_p \sin\theta_j}\right) O_4} \quad 66$$

The corresponding parameters are

$$O_1 = \sum_{p=1}^{P} W_{n,p} H^I_{n,j,p} H^I_{n,j,p} e^{i2k_n(-x_p \cos\theta_j - y_p \sin\theta_j)}$$

$$O_2 = \sum_{p=1}^{P} W_{n,p} H^R_{n,j,p} H^R_{n,j,p} e^{i2k_n(x_p \cos\theta_j - y_p \sin\theta_j)}$$

$$O_3 = \sum_{p=1}^{P} W_{n,p} H^I_{n,j,p} H_{n,j,p} F_{n,j,p} e^{ik_n(-x_p \cos\theta_j - y_p \sin\theta_j)}$$

$$O_4 = \sum_{p=1}^{P} W_{n,p} H^R_{n,j,p} H_{n,j,p} F_{n,j,p} e^{ik_n(x_p \cos\theta_j - y_p \sin\theta_j)}$$

Estimating directional spectrum in terms of directional function

The real ocean is three-dimensional and the corresponding spectrum should be directional spectrum, the two-dimensional spectrum is a spectrum that the energy concentrates on a specific direction (usually at $\theta = 0$) and the energy will spread along the directions directional spectrum. The directional spectra may be estimated as a production of frequency spectrum and directional function, and according the directional spectrum of the reflection coefficients can be presented in Equation 67.

$$K_R(\omega, \theta) = K_R(\omega) D(\omega, \theta) \tag{67}$$

Where: $K_R(\omega)$ is frequency spectrum computed using extended least squares method in previous section; $D(\omega, \theta)$ is direction distribution function or simply as directional function presenting the distribution or dissipation of energy along the direction on both sides of main direction, which satisfies Equation 68.

$$\int_{-\pi}^{\pi} D(\omega, \theta)\, d\theta = 1 \tag{68}$$

Because

$$K_R(\omega) = \int_{-\pi}^{\pi} K_R(\omega, \theta)\, d\theta = K_R(\omega) \int_{-\pi}^{\pi} D(\omega, \theta)\, d\theta$$

Determination of frequency spectrum $K_R(\omega)$ uses the same pattern of wave probe arrays applied in least square method. Estimation of directional spectrum for the reflection coefficients becomes the determination of direction distribution function.

A simple empirical function that is independent from frequency, i.e. $D(\omega, \theta) = D(\theta)$, may be used to present the direction distribution function, which is presented in Equation 69.

$$D(\omega,\theta) = C(s)\cos^{2s}\theta \qquad 69$$

With:

$$C(s) = \frac{1}{\sqrt{\pi}}\frac{\Gamma(s+1)}{\Gamma(s+1/2)} = \frac{2s!!}{\pi(2s-1)!!}$$

Where: the gamma function $\Gamma(s)$ has properties of:

$$\Gamma(s+1) = s\Gamma(s) = (s-1)!$$

$$\Gamma(s+1/2) = \frac{(2s-1)\cdot\ldots\cdot 3\cdot 1}{2^n}\sqrt{\pi} = \frac{(2s-1)!!}{2^n}\sqrt{\pi}$$

$$2s!! = 2s\cdot\ldots\cdot 4\cdot 2$$

$$(2s-1)!! = (2s-1)\cdot\ldots\cdot 3\cdot 1$$

The coefficient s is a direction distribution coefficient, which is a constant in simple empirical function, which need to be determined according to the wave directions. Direction distribution coefficient s may be a function of frequency ω for other direction distribution functions. Some of the other direction distribution functions include equation presented by Longuet-Higgins (1963) using direction distribution coefficient presented by Mitsuyasu, et al. (1975) and Yu and Liu (1994). Measurements are necessary to verify the applicability of these direction distribution function and to develop new functions being applicable for the spectra of incident wave, reflected wave and the reflection coefficients.

Estimating composite wave directions from measurement of probe pairs

The directions of the composite waves may be distributed within an interval of angles θ_n. The direction of the composite waves can be obtained by computing the phase shifts using measurement from a pair of probe, the relationship among the wave direction, orientation of the connecting line of the probe pair and the angle between the wave direction and connecting line of probe pair is illustrated in Figure 5.

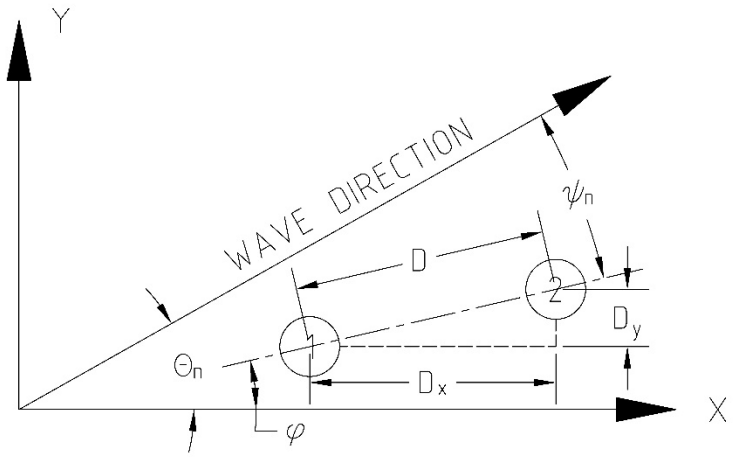

Figure 5. Relationships between wave direction and probe pair orientation.

Considering the time series of surface elevation captured by two wave probes presented in Equation 70.

$$\eta_{m,1} = \sum_{n=1}^{N} A_{n,1} e^{i(-k_n x_1 \cos\theta_n - k_n y_1 \sin\theta_n + \omega_n t_m)}$$

$$\eta_{m,2} = \sum_{n=1}^{N} A_{n,2} e^{i\left[-k_n (x_1 + D_x)\cos\theta_n - k_n (y_1 + D_y)\sin\theta_n\right]} \quad 70$$

The Fourier series of the time series are presented in Equation 71.

$$\mathcal{F}(\eta_{m,1}) = A_{n,1}e^{-i(k_n x_1 \cos\theta_n + k_n y_1 \sin\theta_n)}$$
$$\mathcal{F}(\eta_{m,2}) = A_{n,2}e^{-i[k_n(x_1+D_x)\cos\theta_n + k_n(y_1+D_y)\sin\theta_n]} \quad (71)$$

Since

$$D_x = D\cos\varphi$$
$$D_y = D\sin\varphi$$
$$\psi_n = \theta_n - \varphi$$

The equation pair can be written as Equation 72

$$\mathcal{F}(\eta_{m,1}) = A_{n,1}e^{-i(k_n x_1 \cos\theta_n + k_n y_1 \sin\theta_n)}$$
$$\mathcal{F}(\eta_{m,2}) = A_{n,2}e^{-i[(k_n x_1 \cos\theta_n + k_n y_1 \sin\theta_n) + k_n D\cos\psi_n]} \quad (72)$$

Using Euler's formula that is presented in Equation 73.

$$\cos(k_n D\cos\psi_n) = \frac{\mathcal{F}(\eta_{m,1})\mathcal{F}^*(\eta_{m,2}) + \mathcal{F}^*(\eta_{m,1})\mathcal{F}(\eta_{m,2})}{2\left|\mathcal{F}(\eta_{m,1})\mathcal{F}^*(\eta_{m,2})\right|}$$
$$\sin(k_n D\cos\psi_n) = \frac{\mathcal{F}(\eta_{m,1})\mathcal{F}^*(\eta_{m,2}) - \mathcal{F}^*(\eta_{m,1})\mathcal{F}(\eta_{m,2})}{i2\left|\mathcal{F}(\eta_{m,1})\mathcal{F}^*(\eta_{m,2})\right|} \quad (73)$$

Where:

$$\mathcal{F}(\eta_{m,1})\mathcal{F}^*(\eta_{m,2}) = A_{n,1}A_{n,2}e^{ik_n D\cos\psi_n}$$
$$\mathcal{F}^*(\eta_{m,1})\mathcal{F}(\eta_{m,2}) = A_{n,1}A_{n,2}e^{-ik_n D\cos\psi_n}$$

to have Equation 74.

$$\tan(k_n D\cos\psi_n) = -i\frac{\mathcal{F}(\eta_{m,1})\mathcal{F}^*(\eta_{m,2}) - \mathcal{F}^*(\eta_{m,1})\mathcal{F}(\eta_{m,2})}{\mathcal{F}(\eta_{m,1})\mathcal{F}^*(\eta_{m,2}) + \mathcal{F}^*(\eta_{m,1})\mathcal{F}(\eta_{m,2})} \quad (74)$$

Hence to get the relative angle between the connection line of probe pair and the wave direction, which is presented in Equation 75.

$$\psi_n = \cos^{-1}\left\{\frac{\tan^{-1}\left[-i\dfrac{\mathcal{F}(\eta_{m,1})\mathcal{F}^*(\eta_{m,2}) - \mathcal{F}^*(\eta_{m,1})\mathcal{F}(\eta_{m,2})}{\mathcal{F}(\eta_{m,1})\mathcal{F}^*(\eta_{m,2}) + \mathcal{F}^*(\eta_{m,1})\mathcal{F}(\eta_{m,2})}\right]}{k_n D}\right\} \quad 75$$

And the directions of one of the composite wave is presented in Equation 76.

$$\theta_n = \cos^{-1}\left\{\frac{\tan^{-1}\left[-i\dfrac{\mathcal{F}(\eta_{m,1})\mathcal{F}^*(\eta_{m,2}) - \mathcal{F}^*(\eta_{m,1})\mathcal{F}(\eta_{m,2})}{\mathcal{F}(\eta_{m,1})\mathcal{F}^*(\eta_{m,2}) + \mathcal{F}^*(\eta_{m,1})\mathcal{F}(\eta_{m,2})}\right]}{k_n D}\right\} + \varphi \quad 76$$

This gives wave directions θ_n, including the extremes of the wave directions, the distribution of composite wave directions can be accordingly computed.

CHAPTER IV

PROBE POSITION CRITERIA

Principles for Probe Arrangement

The principle for probe arrangement is to measure wave parameters with known phase and time lag, measurements shall be either at the same location with known time lag or at different locations with known relative probe positions. The techniques for wave measurement employ direct technique using instrument in the water, including capacitance wave gauge measuring the surface elevation, current meter measuring particle velocity, free float buoy measuring particle velocity and wave slope, pressure gauge measuring wave pressure, and so on. Indirect technique such as stereography using optical methods including camera to capture the image of surface elevation. The indirect method is usually used for the directional waves

This section emphasizing on introducing a method using five wave probes and three of them are selected for spectra estimation and reflection analysis (three-of-five), which is based on the least square technique. The weighted coefficient used in the method employing an arbitrary number wave gauge is also introduced. Both methods are based on the principles of how to properly select a set of wave probes and both of them can reduce the labor in relocating wave probes when the test conditions employing multiple wavelengths. Also, these two methods are for long-crested waves. A software is developed for automatically arranging and selecting wave probes and its applicability based on the three-of-five technique are presented with instruction and sample results.

For short-crested waves, the methods of probes arrangement for capturing directional spectrum are introduced and are categorized in to narrow and wide spreading angles of the composite waves.

Probe Position for Long-Crest Waves

For long-crested waves, probe arrays employing at least two probes or one probe measuring at least two wave parameters simultaneously is usually used to capture the surface elevations and other wave parameters for estimating wave spectrum and further used for reflection analysis, and the probe arrays consist of arrangements such as spatially-spaced array, vertical array, co-located array, and wave probe matrix. A spatially-spaced array presented in top left of Figure 6 uses two (Thornton and Calhoun 1972); (Goda and Suzuki 1976), three (Mansard and Funke 1980), or an arbitrary number of (Zelt and Sejelbreia 1992) wave probes positioned parallel to wave propagation direction to measure surface elevations. A vertical array (S. A. Hughes 1993) presented in left middle of Figure 6 uses a wave probe measuring surface elevation and a current meter positioned vertically at the same horizontal position measuring particle velocity simultaneously. A co-located array (S. A. Hughes 1993) employs a current meter measuring the particle velocities of two directions simultaneously, which is presented in left bottom of Figure 6. Estimating wave spectrum according to the measurement for long-crest oblique wave may employ a wave probes matrix presented in right of Figure 6, and there is no need to restrict the positions of wave probes parallel to the orthogonal of reflection object (or wavemaker). The wave probe matrix technique is an extension of spatially-spaced array technique, however according to calculation by Issacson (1991) and by the author in the previous chapter, the offset of wave probes relative to the wavemaker orthogonal may not be necessary and the spatially spaced technique is still applicable for oblique long-crest wave.

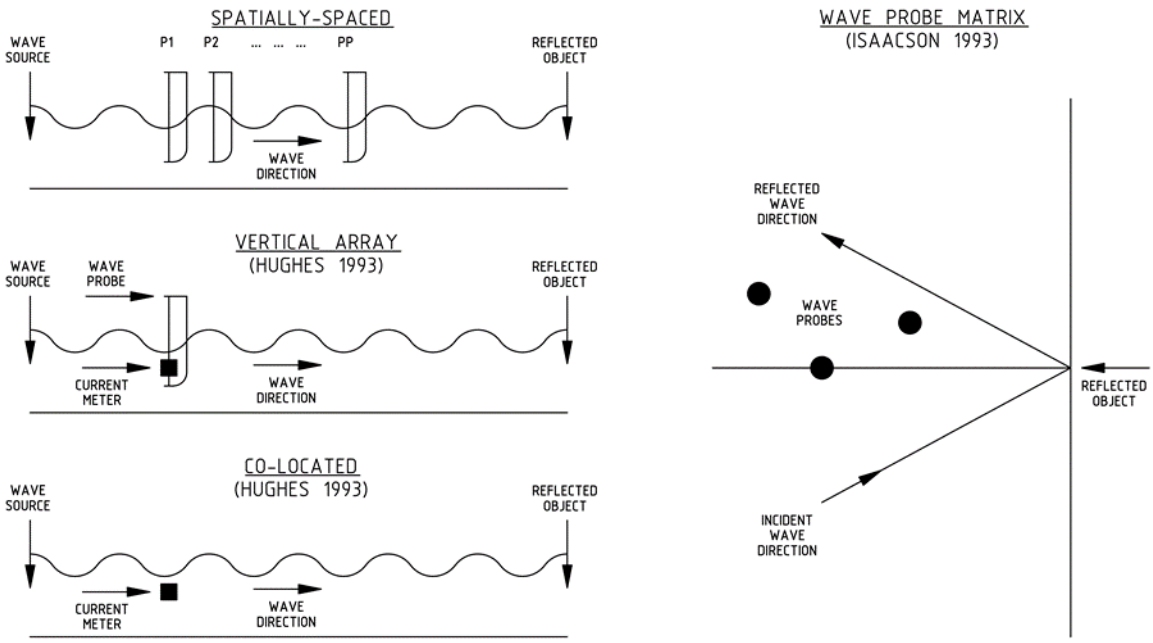

Figure 6. Probes array used in reflection analysis for long-crest wave.

For both single wavelength condition, distance between any of the two wave probes shall never be any integer multiplying half wavelength, and the distances between any wave probe and the wave source/reflected object shall be at least one wavelength. For a single wave condition with one wavelength only, a criterion determining the positions of the three wave probes recommended by Mansard and Funke (1980) is used, which is presented in Equation 77.

$$x_{12} = \frac{\lambda}{10}$$

$$\frac{\lambda}{6} < x_{13} < \frac{\lambda}{5} \text{ or } \frac{\lambda}{5} < x_{13} < \frac{3\lambda}{10} \text{ or } \frac{3\lambda}{10} < x_{13} < \frac{\lambda}{3} \quad (77)$$

Where: x_{12} and x_{13} are the probe distances between probes 1 and 2, and between probes 1 and 3 respectively, and probe 1 is the probe closest to the wave maker; λ is the wavelength corresponding to peak period of the wave spectrum.

Singularities that causing zero denominator for waves propagating normal to the toe of structure, i.e. $\theta = 0$, in Equation 37 for calculating F_I and F_R, respectively, happens when the probe distance between the first and the p^{th}, i.e. x_{1p}, equals to an integer multiplied by half wavelength. This situation presented in Equation 78 needs to be carefully avoided.

$$e^{i2k_n x_{1p}} = 1 \xrightarrow{yields} k_n x_{1p} = z_p \pi \xrightarrow{yields} x_{1p} = z_p \frac{\lambda}{2}, \qquad z_p \in \mathbb{Z} \tag{78}$$

A model basin test usually involves one or multiple wave conditions featuring single and variable wavelengths, respectively. For multiple wave conditions featuring specific wavelength for each scenario, two methods may be used, one of the methods is applying the weighted coefficients proposed by Zelt and Skejebreia (1992) and choosing three or more wave gauges from the wave probe array, the other method is using five probes, and three of the wave probes are used for reflection analysis for each specific wavelength of each corresponding wave condition or for several wavelengths of several corresponding wave conditions.

Three-of-five probes method

The breakwater project that let several wave conditions sharing a set of three wave probes for reflection analysis using least square technique indicates that margins maybe tolerable for the above probe spacing criterion. Also, the actual probe position may be an approximate to the probe spacing criteria. Accordingly, in the latter method, sharing three wave probes for several wavelengths to compute reflection coefficient using least squares method following spacing criteria above when only five probes are available may be a feasible method in basin test.

Let the five wave probes from the position closest to the wavemaker to the reflected structure as probes 1, 2, 3, 4, and 5 and the three wave probes used for reflection analysis from the position closest to the wave maker to the reflected structure as probes A, B, and C. The probe

distances relative to probe 1 are x_{12}, x_{13}, x_{14}, and x_{15}, and the probe distance relative to probe A are x_{AB}, and x_{AC}. Also, for conditions of wavelengths with totally M wavelengths, let λ^m be each wave condition and $m = 1,2, \dots, m, \dots M$. According to the breakwater project, margin of 1% of wave length may be added to the probe position criteria by Mansard and Funke (1980) for the distance between the first and the second wave probes, i.e. x_{AB}, and use the same probe criteria for the distance between the first and the third wave probes, i.e. x_{AC}, the singularities are also need to be carefully avoided and the distance between the wavemaker to probe A and the toe of reflected structure to probe C shall be equal or larger than one wave length. Hence, the revised probe criteria for x_{AB} and x_{AC} may be presented in Equation 79.

$$\frac{9\lambda}{100} \leq x_{AB} \leq \frac{11\lambda}{100}$$
$$\frac{\lambda}{6} < x_{AC} < \frac{\lambda}{3} \qquad 79$$

Accordingly, the conditions that allow two wavelengths λ^1 and λ^m ($\lambda^m > \lambda^1$) to share wave probes for reflection analysis can be established. The probe space distance between the probes A and B for λ^1 and λ^m are x_{AB}^1 and x_{AB}^m, respectively; The probe space distance between the probes A and C for λ^1 and λ^m are x_{AC}^1 and x_{AC}^m, respectively.

λ^m and λ^1 share the same x_{AB} when the lower limit of probe distance between the probes A and B for the m^{th} wavelength λ^m, i.e. $x_{AB}^m = (9/100)\lambda^m$, falls between the interval of the probe distance between the probes A and B for the first wavelength λ^1, i.e. x_{AB}^1. This condition is presented in Equation 80.

$$\frac{9}{100}\lambda^1 < \frac{9}{100}\lambda^m < \frac{11}{100}\lambda^1 \xrightarrow{yields} \lambda^1 < \lambda^m < \frac{11}{9}\lambda^1 \qquad 80$$

λ^m and λ^1 share the same x_{AC} when the lower limit of probe distance between the probes A and C for the m^{th} wavelength λ^m, i.e. $x_{AC}^m = (1/6)\lambda^m$, falls between the interval of the probe distance between the probes A and C for the first wavelength λ^1, i.e. x_{AC}^1. This condition is presented in Equation 81.

$$\frac{1}{6}\lambda^1 < \frac{1}{6}\lambda^m < \frac{1}{3}\lambda^1 \xrightarrow{yields} \lambda^1 < \lambda^m < 2\lambda^1 \quad (81)$$

The probe distance between the probes A and B for the m^{th} wavelength λ^m, i.e. x_{AB}^m, overlaps the probe distance between the probes A and C for the 1^{th} wavelength of λ^1, i.e. x_{AC}^1, when the lower limit of x_{AB}^m, i.e. $x_{AB}^m = (9/100)\lambda^m$, falls between the interval of x_{AC}^1. This condition is presented in Equation 82.

$$\frac{1}{6}\lambda^1 < \frac{9}{100}\lambda^m < \frac{1}{3}\lambda^1 \xrightarrow{yields} \frac{50}{27}\lambda^1 < \lambda^m < \frac{100}{27}\lambda^1 \quad (82)$$

These relations from Equation 79 to 82 are tabulated in Table 5 below.

Table 5. The conditions for sharing wave probes.

λ^m	$x_{AB}^1 \cap x_{AB}^m$	$x_{AC}^1 \cap x_{AC}^m$	$x_{AC}^1 \cap x_{AB}^m$
$\left(\lambda^1, \frac{11}{9}\lambda^1\right)$	$\neq 0$	$\neq 0$	$= 0$
$\left(\frac{11}{9}\lambda^1, \frac{50}{27}\lambda^1\right)$	$= 0$	$\neq 0$	$= 0$
$\left(\frac{50}{27}\lambda^1, 2\lambda^1\right)$	$= 0$	$\neq 0$	$\neq 0$
$\left(2\lambda^1, \frac{100}{27}\lambda^1\right)$	$= 0$	$= 0$	$\neq 0$
$\left(\frac{100}{27}\lambda^1, \infty\right)$	$= 0$	$= 0$	$= 0$

Based on the conditions tabulated in Table 5, the software can be programed to automatically determine the number of wave probes and their positions, and three of these probes will be selected for reflection analysis according to the wavelength used in the test. The directions are stated as follows:

1. Inputting the wavelengths used in a test and sorting them ascendingly to get an array of wavelengths λ^m

$$\lambda^m = \{\lambda^1, \lambda^2, \dots, \lambda^M\}$$

2. Comparing each wavelength that is larger than the first wavelength, i.e. $\lambda^{m\prime} = \{\lambda^2, \dots, \lambda^M\}$, to the first wavelengths λ^1 until there is zero overlapping between x_{AC}^1 and x_{AB}^m. Marking the longest wavelength having its x_{AB} overlap with x_{AC}^1 as λ^{M_1}, and marking the shortest wavelength that does not have its x_{AB} overlap with x_{AC}^1 as λ^{M_1+1}, and $1 \leq M_1 < M$. Wavelength λ^{M_1+1} and λ^1 have the following relationship derived from Equation 82.

$$\lambda^{M_1+1} > \frac{100}{27}\lambda^1$$

A group of the wavelengths (main group 1 – MG (1)) having overlapping to λ^1 can be formed, such that

$$MG(1) = \{\lambda^1, \dots, \lambda^{M_1}\}$$

3. Comparing each wavelength that is larger than λ^{M_1+1}, i.e. $\lambda^{m\prime} = \{\lambda^{M_1+2}, \dots, \lambda^M\}$, to the λ^{M_1+1} until there is zero overlapping between $x_{AC}^{M_1+1}$ and x_{AB}^m. Marking the longest wavelength having its x_{AB} overlap with $x_{AC}^{M_1+1}$ as λ^{M_2}, and marking the shortest wavelength that does not have its x_{AB} overlap with $x_{AC}^{M_1+1}$ as λ^{M_2+1}, and $M_1 + 1 \leq M_2 <$

M. Wavelength λ^{M_2+1} and λ^{M_1+1} have the following relationship derived from Equation 82.

$$\lambda^{M_2+1} > \frac{100}{27}\lambda^{M_1+1}$$

A group of the wavelengths (main group 2 – MG (2)) having overlapping to λ^1 can be formed, such that

$$MG(2) = \{\lambda^{M_1+1}, \dots, \lambda^{M_2}\}$$

4. Repeating the steps 2 and 3 until finishing comparing all wavelengths and categorizing all wavelengths, i.e. $\lambda^m = \{\lambda^1, \lambda^2, \dots, \lambda^M\}$, into the main groups of

$$MG(1) = \{\lambda^1, \dots, \lambda^{M_1}\}$$

$$MG(2) = \{\lambda^{M_1+1}, \dots, \lambda^{M_2}\}$$

…

$$MG(i) = \{\lambda^{M_{i-1}+1}, \dots, \lambda^{M}\}$$

5. Categorizing each main group, the 1st group, i.e. $\{\lambda^1, \dots, \lambda^{M_1}\}$, for example, into the subgroups SGs

    a. Categorizing the wavelengths according to Table 5 into four subgroups: a group that all wavelengths sharing the same x_{AB} and the same x_{AC} with those of λ^1; a group sharing the same x_{AC} while having zero overlapping of x_{AB} with those of λ^1; a group sharing the same x_{AC} and the x_{AB} of the longer wavelengths have the overlap with the x_{AC} of λ^1; a group that the x_{AB} of the longer wavelengths have the overlap with the x_{AC} of λ^1.

$$\lambda^1 \leq \{\lambda^1, \dots, \lambda^{S_1}\} < \frac{11}{9}\lambda^1$$

$$\frac{11}{9}\lambda^1 < \{\lambda^{S_1+1}, \dots, \lambda^{S_2}\} < \frac{50}{27}\lambda^1$$

$$\frac{50}{27}\lambda^1 < \{\lambda^{S_2+1}, \dots, \lambda^{S_3}\} < \frac{550}{243}\lambda^1$$

$$\frac{550}{243}\lambda^1 < \{\lambda^{S_3+1}, \dots, \lambda^{M_1}\} < \frac{100}{27}\lambda^1$$

b. For a subgroup $SG(1)$ sharing the same x_{AB} and the same x_{AC}, i.e. $\lambda^1 < \{\lambda^1, \dots, \lambda^{a_1}\} < (11/9)\lambda^1$, three wave probes are needed. The distance between the first and the second probes, i.e. x_{12}, are used as distance between the probes A and B, i.e. x_{AB}, and the distance between the first and the third probes, i.e. x_{13}, are used as distance between the probes A and C, i.e. x_{AC}.

$$x_{12}^{1\sim S_1} = \{x_{AB}^1, \dots, x_{AB}^{S_1}\}$$

$$x_{13}^{1\sim S_1} = \{x_{AC}^1, \dots, x_{AC}^{S_1}\}$$

c. For a subgroup $SG(2)$ sharing the same x_{AC} while having zero overlapping of x_{AB} with those of λ^1, i.e. $(11/9)\lambda^1 < \{\lambda^{S_1+1}, \dots, \lambda^{S_2}\} < (50/27)\lambda^1$, up to five wave probes are needed. These wavelengths share the same x_{AC} with the previous subgroup can be categorized into up to three groups, and each group shares the same x_{AB}.

$$x_{12}^{S_1+1\sim a_1} = \{x_{AB}^{S_1+1}, \dots, x_{AB}^{a_1}\}$$

$$x_{13}^{a_1+1\sim a_2} = \{x_{AB}^{a_1+1}, \dots, x_{AB}^{a_2}\}$$

$$x_{14}^{a_2+1\sim S_2} = \{x_{AB}^{a_2+1}, \dots, x_{AB}^{S_2}\}$$

$$x_{15}^{S_1+1\sim S_2} = \{x_{AC}^{S_1+1}, \dots, x_{AC}^{S_2}\}$$

d. The subgroup, i.e. $SG(3)$, of $(50/27)\lambda^1 < \{\lambda^{S_2+1}, \dots, \lambda^{S_3}\} < (550/243)\lambda^1$ is re-written from $\lambda^{S_2+1} < \{\lambda^{S_2+1}, \dots, \lambda^{S_3}\} < (11/9)\lambda^{S_2+1}$, and the wavelengths in this group share the same x_{AB} and the same x_{AC}. Three wave probes are needed. The distance between the first and the second probes, i.e. x_{12}, are used as distance between the probes A and B, i.e. x_{AB}, and the distance between the first and the third probes, i.e. x_{13}, are used as distance between the probes A and C, i.e. x_{AC}.

$$x_{12}^{S_2+1\sim S_3} = \{x_{AB}^{S_2+1}, \dots, x_{AB}^{S_3}\}$$

$$x_{13}^{S_2+1\sim S_3} = \{x_{AC}^{S_2+1}, \dots, x_{AC}^{S_3}\}$$

e. The wavelengths in subgroup $SG(4)$ of $(550/243)\lambda^1 < \{\lambda^{S_3+1}, \dots, \lambda^{M_1}\} < (100/27)\lambda^1$ share their distance x_{AB} with the distance between the first and the third probe of the shortest wavelength λ^1, i.e. x_{AC}^1. The interval of this subgroup can be rewritten as $\lambda^{S_3+1} < \{\lambda^{S_3+1}, \dots, \lambda^{M_1}\} < (18/11)\lambda^{S_3+1}$ and knowing that $(11/9)\lambda^{S_3+1} < (18/11)\lambda^{S_3+1} < (50/27)\lambda^{S_3+1}$, the wavelengths in this subgroup share the same distance x_{AC} with that of the shortest wavelength λ^{S_3+1} in this group, i.e. $x_{AC}^{S_3+1}$. Up to five wave probes are needed in this group.

$$x_{12}^{S_3+1\sim b_1} = \{x_{AB}^{S_3+1}, \dots, x_{AB}^{b_1}\}$$

$$x_{13}^{b_1+1\sim b_2} = \{x_{AB}^{b_1+1}, \dots, x_{AB}^{b_2}\}$$

$$x_{14}^{b_2+1\sim M_1} = \{x_{AB}^{b_2+1}, \dots, x_{AB}^{M_1}\}$$

$$x_{15}^{S_3+1\sim M_1} = \{x_{AC}^{S_3+1}, \dots, x_{AC}^{M_1}\}$$

f. According to Table 5, knowing that $x_{1p}^{a_2+1\sim S_2}$ in $SG(2)$ overlaps $x_{13}^{1\sim S_1}$ in $SG(1)$ Also $x_{13}^{S_3+1\sim M_1}$ in $SG(4)$ has overlap with overlap of $x_{1p}^{a_2+1\sim S_2}$ in $SG(2)$ and $x_{13}^{1\sim S_1}$ in $SG(1)$. Accordingly Merging can be applied to those subgroups:

   i. Merging $\{x_{AC}^1, \dots, x_{AC}^{S_1}\}$ and $\{x_{AC}^{S_1+1}, \dots, x_{AC}^{S_2}\}$

   ii. Merging, $\{x_{AC}^1, \dots, x_{AC}^{S_1}\}$, $\{x_{AC}^{S_1+1}, \dots, x_{AC}^{S_2}\}$, and $\{x_{AB}^{S_2+1}, \dots, x_{AB}^{S_3}\}$

g. To get the result that

$$x_{12} = \{x_{AB}^1, \dots, x_{AB}^{S_1}\}$$

$$x_{13} = \{x_{AB}^{S_1+1}, \dots, x_{AB}^{a_1}\}$$

$$x_{14} = \{x_{AB}^{a_1+1}, \dots, x_{AB}^{a_2}\}$$

$$x_{15} = \{x_{AB}^{a_2+1}, \dots, x_{AB}^{S_2}\}$$

$$x_{16} = \{x_{AC}^1, \dots, x_{AC}^{S_2}\}$$

$$= \{x_{AB}^{S_2+1}, \dots, x_{AB}^{S_3}\}$$

$$x_{17} = \{x_{AB}^{S_3+1}, \dots, x_{AB}^{b_1}\}$$

$$x_{18} = \{x_{AB}^{b_1+1}, \dots, x_{AB}^{b_2}\}$$

$$x_{19} = \{x_{AB}^{b_2+1}, \dots, x_{AB}^{M_1}\}$$

$$x_{1,10} = \{x_{AC}^{S_3}, \dots, x_{AC}^{M_1}\}$$

6. Repeating step 5 to complete the other main groups

Accordingly, by using the procedures above, several cases using up to five wave probes with the corresponding required number of probes and their positions can be obtained and are presented in Table 6 to Table 18.

The Case I presented in Table 6 indicating that all the wavelengths fall into the subgroup $SG(1)$. The wavelengths in this case share the same x_{AB} and the same x_{AC}, and only three wave probes are required. Distance x_{12} is for x_{AB} of all wavelengths, and distance x_{12} is for x_{AC} of all wavelengths.

Table 6. Cases and required number of probes – Case I.

$\{\lambda^1, \dots, \lambda^M\}$	Probe Position	P
$\lambda^1 \leq \{\lambda^1, \dots, \lambda^M\} < \frac{11}{9}\lambda^1$	$x_{12} = \{x_{AB}^1, \dots, x_{AB}^M\}$ $x_{13} = \{x_{AC}^1, \dots, x_{AC}^M\}$	3

The wavelengths in Case II fall into two subgroups, including Case II-1 presented in Table 7. Cases and required number of probes – Case II-1. that wavelengths fall into $SG(1)$ and $SG(2)$, Case II-2 presented in Table 8 that wavelengths fall into $SG(1)$ and $SG(3)$, and Case II-3 presented in Table 9 that wavelengths fall into $SG(1)$ and $SG(4)$.

Case II-1 presented in Table 7 that all wavelengths fall into $SG(1)$ and $SG(2)$ indicates that at least four wave probes and up to six wave probes are needed in this case. All wavelengths in this case share the same x_{AC}. The wavelengths fall into $SG(1)$ share the same x_{AB} that is independent from those of the wavelengths fall into $SG(2)$. The wavelengths fall into $SG(2)$ may need up to three x_{AB}s depending on how many intervals that these wavelengths fall into, and each interval using the same criteria of $SG(1)$ that guarantees all wavelengths in this interval share the same x_{AB} and x_{AC}. When the wavelengths in $SG(2)$ fall into three intervals, six wave probes are needed and this above the limit of five probe method.

Table 7. Cases and required number of probes – Case II-1.

$\{\lambda^1, \dots, \lambda^M\}$	Probe Position	P
$\lambda^1 \le \{\lambda^1, \dots, \lambda^{S_1}\} < \frac{11}{9}\lambda^1$ $\frac{11}{9}\lambda^1 < \{\lambda^{S_1+1}, \dots, \lambda^M\} < \left(\frac{11}{9}\right)^2 \lambda^1$	$x_{12} = \{x_{AB}^1, \dots, x_{AB}^{S_1}\}$ $x_{13} = \{x_{AB}^{S_1+1}, \dots, x_{AB}^M\}$ $x_{14} = \{x_{AC}^1, \dots, x_{AC}^M\}$	4
$\lambda^1 \le \{\lambda^1, \dots, \lambda^{S_1}\} < \frac{11}{9}\lambda^1$ $\left(\frac{11}{9}\right)^2 \lambda^1 < \{\lambda^{S_1+1}, \dots, \lambda^M\} < \left(\frac{11}{9}\right)^3 \lambda^1$	$x_{12} = \{x_{AB}^1, \dots, x_{AB}^{S_1}\}$ $x_{13} = \{x_{AB}^{S_1+1}, \dots, x_{AB}^M\}$ $x_{14} = \{x_{AC}^1, \dots, x_{AC}^M\}$	4
$\lambda^1 \le \{\lambda^1, \dots, \lambda^{S_1}\} < \frac{11}{9}\lambda^1$ $\left(\frac{11}{9}\right)^3 \lambda^1 < \{\lambda^{S_1+1}, \dots, \lambda^M\} < \frac{50}{27}\lambda^1$	$x_{12} = \{x_{AB}^1, \dots, x_{AB}^{S_1}\}$ $x_{13} = \{x_{AB}^{S_1+1}, \dots, x_{AB}^M\}$ $x_{14} = \{x_{AC}^1, \dots, x_{AC}^M\}$	4
$\lambda^1 \le \{\lambda^1, \dots, \lambda^{S_1}\} < \frac{11}{9}\lambda^1$ $\frac{11}{9}\lambda^1 < \{\lambda^{S_1+1}, \dots, \lambda^{a_1}\} < \left(\frac{11}{9}\right)^2 \lambda^1$ $\left(\frac{11}{9}\right)^2 \lambda^1 < \{\lambda^{a_1+1}, \dots, \lambda^M\} < \left(\frac{11}{9}\right)^3 \lambda^1$	$x_{12} = \{x_{AB}^1, \dots, x_{AB}^{S_1}\}$ $x_{13} = \{x_{AB}^{S_1+1}, \dots, x_{AB}^{a_1}\}$ $x_{14} = \{x_{AB}^{a_1+1}, \dots, x_{AB}^M\}$ $x_{15} = \{x_{AC}^1, \dots, x_{AC}^M\}$	5
$\lambda^1 \le \{\lambda^1, \dots, \lambda^{S_1}\} < \frac{11}{9}\lambda^1$ $\frac{11}{9}\lambda^1 < \{\lambda^{S_1+1}, \dots, \lambda^{a_1}\} < \left(\frac{11}{9}\right)^2 \lambda^1$ $\left(\frac{11}{9}\right)^3 \lambda^1 < \{\lambda^{a_1+1}, \dots, \lambda^M\} < \frac{50}{27}\lambda^1$	$x_{12} = \{x_{AB}^1, \dots, x_{AB}^{S_1}\}$ $x_{13} = \{x_{AB}^{S_1+1}, \dots, x_{AB}^{a_1}\}$ $x_{14} = \{x_{AB}^{a_1+1}, \dots, x_{AB}^M\}$ $x_{15} = \{x_{AC}^1, \dots, x_{AC}^M\}$	5
$\lambda^1 \le \{\lambda^1, \dots, \lambda^{S_1}\} < \frac{11}{9}\lambda^1$ $\left(\frac{11}{9}\right)^2 \lambda^1 < \{\lambda^{S_1+1}, \dots, \lambda^{a_1}\} < \left(\frac{11}{9}\right)^3 \lambda^1$ $\left(\frac{11}{9}\right)^3 \lambda^1 < \{\lambda^{a_1+1}, \dots, \lambda^M\} < \frac{50}{27}\lambda^1$	$x_{12} = \{x_{AB}^1, \dots, x_{AB}^{S_1}\}$ $x_{13} = \{x_{AB}^{S_1+1}, \dots, x_{AB}^{a_1}\}$ $x_{14} = \{x_{AB}^{a_1+1}, \dots, x_{AB}^M\}$ $x_{15} = \{x_{AC}^1, \dots, x_{AC}^M\}$	5

Table 7. Continued.

$\{\lambda^1, \dots, \lambda^M\}$	Probe Position	P
$\lambda^1 \le \{\lambda^1, \dots, \lambda^{S_1}\} < \frac{11}{9}\lambda^1$ $\frac{11}{9}\lambda^1 < \{\lambda^{S_1+1}, \dots, \lambda^{a_1}\} < \left(\frac{11}{9}\right)^2 \lambda^1$ $\left(\frac{11}{9}\right)^2 \lambda^1 < \{\lambda^{a_1+1}, \dots, \lambda^{a_2}\} < \left(\frac{11}{9}\right)^3 \lambda^1$ $\left(\frac{11}{9}\right)^3 \lambda^1 < \{\lambda^{a_2+1}, \dots, \lambda^M\} < \frac{50}{27}\lambda^1$	$x_{12} = \{x_{AB}^1, \dots, x_{AB}^{S_1}\}$ $x_{13} = \{x_{AB}^{S_1+1}, \dots, x_{AB}^{a_1}\}$ $x_{14} = \{x_{AB}^{a_1+1}, \dots, x_{AB}^{a_2}\}$ $x_{15} = \{x_{AB}^{a_2+1}, \dots, x_{AB}^{M}\}$ $x_{16} = \{x_{AC}^1, \dots, x_{AC}^M\}$	6

Case II-2 presented in Table 8 that all wavelengths fall into $SG(1)$ and $SG(3)$ indicates that at only four wave probes are needed in this case. The x_{AB}s of the wavelengths in these subgroups have no overlap. All wavelengths in this case share the same x_{AC} if the wavelengths in $SG(3)$ are shorter than $2\lambda^1$. x_{AC} of $SG(1)$ is independent from that of $SG(3)$ when some wavelengths in the latter subgroup are longer than $2\lambda^1$, and the x_{AB} of $SG(3)$ share the probes with x_{AC} of $SG(1)$.

Table 8. Cases and required number of probes – Case II-2.

$\{\lambda^2, \dots, \lambda^M\}$	Probe Position	P
$\lambda^1 \le \{\lambda^1, \dots, \lambda^{S_1}\} < \frac{11}{9}\lambda^1$ $\frac{50}{27}\lambda^1 < \{\lambda^{S_1+1}, \dots, \lambda^M\} < 2\lambda^1$	$x_{12} = \{x_{AB}^1, \dots, x_{AB}^{S_1}\}$ $x_{13} = \{x_{AB}^{S_1+1}, \dots, x_{AB}^{M}\}$ $x_{14} = \{x_{AC}^1, \dots, x_{AC}^M\}$	4
$\lambda^1 \le \{\lambda^1, \dots, \lambda^{S_1}\} < \frac{11}{9}\lambda^1$ $\frac{50}{27}\lambda^1 < \{\lambda^{S_1+1}, \dots, \lambda^M\} < \frac{550}{243}\lambda^1$	$x_{12} = \{x_{AB}^1, \dots, x_{AB}^{S_1}\}$ $x_{13} = \{x_{AC}^1, \dots, x_{AC}^{S_1}\}$ $= \{x_{AB}^{S_1+1}, \dots, x_{AB}^{M}\}$ $x_{14} = \{x_{AC}^{S_1+1}, \dots, x_{AC}^{M}\}$	4

Case II-3 presented in Table 9 that all wavelengths fall into $SG(1)$ and $SG(4)$ indicates that at least four wave probes and up to six wave probes are needed in this case. The wavelengths in subcase $SG(1)$ share the same x_{AB} and x_{AC}. The wavelengths in $SG(4)$ share the same x_{AC} and may need up to three x_{AB}s depending on how many intervals that these wavelengths fall into, and each interval using the same criteria of $SG(1)$ that guarantees all wavelengths in this interval share the same x_{AB} and x_{AC}. The x_{AB}s of $SG(4)$ overlap the x_{AC} of $SG(4)$ and letting one of the x_{AB}s of $SG(4)$ share the wave probe with the x_{AC} of $SG(4)$. When the wavelengths in $SG(2)$ fall into three intervals, six wave probes are needed and this above the limit of five probe method.

Table 9. Cases and required number of probes – Case II-3.

$\{\lambda^2, \dots, \lambda^M\}$	Probe Position	P
$\lambda^1 \le \{\lambda^1, \dots, \lambda^{S_1}\} < \frac{11}{9}\lambda^1$ $\frac{550}{243}\lambda^1 \le \{\lambda^{S_1+1}, \dots, \lambda^M\} < \frac{550}{243}\left(\frac{11}{9}\right)\lambda^1$	$x_{12} = \{x_{AB}^1, \dots, x_{AB}^{S_1}\}$ $x_{13} = \{x_{AC}^1, \dots, x_{AC}^{S_1}\}$ $= \{x_{AB}^{S_1+1}, \dots, x_{AB}^M\}$ $x_{14} = \{x_{AC}^{S_1+1}, \dots, x_{AC}^M\}$	4
$\lambda^1 \le \{\lambda^1, \dots, \lambda^{S_1}\} < \frac{11}{9}\lambda^1$ $\frac{550}{243}\left(\frac{11}{9}\right)\lambda^1 < \{\lambda^{S_1+1}, \dots, \lambda^M\} < \frac{550}{243}\left(\frac{11}{9}\right)^2\lambda^1$	$x_{12} = \{x_{AB}^1, \dots, x_{AB}^{S_1}\}$ $x_{13} = \{x_{AC}^1, \dots, x_{AC}^{S_1}\}$ $= \{x_{AB}^{S_1+1}, \dots, x_{AB}^M\}$ $x_{14} = \{x_{AC}^{S_1+1}, \dots, x_{AC}^M\}$	4
$\lambda^1 \le \{\lambda^1, \dots, \lambda^{S_1}\} < \frac{11}{9}\lambda^1$ $\frac{550}{243}\left(\frac{11}{9}\right)^2\lambda^1 < \{\lambda^{S_1+1}, \dots, \lambda^M\} < \frac{550}{243}\left(\frac{18}{11}\right)\lambda^1$	$x_{12} = \{x_{AB}^1, \dots, x_{AB}^{S_1}\}$ $x_{13} = \{x_{AC}^1, \dots, x_{AC}^{S_1}\}$ $= \{x_{AB}^{S_1+1}, \dots, x_{AB}^M\}$ $x_{14} = \{x_{AC}^{S_1+1}, \dots, x_{AC}^M\}$	4

Table 9. Continued.

$\{\lambda^2, \dots, \lambda^M\}$	Probe Position	P
$\lambda^1 \le \{\lambda^1, \dots, \lambda^{S_1}\} < \frac{11}{9}\lambda^1$ $\frac{550}{243}\lambda^1 < \{\lambda^{S_1+1}, \dots, \lambda^{b_1}\} < \frac{550}{243}\left(\frac{11}{9}\right)\lambda^1$ $\frac{550}{243}\left(\frac{11}{9}\right)\lambda^1 < \{\lambda^{b_1+1}, \dots, \lambda^M\} < \frac{550}{243}\left(\frac{11}{9}\right)^2\lambda^1$	$x_{12} = \{x_{AB}^1, \dots, x_{AB}^{S_1}\}$ $x_{13} = \{x_{AC}^1, \dots, x_{AC}^{S_1}\}$ $= \{x_{AB}^{S_1+1}, \dots, x_{AB}^{b_1}\}$ $x_{14} = \{x_{AB}^{b_1+1}, \dots, x_{AB}^{M}\}$ $x_{15} = \{x_{AC}^{S_1+1}, \dots, x_{AC}^{M}\}$	5
$\lambda^1 \le \{\lambda^1, \dots, \lambda^{S_1}\} < \frac{11}{9}\lambda^1$ $\frac{550}{243}\lambda^1 < \{\lambda^{S_1+1}, \dots, \lambda^{b_1}\} < \frac{550}{243}\left(\frac{11}{9}\right)\lambda^1$ $\frac{550}{243}\left(\frac{11}{9}\right)^2\lambda^1 < \{\lambda^{b_1+1}, \dots, \lambda^M\} < \frac{550}{243}\left(\frac{18}{11}\right)\lambda^1$	$x_{12} = \{x_{AB}^1, \dots, x_{AB}^{S_1}\}$ $x_{13} = \{x_{AC}^1, \dots, x_{AC}^{S_1}\}$ $= \{x_{AB}^{S_1+1}, \dots, x_{AB}^{b_1}\}$ $x_{14} = \{x_{AB}^{b_1+1}, \dots, x_{AB}^{M}\}$ $x_{15} = \{x_{AC}^{S_1+1}, \dots, x_{AC}^{M}\}$	5
$\lambda^1 \le \{\lambda^1, \dots, \lambda^{S_1}\} < \frac{11}{9}\lambda^1$ $\frac{550}{243}\left(\frac{11}{9}\right)\lambda^1 < \{\lambda^{S_1+1}, \dots, \lambda^{b_1}\} < \frac{550}{243}\left(\frac{11}{9}\right)^2\lambda^1$ $\frac{550}{243}\left(\frac{11}{9}\right)^2\lambda^1 < \{\lambda^{b_1+1}, \dots, \lambda^M\} < \frac{550}{243}\left(\frac{18}{11}\right)\lambda^1$	$x_{12} = \{x_{AB}^1, \dots, x_{AB}^{S_1}\}$ $x_{13} = \{x_{AC}^1, \dots, x_{AC}^{S_1}\}$ $= \{x_{AB}^{S_1+1}, \dots, x_{AB}^{b_1}\}$ $x_{14} = \{x_{AB}^{b_1+1}, \dots, x_{AB}^{M}\}$ $x_{15} = \{x_{AC}^{S_1+1}, \dots, x_{AC}^{M}\}$	5
$\lambda^1 \le \{\lambda^1, \dots, \lambda^{S_1}\} < \frac{11}{9}\lambda^1$ $\frac{550}{243}\lambda^1 < \{\lambda^{S_1+1}, \dots, \lambda^{b_1}\} < \frac{550}{243}\left(\frac{11}{9}\right)\lambda^1$ $\frac{550}{243}\left(\frac{11}{9}\right)\lambda^1 < \{\lambda^{b_1+1}, \dots, \lambda^{b_2}\} < \frac{550}{243}\left(\frac{11}{9}\right)^2\lambda^1$ $\frac{550}{243}\left(\frac{11}{9}\right)^2\lambda^1 < \{\lambda^{b_2+1}, \dots, \lambda^M\} < \frac{550}{243}\left(\frac{18}{11}\right)\lambda^1$	$x_{12} = \{x_{AB}^1, \dots, x_{AB}^{S_1}\}$ $x_{13} = \{x_{AC}^1, \dots, x_{AC}^{S_1}\}$ $= \{x_{AB}^{S_1+1}, \dots, x_{AB}^{b_1}\}$ $x_{14} = \{x_{AB}^{b_1+1}, \dots, x_{AB}^{b_2}\}$ $x_{15} = \{x_{AC}^{b_2+1}, \dots, x_{AC}^{M}\}$ $x_{16} = \{x_{AC}^{S_1+1}, \dots, x_{AC}^{M}\}$	6

The wavelengths in Case III fall into three subgroups, including Case III-1 presented in Table 10 and Table 11 that wavelengths fall into $SG(1)$, $SG(2)$, and, $SG(3)$, Case III-2 presented

in Table 12, Table 13, and Table 14 that wavelengths fall into $SG(1)$, $SG(2)$, and, $SG(4)$, and Case III-3 presented in Table 15 and Table 16 that wavelengths fall into $SG(1)$, $SG(3)$, and, $SG(4)$.

Case III-1 presented in Table 10 for Case III-1a and Table 11 for Case III-1b that all wavelengths fall into $SG(1)$, $SG(2)$, and, $SG(3)$ indicates that five wave probes are needed in this case if the wavelengths in $SG(2)$ fall into only one of its intervals. All wavelengths in this case share the same x_{AC} if the wavelengths in $SG(3)$ are shorter than $2\lambda^1$, which are presented in Case III-1a. x_{AC} of $SG(1)$ and $SG(2)$ is independent from that of $SG(3)$ when some wavelengths in the subgroup $SG(3)$ are longer than $2\lambda^1$, and the x_{AB} of $SG(3)$ share the probes with x_{AC} of $SG(1)$ and $SG(2)$, which are presented in Case III-1b.

Table 10. Cases and required number of probes – Case III-1a.

$\{\lambda^1, \dots, \lambda^M\}$	Probe Position	P
$\lambda^1 \le \{\lambda^1, \dots, \lambda^{S_1}\} < \frac{11}{9}\lambda^1$ $\frac{11}{9}\lambda^1 < \{\lambda^{S_1+1}, \dots, \lambda^{S_2}\} < \left(\frac{11}{9}\right)^2 \lambda^1$ $\frac{50}{27}\lambda^1 < \{\lambda^{S_2+1}, \dots, \lambda^M\} < 2\lambda^1$	$x_{12} = \{x_{AB}^1, \dots, x_{AB}^{S_1}\}$ $x_{13} = \{x_{AB}^{S_1+1}, \dots, x_{AB}^{S_2}\}$ $x_{14} = \{x_{AC}^{S_2+1}, \dots, x_{AC}^M\}$ $x_{15} = \{x_{AC}^1, \dots, x_{AC}^M\}$	5
$\lambda^1 \le \{\lambda^1, \dots, \lambda^{S_1}\} < \frac{11}{9}\lambda^1$ $\left(\frac{11}{9}\right)^2 \lambda^1 < \{\lambda^{S_1+1}, \dots, \lambda^{S_2}\} < \left(\frac{11}{9}\right)^3 \lambda^1$ $\frac{50}{27}\lambda^1 < \{\lambda^{S_2+1}, \dots, \lambda^M\} < 2\lambda^1$	$x_{12} = \{x_{AB}^1, \dots, x_{AB}^{S_1}\}$ $x_{13} = \{x_{AB}^{S_1+1}, \dots, x_{AB}^{S_2}\}$ $x_{14} = \{x_{AC}^{S_2+1}, \dots, x_{AC}^M\}$ $x_{15} = \{x_{AC}^1, \dots, x_{AC}^M\}$	5

Table 10. Continued.

$\{\lambda^1, \dots, \lambda^M\}$	Probe Position	P
$\lambda^1 \le \{\lambda^1, \dots, \lambda^{S_1}\} < \frac{11}{9}\lambda^1$ $\left(\frac{11}{9}\right)^3 \lambda^1 < \{\lambda^{S_1+1}, \dots, \lambda^{S_2}\} < \frac{50}{27}\lambda^1$ $\frac{50}{27}\lambda^1 < \{\lambda^{S_2+1}, \dots, \lambda^M\} < 2\lambda^1$	$x_{12} = \{x_{AB}^1, \dots, x_{AB}^{S_1}\}$ $x_{13} = \{x_{AB}^{S_1+1}, \dots, x_{AB}^{S_2}\}$ $x_{14} = \{x_{AC}^{S_2+1}, \dots, x_{AC}^M\}$ $x_{15} = \{x_{AC}^1, \dots, x_{AC}^M\}$	5

Table 11. Cases and required number of probes – Case III-1b.

$\{\lambda^1, \dots, \lambda^M\}$	Probe Position	P
$\lambda^1 \le \{\lambda^1, \dots, \lambda^{S_1}\} < \frac{11}{9}\lambda^1$ $\frac{11}{9}\lambda^1 < \{\lambda^{S_1+1}, \dots, \lambda^{S_2}\} < \left(\frac{11}{9}\right)^2 \lambda^1$ $\frac{50}{27}\lambda^1 < \{\lambda^{S_2+1}, \dots, \lambda^M\} < \frac{550}{243}\lambda^1$	$x_{12} = \{x_{AB}^1, \dots, x_{AB}^{S_1}\}$ $x_{13} = \{x_{AB}^{S_1+1}, \dots, x_{AB}^{S_2}\}$ $x_{14} = \{x_{AC}^1, \dots, x_{AC}^{S_2}\}$ $= \{x_{AB}^{S_2+1}, \dots, x_{AB}^M\}$ $x_{15} = \{x_{AC}^{S_2+1}, \dots, x_{AC}^M\}$	5
$\lambda^1 \le \{\lambda^1, \dots, \lambda^{S_1}\} < \frac{11}{9}\lambda^1$ $\left(\frac{11}{9}\right)^2 \lambda^1 < \{\lambda^{S_1+1}, \dots, \lambda^{S_2}\} < \left(\frac{11}{9}\right)^3 \lambda^1$ $\frac{50}{27}\lambda^1 < \{\lambda^{S_2+1}, \dots, \lambda^M\} < \frac{550}{243}\lambda^1$	$x_{12} = \{x_{AB}^1, \dots, x_{AB}^{S_1}\}$ $x_{13} = \{x_{AB}^{S_1+1}, \dots, x_{AB}^{S_2}\}$ $x_{14} = \{x_{AC}^1, \dots, x_{AC}^{S_2}\}$ $= \{x_{AB}^{S_2+1}, \dots, x_{AB}^M\}$ $x_{15} = \{x_{AC}^{S_2+1}, \dots, x_{AC}^M\}$	5
$\lambda^1 \le \{\lambda^1, \dots, \lambda^{S_1}\} < \frac{11}{9}\lambda^1$ $\left(\frac{11}{9}\right)^3 \lambda^1 < \{\lambda^{S_1+1}, \dots, \lambda^{S_2}\} < \frac{50}{27}\lambda^1$ $\frac{50}{27}\lambda^1 < \{\lambda^{S_2+1}, \dots, \lambda^M\} < \frac{550}{243}\lambda^1$	$x_{12} = \{x_{AB}^1, \dots, x_{AB}^{S_1}\}$ $x_{13} = \{x_{AB}^{S_1+1}, \dots, x_{AB}^{S_2}\}$ $x_{14} = \{x_{AC}^1, \dots, x_{AC}^{S_2}\}$ $= \{x_{AB}^{S_2+1}, \dots, x_{AB}^M\}$ $x_{15} = \{x_{AC}^{S_2+1}, \dots, x_{AC}^M\}$	5

Case III-2 presented in Table 12 for Case III-2a and in Table 13 for Case III-2b and in Table 14 for Case III-2c that all wavelengths fall into $SG(1)$, $SG(2)$, and, $SG(4)$ indicates that five wave probes are needed in this case if the wavelengths in $SG(2)$ and $SG(4)$ fall into only one of their intervals. All wavelengths in $SG(1)$ and $SG(2)$ in this case share the same x_{AC} that is independent from that of $SG(4)$. x_{AB} of the wavelengths in $SG(4)$ share the probes with x_{AC} of the wavelengths in $SG(1)$ and $SG(2)$.

Table 12. Cases and required number of probes – Case III-2a.

$\{\lambda^1, \dots, \lambda^M\}$	Probe Position	P
$\lambda^1 \le \{\lambda^1, \dots, \lambda^{S_1}\} < \frac{11}{9}\lambda^1$ $\frac{11}{9}\lambda^1 < \{\lambda^{S_1+1}, \dots, \lambda^{S_2}\} < \left(\frac{11}{9}\right)^2 \lambda^1$ $\frac{550}{243}\lambda^1 \le \{\lambda^{S_2+1}, \dots, \lambda^M\} < \frac{550}{243}\left(\frac{11}{9}\right)\lambda^1$	$x_{12} = \{x_{AB}^1, \dots, x_{AB}^{S_1}\}$ $x_{13} = \{x_{AB}^{S_1+1}, \dots, x_{AB}^{S_2}\}$ $x_{14} = \{x_{AC}^1, \dots, x_{AC}^{S_2}\}$ $= \{x_{AB}^{S_2+1}, \dots, x_{AB}^M\}$ $x_{15} = \{x_{AC}^{S_2+1}, \dots, x_{AC}^M\}$	5
$\lambda^1 \le \{\lambda^1, \dots, \lambda^{S_1}\} < \frac{11}{9}\lambda^1$ $\left(\frac{11}{9}\right)^2 \lambda^1 < \{\lambda^{S_1+1}, \dots, \lambda^{S_2}\} < \left(\frac{11}{9}\right)^3 \lambda^1$ $\frac{550}{243}\lambda^1 \le \{\lambda^{S_2+1}, \dots, \lambda^M\} < \frac{550}{243}\left(\frac{11}{9}\right)\lambda^1$	$x_{12} = \{x_{AB}^1, \dots, x_{AB}^{S_1}\}$ $x_{13} = \{x_{AB}^{S_1+1}, \dots, x_{AB}^{S_2}\}$ $x_{14} = \{x_{AC}^1, \dots, x_{AC}^{S_2}\}$ $= \{x_{AB}^{S_2+1}, \dots, x_{AB}^M\}$ $x_{15} = \{x_{AC}^{S_2+1}, \dots, x_{AC}^M\}$	5
$\lambda^1 \le \{\lambda^1, \dots, \lambda^{S_1}\} < \frac{11}{9}\lambda^1$ $\left(\frac{11}{9}\right)^3 \lambda^1 < \{\lambda^{S_1+1}, \dots, \lambda^{S_2}\} < \frac{50}{27}\lambda^1$ $\frac{550}{243}\lambda^1 \le \{\lambda^{S_2+1}, \dots, \lambda^M\} < \frac{550}{243}\left(\frac{11}{9}\right)\lambda^1$	$x_{12} = \{x_{AB}^1, \dots, x_{AB}^{S_1}\}$ $x_{13} = \{x_{AB}^{S_1+1}, \dots, x_{AB}^{S_2}\}$ $x_{14} = \{x_{AC}^1, \dots, x_{AC}^{S_2}\}$ $= \{x_{AB}^{S_2+1}, \dots, x_{AB}^M\}$ $x_{15} = \{x_{AC}^{S_2+1}, \dots, x_{AC}^M\}$	5

Table 13. Cases and required number of probes – Case III-2b.

$\{\lambda^1, \dots, \lambda^M\}$	Probe Position	P
$\lambda^1 \le \{\lambda^1, \dots, \lambda^{S_1}\} < \frac{11}{9}\lambda^1$ $\frac{11}{9}\lambda^1 < \{\lambda^{S_1+1}, \dots, \lambda^{S_2}\} < \left(\frac{11}{9}\right)^2 \lambda^1$ $\frac{550}{243}\left(\frac{11}{9}\right)\lambda^1 \le \{\lambda^{S_2+1}, \dots, \lambda^M\} < \frac{550}{243}\left(\frac{11}{9}\right)^2 \lambda^1$	$x_{12} = \{x_{AB}^1, \dots, x_{AB}^{S_1}\}$ $x_{13} = \{x_{AB}^{S_1+1}, \dots, x_{AB}^{S_2}\}$ $x_{14} = \{x_{AC}^1, \dots, x_{AC}^{S_2}\}$ $= \{x_{AB}^{S_2+1}, \dots, x_{AB}^M\}$ $x_{15} = \{x_{AC}^{S_2+1}, \dots, x_{AC}^M\}$	5
$\lambda^1 \le \{\lambda^1, \dots, \lambda^{S_1}\} < \frac{11}{9}\lambda^1$ $\left(\frac{11}{9}\right)^2 \lambda^1 < \{\lambda^{S_1+1}, \dots, \lambda^{S_2}\} < \left(\frac{11}{9}\right)^3 \lambda^1$ $\frac{550}{243}\left(\frac{11}{9}\right)\lambda^1 \le \{\lambda^{S_2+1}, \dots, \lambda^M\} < \frac{550}{243}\left(\frac{11}{9}\right)^2 \lambda^1$	$x_{12} = \{x_{AB}^1, \dots, x_{AB}^{S_1}\}$ $x_{13} = \{x_{AB}^{S_1+1}, \dots, x_{AB}^{S_2}\}$ $x_{14} = \{x_{AC}^1, \dots, x_{AC}^{S_2}\}$ $= \{x_{AB}^{S_2+1}, \dots, x_{AB}^M\}$ $x_{15} = \{x_{AC}^{S_2+1}, \dots, x_{AC}^M\}$	5
$\lambda^1 \le \{\lambda^1, \dots, \lambda^{S_1}\} < \frac{11}{9}\lambda^1$ $\left(\frac{11}{9}\right)^3 \lambda^1 < \{\lambda^{S_1+1}, \dots, \lambda^{S_2}\} < \frac{50}{27}\lambda^1$ $\frac{550}{243}\left(\frac{11}{9}\right)\lambda^1 \le \{\lambda^{S_2+1}, \dots, \lambda^M\} < \frac{550}{243}\left(\frac{11}{9}\right)^2 \lambda^1$	$x_{12} = \{x_{AB}^1, \dots, x_{AB}^{S_1}\}$ $x_{13} = \{x_{AB}^{S_1+1}, \dots, x_{AB}^{S_2}\}$ $x_{14} = \{x_{AC}^1, \dots, x_{AC}^{S_2}\}$ $= \{x_{AB}^{S_2+1}, \dots, x_{AB}^M\}$ $x_{15} = \{x_{AC}^{S_2+1}, \dots, x_{AC}^M\}$	5

Table 14. Cases and required number of probes – Case III-2c.

$\{\lambda^1, \dots, \lambda^M\}$	Probe Position	P
$\lambda^1 \le \{\lambda^1, \dots, \lambda^{S_1}\} < \frac{11}{9}\lambda^1$ $\frac{11}{9}\lambda^1 < \{\lambda^{S_1+1}, \dots, \lambda^{S_2}\} < \left(\frac{11}{9}\right)^2 \lambda^1$ $\frac{550}{243}\left(\frac{11}{9}\right)^2 \lambda^1 < \{\lambda^{S_2+1}, \dots, \lambda^M\} < \frac{550}{243}\left(\frac{18}{11}\right)\lambda^1$	$x_{12} = \{x_{AB}^1, \dots, x_{AB}^{S_1}\}$ $x_{13} = \{x_{AB}^{S_1+1}, \dots, x_{AB}^{S_2}\}$ $x_{14} = \{x_{AC}^1, \dots, x_{AC}^{S_2}\}$ $= \{x_{AB}^{S_2+1}, \dots, x_{AB}^M\}$ $x_{15} = \{x_{AC}^{S_2+1}, \dots, x_{AC}^M\}$	5
$\lambda^1 \le \{\lambda^1, \dots, \lambda^{S_1}\} < \frac{11}{9}\lambda^1$ $\left(\frac{11}{9}\right)^2 \lambda^1 < \{\lambda^{S_1+1}, \dots, \lambda^{S_2}\} < \left(\frac{11}{9}\right)^3 \lambda^1$ $\frac{550}{243}\left(\frac{11}{9}\right)^2 \lambda^1 < \{\lambda^{S_2+1}, \dots, \lambda^M\} < \frac{550}{243}\left(\frac{18}{11}\right)\lambda^1$	$x_{12} = \{x_{AB}^1, \dots, x_{AB}^{S_1}\}$ $x_{13} = \{x_{AB}^{S_1+1}, \dots, x_{AB}^{S_2}\}$ $x_{14} = \{x_{AC}^1, \dots, x_{AC}^{S_2}\}$ $= \{x_{AB}^{S_2+1}, \dots, x_{AB}^M\}$ $x_{15} = \{x_{AC}^{S_2+1}, \dots, x_{AC}^M\}$	5
$\lambda^1 \le \{\lambda^1, \dots, \lambda^{S_1}\} < \frac{11}{9}\lambda^1$ $\left(\frac{11}{9}\right)^3 \lambda^1 < \{\lambda^{S_1+1}, \dots, \lambda^{S_2}\} < \frac{50}{27}\lambda^1$ $\frac{550}{243}\left(\frac{11}{9}\right)^2 \lambda^1 < \{\lambda^{S_2+1}, \dots, \lambda^M\} < \frac{550}{243}\left(\frac{18}{11}\right)\lambda^1$	$x_{12} = \{x_{AB}^1, \dots, x_{AB}^{S_1}\}$ $x_{13} = \{x_{AB}^{S_1+1}, \dots, x_{AB}^{S_2}\}$ $x_{14} = \{x_{AC}^1, \dots, x_{AC}^{S_2}\}$ $= \{x_{AB}^{S_2+1}, \dots, x_{AB}^M\}$ $x_{15} = \{x_{AC}^{S_2+1}, \dots, x_{AC}^M\}$	5

Case III-3 presented in Table 15 for Case III-3a and Table 16 for Case III-3b that all wavelengths fall into $SG(1)$, $SG(3)$, and, $SG(4)$ indicates that five wave probes are needed in this case if the wavelengths in $SG(4)$ fall into only one of its intervals. All wavelengths in $SG(1)$ and $SG(3)$ share the same x_{AC} if the wavelengths in $SG(3)$ are shorter than $2\lambda^1$, which are presented in Case III-3a, and x_{AB} of the wavelengths in $SG(4)$ overlaps with the x_{AC} of $SG(1)$ and $SG(3)$. The x_{AC}s of $SG(1)$ and $SG(3)$ are independent to each other if the wavelengths in $SG(3)$ are longer than $2\lambda^1$, x_{AB} of the wavelengths in $SG(3)$ share the probes with x_{AC} of $SG(1)$ and $SG(2)$, and wavelengths in $SG(3)$ and $SG(4)$ share the probes for x_{AC}, which are presented in Case III-3b.

Table 15. Cases and required number of probes – Case III-3a.

$\{\lambda^2, \dots, \lambda^M\}$	Probe Position	P
$\lambda^1 \leq \{\lambda^1, \dots, \lambda^{S_1}\} < \frac{11}{9}\lambda^1$ $\frac{50}{27}\lambda^1 < \{\lambda^{S_1+1}, \dots, \lambda^{S_2}\} < 2\lambda^1$ $\frac{550}{243}\lambda^1 < \{\lambda^{S_2+1}, \dots, \lambda^M\} < \frac{550}{243}\left(\frac{11}{9}\right)\lambda^1$	$x_{12} = \{x_{AB}^1, \dots, x_{AB}^{S_1}\}$ $x_{13} = \{x_{AB}^{S_1+1}, \dots, x_{AB}^{S_2}\}$ $x_{14} = \{x_{AC}^1, \dots, x_{AC}^{S_2}\}$ $= \{x_{AB}^{S_2+1}, \dots, x_{AB}^M\}$ $x_{15} = \{x_{AC}^{S_2+1}, \dots, x_{AC}^M\}$	5
$\lambda^1 \leq \{\lambda^1, \dots, \lambda^{S_1}\} < \frac{11}{9}\lambda^1$ $\frac{50}{27}\lambda^1 < \{\lambda^{S_1+1}, \dots, \lambda^{S_2}\} < 2\lambda^1$ $\frac{550}{243}\left(\frac{11}{9}\right)\lambda^1 < \{\lambda^{S_2+1}, \dots, \lambda^M\} < \frac{550}{243}\left(\frac{11}{9}\right)^2\lambda^1$	$x_{12} = \{x_{AB}^1, \dots, x_{AB}^{S_1}\}$ $x_{13} = \{x_{AB}^{S_1+1}, \dots, x_{AB}^{S_2}\}$ $x_{14} = \{x_{AC}^1, \dots, x_{AC}^{S_2}\}$ $= \{x_{AB}^{S_2+1}, \dots, x_{AB}^M\}$ $x_{15} = \{x_{AC}^{S_2+1}, \dots, x_{AC}^M\}$	5
$\lambda^1 \leq \{\lambda^1, \dots, \lambda^{S_1}\} < \frac{11}{9}\lambda^1$ $\frac{50}{27}\lambda^1 < \{\lambda^{S_1+1}, \dots, \lambda^{S_2}\} < 2\lambda^1$ $\frac{550}{243}\left(\frac{11}{9}\right)^2\lambda^1 < \{\lambda^{S_2+1}, \dots, \lambda^M\} < \frac{550}{243}\left(\frac{18}{11}\right)\lambda^1$	$x_{12} = \{x_{AB}^1, \dots, x_{AB}^{S_1}\}$ $x_{13} = \{x_{AB}^{S_1+1}, \dots, x_{AB}^{S_2}\}$ $x_{14} = \{x_{AC}^1, \dots, x_{AC}^{S_2}\}$ $= \{x_{AB}^{S_2+1}, \dots, x_{AB}^M\}$ $x_{15} = \{x_{AC}^{S_2+1}, \dots, x_{AC}^M\}$	5

Table 16. Cases and required number of probes – Case III-3b.

$\{\lambda^2, \dots, \lambda^M\}$	Probe Position	P
$\lambda^1 \le \{\lambda^1, \dots, \lambda^{S_1}\} < \frac{11}{9}\lambda^1$ $\frac{50}{27}\lambda^1 < \{\lambda^{S_1+1}, \dots, \lambda^{S_2}\} < \frac{550}{243}\lambda^1$ $\frac{550}{243}\lambda^1 < \{\lambda^{S_2+1}, \dots, \lambda^M\} < \frac{550}{243}\left(\frac{11}{9}\right)\lambda^1$	$x_{12} = \{x_{AB}^1, \dots, x_{AB}^{S_1}\}$ $x_{13} = \{x_{AC}^1, \dots, x_{AC}^{S_1}\}$ $= \{x_{AB}^{S_1+1}, \dots, x_{AB}^{S_2}\}$ $x_{14} = \{x_{AB}^{S_1+1}, \dots, x_{AB}^{S_2}\}$ $x_{15} = \{x_{AC}^{S_2+1}, \dots, x_{AC}^{M}\}$	5
$\lambda^1 \le \{\lambda^1, \dots, \lambda^{S_1}\} < \frac{11}{9}\lambda^1$ $\frac{50}{27}\lambda^1 < \{\lambda^{S_1+1}, \dots, \lambda^{S_2}\} < \frac{550}{243}\lambda^1$ $\frac{550}{243}\left(\frac{11}{9}\right)\lambda^1 < \{\lambda^{S_2+1}, \dots, \lambda^M\} < \frac{550}{243}\left(\frac{11}{9}\right)^2\lambda^1$	$x_{12} = \{x_{AB}^1, \dots, x_{AB}^{S_1}\}$ $x_{13} = \{x_{AC}^1, \dots, x_{AC}^{S_1}\}$ $= \{x_{AB}^{S_1+1}, \dots, x_{AB}^{S_2}\}$ $x_{14} = \{x_{AB}^{S_1+1}, \dots, x_{AB}^{S_2}\}$ $x_{15} = \{x_{AC}^{S_2+1}, \dots, x_{AC}^{M}\}$	5
$\lambda^1 \le \{\lambda^1, \dots, \lambda^{S_1}\} < \frac{11}{9}\lambda^1$ $\frac{50}{27}\lambda^1 < \{\lambda^{S_1+1}, \dots, \lambda^{S_2}\} < \frac{550}{243}\lambda^1$ $\frac{550}{243}\left(\frac{11}{9}\right)^2\lambda^1 < \{\lambda^{S_2+1}, \dots, \lambda^M\} < \frac{550}{243}\left(\frac{18}{11}\right)\lambda^1$	$x_{12} = \{x_{AB}^1, \dots, x_{AB}^{S_1}\}$ $x_{13} = \{x_{AC}^1, \dots, x_{AC}^{S_1}\}$ $= \{x_{AB}^{S_1+1}, \dots, x_{AB}^{S_2}\}$ $x_{14} = \{x_{AB}^{S_1+1}, \dots, x_{AB}^{S_2}\}$ $x_{15} = \{x_{AC}^{S_2+1}, \dots, x_{AC}^{M}\}$	5

The wavelengths in Case IV fall into four subgroups $SG(1)$, $SG(2)$, $SG(3)$, and, $SG(4)$. In this case, at least six and up to ten wave probes are required, and one of the cases in presented in Table 17, below.

Table 17. Cases and required number of probes – Case IV.

$\{\lambda^1, \dots, \lambda^M\}$	Probe Position	P
$\lambda^1 \le \{\lambda^1, \dots, \lambda^{S_1}\} < \frac{11}{9}\lambda^1$ $\frac{11}{9}\lambda^1 < \{\lambda^{S_1+1}, \dots, \lambda^{S_2}\} < \left(\frac{11}{9}\right)^2 \lambda^1$ $\frac{50}{27}\lambda^1 < \{\lambda^{S_2+1}, \dots, \lambda^{S_3}\} < 2\lambda^1$ $\frac{550}{243}\lambda^1 \le \{\lambda^{S_3+1}, \dots, \lambda^M\} < \frac{550}{243}\left(\frac{11}{9}\right)\lambda^1$	$x_{12} = \{x_{AB}^1, \dots, x_{AB}^{S_1}\}$ $x_{13} = \{x_{AB}^{S_1+1}, \dots, x_{AB}^{S_2}\}$ $x_{14} = \{x_{AB}^{S_2+1}, \dots, x_{AB}^{S_3}\}$ $x_{15} = \{x_{AC}^1, \dots, x_{AC}^{S_3}\}$ $= \{x_{AB}^{S_3+1}, \dots, x_{AB}^M\}$ $x_{16} = \{x_{AC}^{S_3+1}, \dots, x_{AC}^M\}$	6

The wavelengths in Case V fall into the first subgroups of two main groups, such as $SG(1)$ of $MG(1)$ and $SG(1)$ of $MG(2)$ and five wave probes are needed in this scenario. This is presented in Table 18.

Table 18. Cases and required number of probes – Case V.

$\{\lambda^1, \dots, \lambda^M\}$	Probe Position	P
$\lambda^1 \le \{\lambda^1, \dots, \lambda^{M_1}\} < \frac{11}{9}\lambda^1$ $\lambda^{M_1+1} \le \{\lambda^{M_1+1}, \dots, \lambda^M\} < \frac{11}{9}\lambda^{M_1+1}$	$x_{12} = \{x_{AB}^1, \dots, x_{AB}^{M_1}\}$ $x_{13} = \{x_{AC}^1, \dots, x_{AC}^{M_1}\}$ $x_{14} = \{x_{AB}^{M_1+1}, \dots, x_{AB}^M\}$ $x_{15} = \{x_{AC}^{M_1+1}, \dots, x_{AC}^M\}$	5

Software based on the principle stated previously is programed using MATLAB, which is presented in the Appendix. The input file is the wavelengths used in the test that shall be inputted in a format of a linear array such as $[\lambda_1, \lambda_2, \dots \lambda_n]$, and the output files displayed on Command Window, including a table of the wavelengths and their corresponding x_{AB}, x_{AC}, and the

positions of probes A, B, and C denoted as “PA”, “PB”, and “PC”, and a table of the probe distances relative to the first probe denoted as “X1P”. Total probe number and the minimum total distance required from the wavemaker to the toe of probe structure is also displayed. Other variables and output files can be found in Workspace. A sample of input and output is illustrated in Figure 7.

```
Array of Wave Lengths [L1,L2,...,Ln] = [4.33,5.29,6.24,7.18,8.12,9.05]
    Name      L       XAB      XAC      PA     PB     PC
    ____    ____    ____    ____    __    __    __

    "L1"    4.33    0.48    1.13    1     2     4
    "L2"    5.29    0.48    1.13    1     2     4
    "L3"    6.24    0.67    1.13    1     3     4
    "L4"    7.18    0.67    1.13    1     3     4
    "L5"    8.12    1.13    2.11    1     4     5
    "L6"    9.05    1.13    2.11    1     4     5

    Name      X1P
    _____    ____

    "X12"    0.48
    "X13"    0.67
    "X14"    1.13
    "X15"    2.11

Probe Numer = 5
Total Distance = 20.21m
```

Figure 7. Sample of automatic probe arrangement.

Using the wavelength in the breakwater project and computing the number of wave probes required and the corresponding probe positions. The comparison between the probe position used in the breakwater project and the probe positions computed by the software are

stated in the Table 19. The total number or required wave probes is 5 and the total distance between the wavemaker and the toe of breakwater is 20.21 m.

Table 19. Comparison between the probe spaces computed by software and used in project.

λ		x_{AB} [m]			x_{AC} [m]		
[m]		Computed	Project	Diff.	Computed	Project	Diff.
λ_1	4.33	0.48	0.48	0.00	1.13	1.17	0.04
λ_2	5.29	0.48	0.48	0.00	1.13	1.17	0.04
λ_3	6.24	0.67	0.67	0.00	1.13	1.67	0.54
λ_4	7.18	0.67	0.67	0.00	1.13	1.67	0.54
λ_5	8.12	1.13	0.91	0.22	2.11	2.26	0.15
λ_6	9.05	1.13	0.91	0.22	2.11	2.26	0.15

Using the auto probe spacing arrangement software, the total number of wave probes required in the project under the same wave condition are reduced from six to five.

Weighting coefficient

The errors between the measurement and the estimation may be primarily caused by the phase deviations due to the usage of linear dispersion relation, which associate with the relative phase due to the probe spacing between two probes $k(x_p - x_q)$, and a goodness function (Equation 83) proposed by Zelta et al. (1992) quantifies the desirability of the phase difference associated with probe spacing.

$$G(\Delta\varphi_{n,pq}) = \frac{\sin^2 \Delta\varphi_{n,pq}}{1 + (\Delta\varphi_{n,pq}/\pi)^2} \quad 83$$

Where:

$$\Delta\varphi_{n,pq} = \varphi_{n,p} - \varphi_{n,q}$$

$$\varphi_{n,p} = k_n x_p$$

$$\varphi_{n,q} = k_n x_q$$

The goodness function is a function of relative phase change of two probes and the larger value of the goodness functions the better wave gauge spacing. The weighting coefficient for wave probe p is defined as the summation of the goodness function of each probe, which is presented in Equation 84.

$$W_{n,p} = \sum_{q=1}^{P} G\left(\Delta\varphi_{n,pq}\right) \qquad 84$$

Probe spacing criteria for directional wave

The general principle to obtain a directional spectrum of relatively higher resolution is to place as many probes as possible. For estimating directional spectrum using the ELSM method, the gauge pattern used for long-crest wave is also applicable. For directional wave with small spreading angle, a linear array of wave probes is usually used being perpendicular to the main wave direction. When using parameterizing method or maximum likelihood method Wave-gauge array with 4 or more wave gauges are used for waves with larger spreading angles and Penicker and Borgman (1974) and Yu and Liu (2010) presented the directional wave spectrum captured by several types of probe array patterns that are presented in Figure 8, and tabulated in Table 20. Goda (1985) gives the general criteria concluded by Yu and Liu (2010) for probe matrix to capture directional wave spectra using the wave probes capturing surface elevations, such that:

1. The distances and orient of wave instrument-pair shall be identical
2. The Euclidean distances of the instrument-pair vectors shall be homogeneously distributed crossing an extensive range
3. The minimum distance of an instrument-pair shall be smaller than half of the shortest wavelength, and for irregular wave this distance shall be smaller than 0.3 times of peak wavelength.

Table 20. Types of wave probes for capturing directional spectrum.

	Type	Number of Probes	Note
1	Star-shape	4	(Top left, Figure 8)
2	T-shape	5	(Top left, Figure 8)
3	5-probe Plus	5	(Top left, Figure 8)
4	Pentagon	5	(Mid left, Figure 8)
5	SWOC	6	(Mid left, Figure 8)
6	CERC	5	(Mid left, Figure 8)
7	Hexagon	6	(Bottom center, Figure 8)

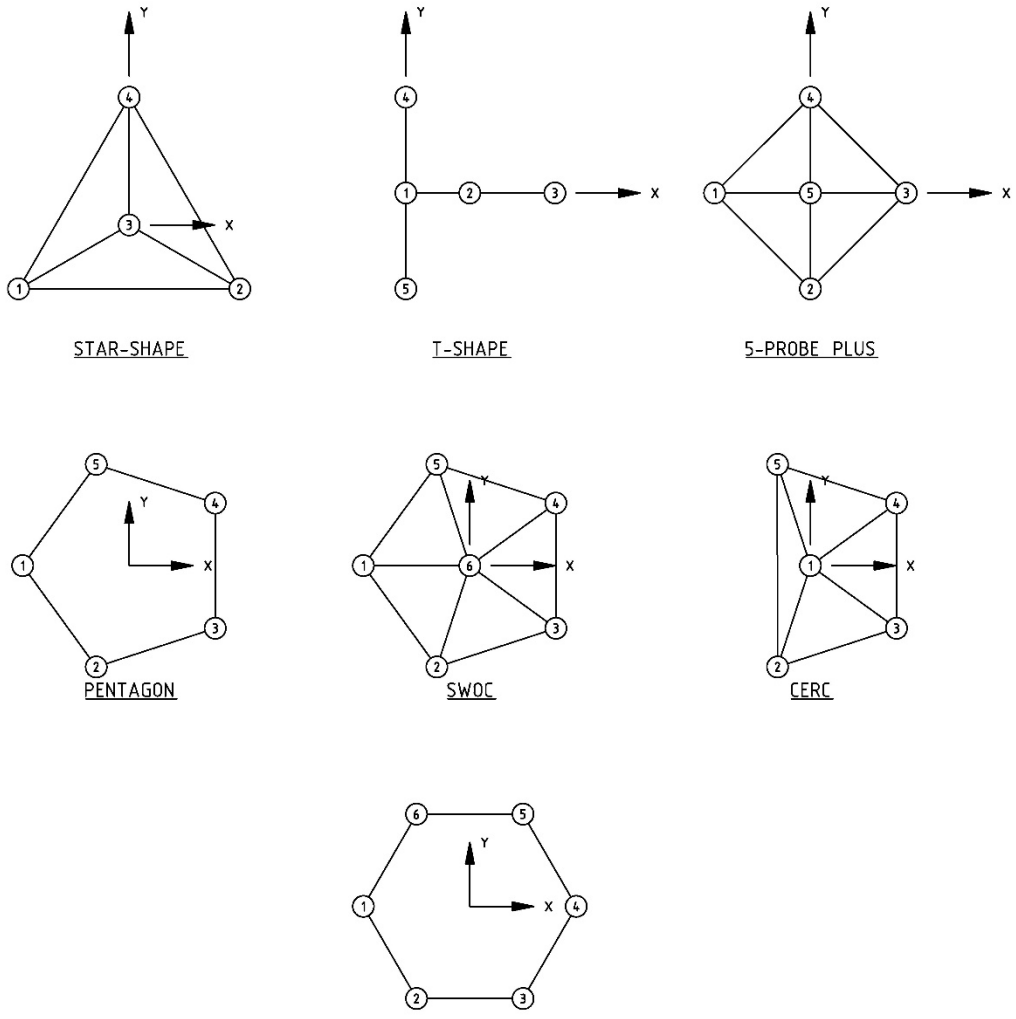

Figure 8. Types of wave probes for capturing directional spectrum.

CHAPTER V

WAVE REFLECTION INFRONT OF RUBBLEMOUNDED BREAKWATERS

Introduction

Validation of least square method used in software REFANA applies reflection analysis on basin test data, since the reflection analysis on this data originally employs a commercial software REFLS (M. D. Miles 1994). Results from REFLS are reliable and are available for validating other customized software using the least squares method. Since the reflection performance of rock beach that is for absorbing wave reflection on the end of model basin is known and consistently low, the spectra captured in front of the rock beach are considered as spectra in open water and are compared with the separated spectra in front of the reflected structures to validate the estimation using the least square method.

Reflection analysis on measurements in Haynes Coastal Engineering Laboratory usually apply REFLS employing least square method that enable users to input wave data and specify cutoff frequencies and data truncation points for auto- and cross- spectra analysis. The reflection analysis using least square method requires the specific probe spacing criteria associated with the wavelengths corresponding to peak frequencies and for a project having more than one wavelengths requires multiple probe-spacing combinations. The probe-spacing combinations that are hand calculated in the breakwater project are compared with the probe-spacing combinations estimated by a software programed by the author to automatically arrange wave probes and to select three of them for a certain peak frequency, which indicates a good agreement.

The measurements come from breakwater tests in the 3D shallow water basin, presented in Figure 9 and Figure 13, with dimensions of 120 ft (36.58 m) in length, 75 ft (22.86 m) in

width, and 4 ft (1.22 m) in depth. The basin is equipped with a wave maker (No. 1 in Figure 9) of 48 piston typed paddles being able to move independently and to generate monochromatic waves, irregular waves with provided spectra, short crested waves, and customized wave input by users. A rock beach with slope of (V:H = 1:6, m = 0.17) is installed for mitigating reflection on the opposite side of wave maker. A motorized bridge (No. 4 in Figure 9) over the basin accommodates computers processing and storing signals from wave gauges and other instruments, details of which are presented in Figure 10.

Capacitance wave gauges made by Reed (2006) are employed for sampling surface elevation, and the varying volts output is recorded and converted automatically using a LabVIEW based software Helios programmed by Yeh (2010), Sonne (2012), and Kim (2013). The conversion from volts to elevation is translated by calibration curves that are linear featuring slope and intercept, and these curves are obtained from calibration procedures employing a motorized calibration stand (No. 5 in Figure 9) designed and programmed by Rosas (2007) and the calibration package of Helios (Sonne 2012). The details of data calibration and acquisition systems, including a computer installed with Helios, a National Instrument DAQ, and a signal amplifier are shown in Figure 10.

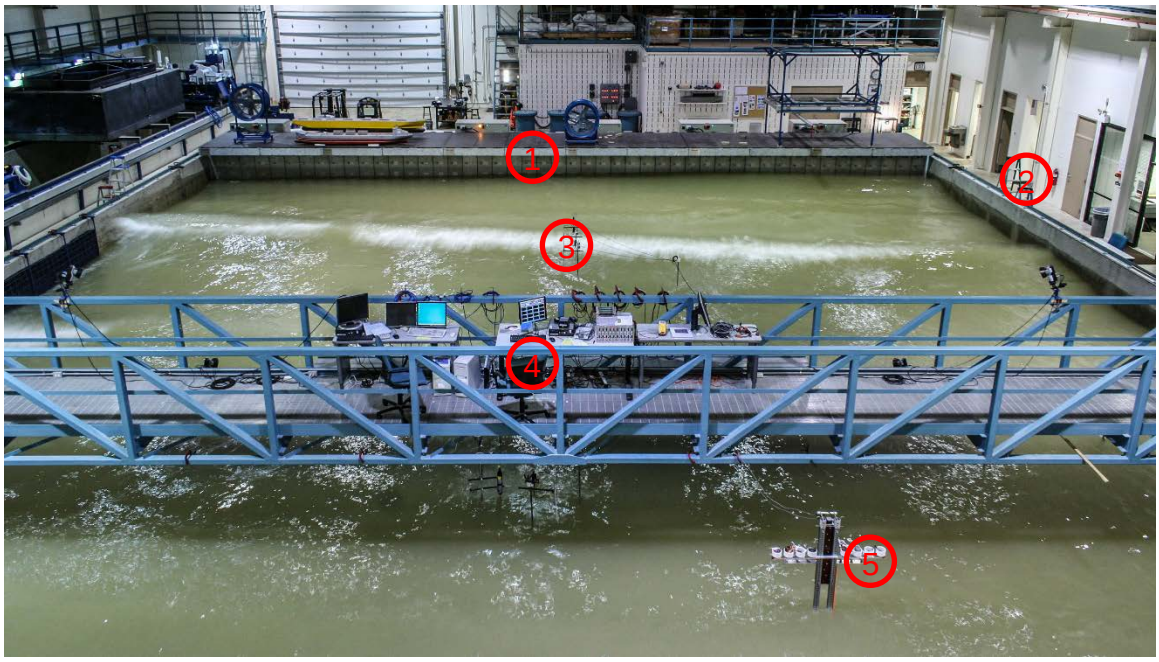

Figure 9. Apparatus for wave generation and data acquisition: (1) wave maker, (2) computer for wave maker, (3) capacitance wave gauge, (4) motorized bridge with data acquisition system, and (5) calibration stand.

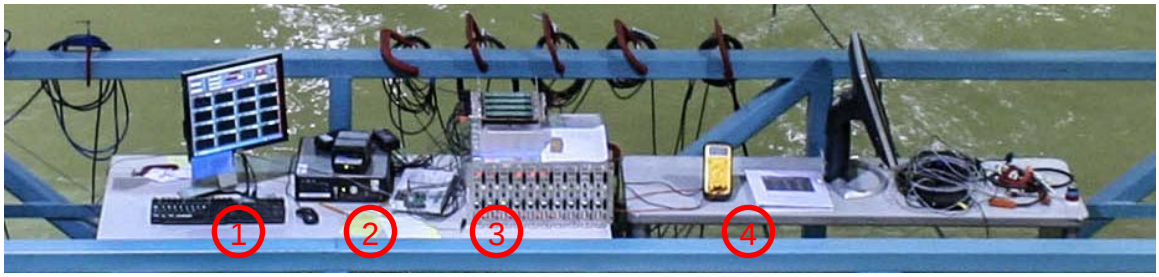

Figure 10. Data acquisition system: (1) computer installed with Helios, (2) National Instrument's DAQ, (3) signal amplifier, and (4) manual for Helios **(Sonne 2012)**.

Test Condition and Setups

One of the projects in Haynes Coastal Engineering Laboratory (Randall, et al. 2016) on rubble mounded breakwaters with both constant-sloped and berm-width types of slope on the head side subjected to wave conditions with wave height of 0.05 m (0.16 ft), wave periods of 2.24 s, 2.68 s, 3.13 s, 3.58 s, 4.02 s, and 4.47 s. and water depth of 0.43 m (1.41 ft). Two

channels were constructed to test two breakwaters simultaneously under the same condition in the wave basin. The layout of the project is represented in Figure 13. The wave conditions and probe positions for reflection analysis are tabulated in Table 21, and each wave condition is repeated for three times for each type of breakwater.

In front of each breakwater, three wave probes were positioned parallel to the orthogonal of the toe of the breakwater and numbered sequentially from the wave maker to the reflected structures were used to record surface elevations simultaneously for reflection analysis, and the criteria of the distance between each pair of probes are discussed in previous chapter. To reduce the labor of moving wave gauges, the distance between the wave maker and the first probe closest to the wave maker was selected to be larger than the longest wavelength in the test at a constant value of 9.73 m (31.92 ft), and the wavelengths λ (sub-script o present deep-water wavelength) are computed using equation derived from linear dispersion relationship. For the probe distance between the probe 1 and probe 2 and between the probe 1 and probe 3, average values are used for wave conditions I and II and for wave conditions III and IV, the larger values are used for wave conditions V and VI. The probe positions are presented in Table 21.

Table 21. Wave conditions and positions for wave gauges.

		Given Condition			Wavelength		Probe Position		
Wave Condition	Test Number	T [s]	h [m]	H_I [m]	λ_o [m]	λ [m]	x_1 [m]	x_{12} [m]	x_{13} [m]
I	1 – 3	2.24	0.43	0.05	7.83	4.33	9.73	0.48	1.17
II	4 – 6	2.68	0.43	0.05	11.21	5.29	9.73	0.48	1.17
III	7 – 9	3.13	0.43	0.05	15.30	6.24	9.73	0.67	1.67
IV	10 – 12	3.58	0.43	0.05	20.01	7.18	9.73	0.67	1.67
V	13 – 15	4.02	0.43	0.05	25.23	8.12	9.73	0.91	2.26
VI	16 – 18	4.47	0.43	0.05	31.20	9.05	9.73	0.91	2.26

The constant-sloped breakwaters have slopes 1:1.5 and 1:2.5 and the berm-width breakwaters have the same slopes of 1:1.5 for both above and below the berm. The average slope presented in Equation 85 and Figure 11 is the slope of connecting line one and half of wave height above and below the plane of berm. The expression of the average slope is identical to that of constant slope when the width of berm equals to zero.

$$\tan\theta = \frac{3H}{B + \frac{1.5H}{\tan\theta_d} \pm \frac{\Delta z}{\tan\theta_d} + \frac{1.5H \mp \Delta z}{\tan\theta_u}} \qquad 85$$

Where: $\tan\theta_d$ and $\tan\theta_u$ are slopes above and below the berm, B is width of berm, and Δz is vertical distance from the plane of berm to still water level (SWL) and Δz has plus or minus signs when the berm is beyond or below the SWL, respectively. Notice that $B = 0$, Δz = 0 and $\theta_d = \theta_u = \theta$ for plain-sloped breakwater. (Shown in Figure 11).

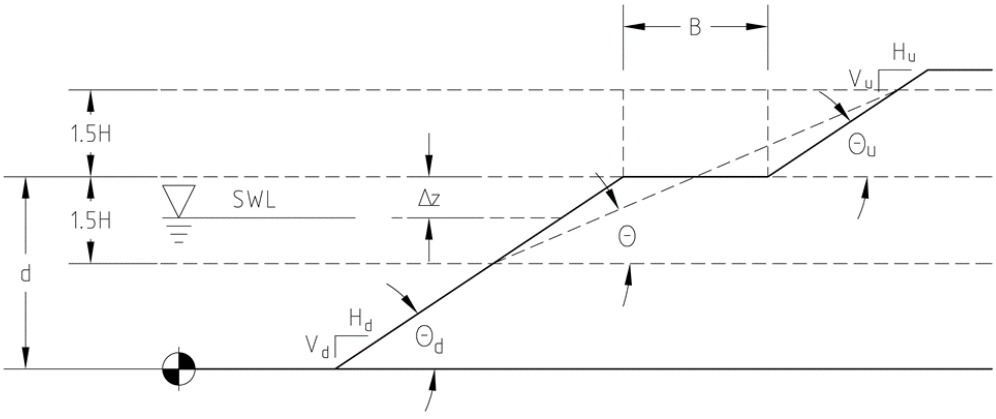

Figure 11. Weighted average slope.

Three rows of cinderblock walls were constructed to form two channels, i.e. North Channel (Channel N) and South Channel (Channel S). The breakwaters having the crest heights (the vertical distance between the crest and the toe of a breakwater) of 0.70 m (2.30 ft) and 0.60 m (1.97 ft) were constructed in the North and the South channels, respectively. The information on the material is tabulated in Table 22 and a cross-section view of the breakwaters in the first scenario (Slope 1) is presented in Figure 12. The breakwater in North Channel was composed by a core covered by an armor layer, and a layer of filter between the core and the armor. The materials for core, filter cloth, and armor were granule/fine pebble, coarse pebble, and very coarse pebble, respectively, and their medium diameters D_{50} varied between 2 mm (0.08 in) and 10 mm (0.39 in), between 20 mm (0.79 in) and 24 mm (0.94 in), and between 44 mm (1.73 in) and 52 mm (2.05 in), respectively. The breakwater in South Channel was composed by a core made of fine/medium pebble having D_{50} varying between 4 mm (0.16 in) and 20 mm (0.79 in), and the core was covered by the armor layer made of medium/coarse pebble having D_{50} varying between 14 mm (0.55 in) and 29 mm (1.14 in). Geotextile filter fabric was applied between the adjacent layers.

Table 22. Material information.

Material Information D_{50} – North Channel						
	Core		Filter		Armor	
	[mm]	[in]	[mm]	[in]	[mm]	[in]
Min	2	0.08	20	0.79	44	1.73
Max	10	0.39	24	0.94	52	2.05
Type	Pebble (Granule/Fine)		Pebble (Coarse)		Pebble (Very Coarse)	
Material Information D_{50} – South Channel						
	Core		Filter		Armor	
	[mm]	[in]	[mm]	[in]	[mm]	[in]
Min	4	0.16	-	-	14	0.55
Max	20	0.79	-	-	29	1.14
Type	Pebble (Fine/Medium)		-		Pebble (Medium/Coarse)	

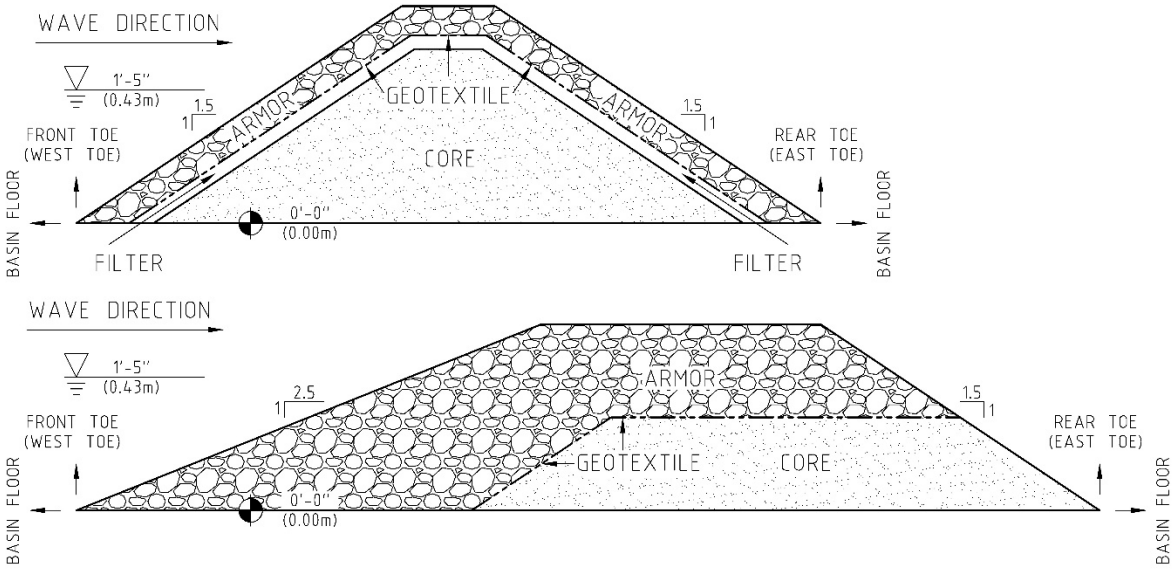

Figure 12. Cross-section illustrating materials of breakwaters in North Channel (top) and in South Channel (bottom) in Slope 1

Three scenarios named as Slope 1, Slope 2, and Slope 3 were involved for both channels. The characteristics of breakwaters are parameterized and tabulated in Table 23. Notice that the crest height C_H in the table is the elevation of breakwater crest relative to the seabed at West toe, and subtraction of still water level may be necessary when calculating overtopping. The cross-section and the corresponding parameters of the breakwaters for these scenarios are presented in Figure 15, Figure 16, and Figure 17.

Table 23. Parameters of breakwater.

Parameters			South Channel			North Channel		
			Slope 1	Slope 2	Slope 3	Slope 1	Slope 2	Slope 3
Slope	m	[-]	0.40	0.67	0.13	0.67	0.38	0.27
Berm Width	B	[m]	0.00	0.00	0.90	0.00	0.17	0.34
Crest Width	C_W	[m]	0.90	1.50	0.61	0.30	0.30	0.30
Crest Height	C_H	[m]	0.60	0.60	0.6	0.70	0.70	0.70

For Slope 1 (Figure 15), both of the breakwaters are plane-sloped, and the slopes of the breakwaters in the North and South Channels are 0.40 ($H:V$ = 1:1.5) and 0.67 ($H:V$ = 1:2.5), respectively. For Slope 2 (Figure 16), additional armor materials were added for the breakwaters in both channels, which forms a berm-width breakwater with berm width of 0.17 m (0.56 ft) in North Channel and forms a plane-slope breakwater in South Channel. The up-slope and the down-slope of the breakwater in North Channel are both 0.67 ($H:V$ = 1:1.5), which composite the average slope of 0.38. The slope for the plane-sloped breakwater in South Channel in Slope 2 is 0.40 ($H:V$ = 1:1.5). For Slope 3 (Figure 17), the breakwaters in both channels are berm-width breakwaters. Additional materials used for armor were added to the breakwater in North Channel with a wider berm doubled the width, i.e. 0.34 m (1.12 ft), than that of previous scenario in North

Channel. In South Channel, materials were removed to constitute a berm-width breakwater having the berm width of 0.90m (2.95 ft). The average slopes for breakwaters of Slope 3 in the North and South Channels are 0.27 and 0.13, respectively, and their up-slopes and down-slopes are both 0.67 ($H:V$ = 1:2.5). These breakwaters are constructed and tested in the dual channels built in wave basin, and their layouts in the basin are presented in Figure 13.

Froude Similarity (Equation 86) was applied such that the temporal scale is the square root of geometrical scale, and the geometrical scale and temporal scale are 1:20 and 1:4.47 (model versus prototype), respectively.

$$\frac{V_m}{\sqrt{g_m L_m}} = \frac{V_p}{\sqrt{g_p L_p}} \xrightarrow{yields} \frac{V_m}{V_p} = \frac{\sqrt{L_m}}{\sqrt{L_p}} \qquad 86$$

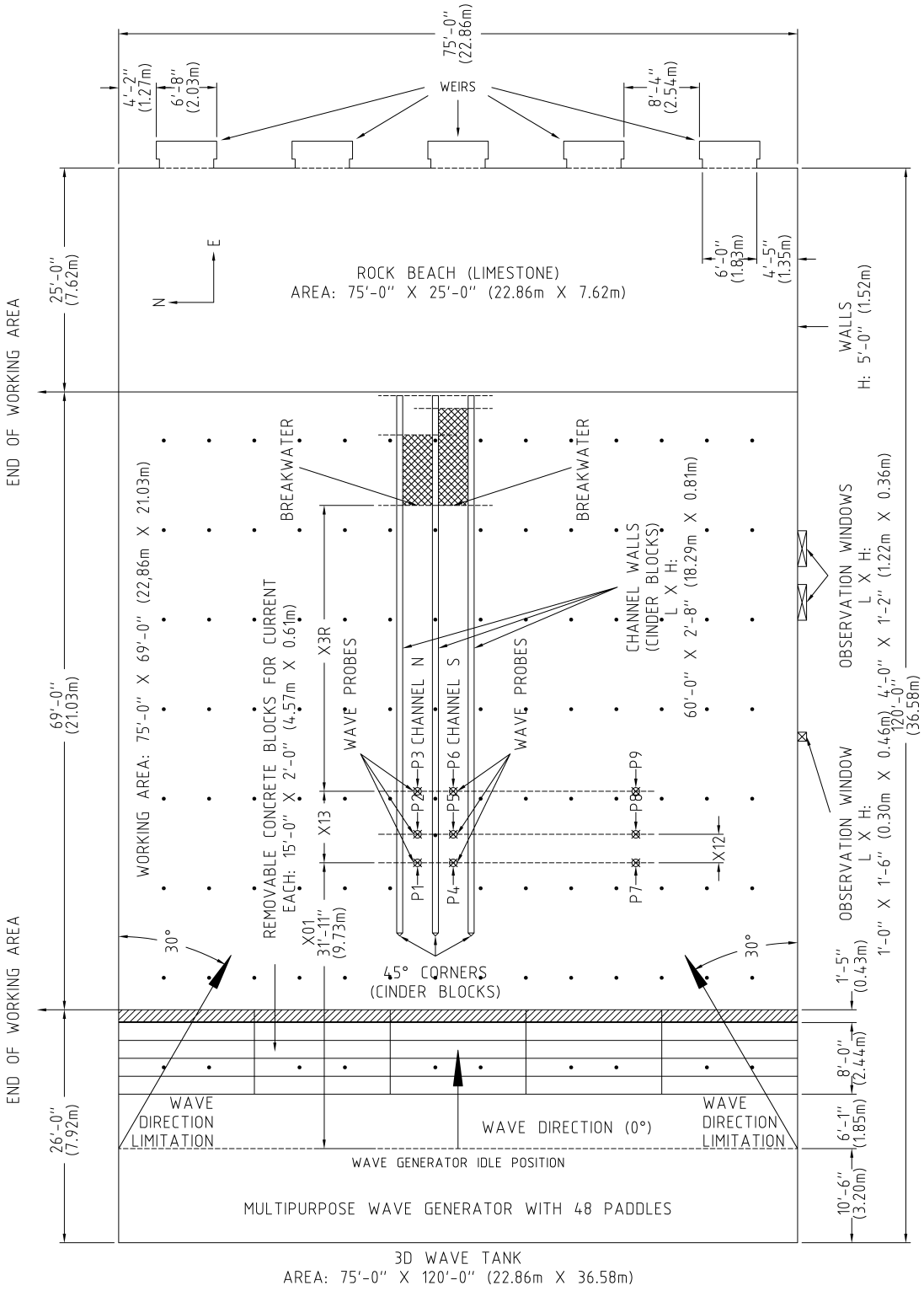

Figure 13. Layout of wave basin and dual breakwater channels.

Software for Reflection Analysis Using Least Square Method

REFLS that is a software package of GEDAP, and REFANA that is a software package programmed using MATLAB by the author are employed for reflection analysis. Both software packages use least squares technique. The results computed by both software are compared to each other and are compared to the reflection coefficients in front of rock beach that is considered as open water causing the minimum reflections to further validate the method for separating the incident and reflected waves. REFANA also has the function for automating the arrangement and selection of wave probes according to the wave conditions for reflection analysis. The probe positions and the selections for reflection computed by REFANA are compared with the wave probe arrangement used in the breakwater project. The reflection coefficients computed by both software are presented in Table 24, Table 25, and Table 26.

REFLS software for reflection analysis

GEDAP proposed by the National Research Council of Canada is a general software system for managing and analyzing laboratory data (Miles and Funke, 1989), which is employed in Haynes Coastal Laboratory for generating waves and reflection analysis. Regular wave signals are synthesized by specifying wave height, wave period, and propagation angle. Irregular wave signals could be generated either by input time series of surface elevations or using PARSPEC or input spectra based on measured data for spectra and then applying RWSYN converting spectra to time series. The time series of surface elevations are then converted to mechanical drive signals for each of the paddles of wave maker using DWREP2. After obtaining surface elevations, the user could use software packages including REFLA, REFLM, and REFLS for refection analysis. The first and the third software are for irregular waves, and the second software is for regular waves.

Besides user input of time series of irregular waves, user could also use PARSPEC, which provides nine expressions of spectra consisting of Pierson-Moskowitz, JONSWAP, Bretschneider, Ochi Double Peak, Scott, TMA Shallow Water, Neumann, Mitsuyasu-Bretschneider (1971), and Mitsuyasu (1972). Depth, significant wave height, and peak frequency are specified for spectra generation. The user can also input spectra from measured data.

RWSYN is then used for synthesizing time series from spectra employing one of the three methods, such as random phase (RP) method, random Fourier coefficient (RFC) method, and RFC method with matched variance. The RP method chooses random phases but determined amplitudes according to spectra for Fourier components. The RFC method has random Fourier coefficients according to Gaussian distribution and the corresponding wave records having variance differ constantly. The third method is a modification of the second method with random variance of each wave records, which, however, would equal to the variance of target spectrum by multiplying a scaling factor. The corresponding algorithms are presented extensively by Funke and Mansard (1984) and Miles (1989).

All of the reflection software provided by GEDAP are based on the least square method presented by Mansard and Funke (1980) according to measurements of surface elevation from three probes spaced at a specified distance parallel to the propagation direction and probe distances are necessary inputs. REFLM is for regular waves without spectra analysis and the truncated time series for analysis should be integer multiples of the wave period, this method offers incident and reflect wave heights and averaged reflection coefficient from measurements of surface elevation. REFLA and REFLS are for reflection analysis for irregular waves. The former method requires inputs of phase lags of cross-spectra between the probe closest to wave maker and other probes using XSPEC2 based on Welch method (Welch et al. 1967) and gives

output of incident wave height and spectrum, peak period, and coherency factor. The latter method uses fast Fourier transform (FFT) for spectra analysis to convert input of wave elevation measurements from three probes to output of averaged reflection coefficient.

Input of REFLS and the other GEDAP software packages applies a batch mode command processor, i.e. GBAT, for the version used in Haynes Coastal Engineering Laboratory, the input file examples can be found in the user guide (M. D. Miles 1994).

REFANA software for reflection analysis

A software, REFANA, programmed using MATLAB employing the least square method is developed for reflection analysis on both two-dimensional regular and irregular waves. This software consists of packages of autospec.m for computing auto-spectrum, crossspec.m for computing spectrum, wave_itr.m for wave length iteration, and ref_ana_leastsquare.m for loading wave file and displaying results of reflection analysis. The packages for computing auto- and cross-spectra employ FFT command in MATLANB. The last package requires inputs of auto- and cross-spectra and wave length from the previous packages, and test information, such as probe distances, water depth, and wave period, loaded from file testinfo.m. Computing of auto- and cross-spectra are based on fast Fourier transform (FFT) function provided by MATLAB.

A sample of the results for the reflection analysis is displayed Figure 14. Results include auto spectral densities for measurements from all the three probes (upper panel of Figure 14), spectral densities of incident and reflect waves, and spectrum of reflection coefficient (lower panel of Figure 14). Significant wave heights of measured surface elevations, incident waves and reflect waves, averaged reflection coefficient are displayed in the legends of spectra plots.

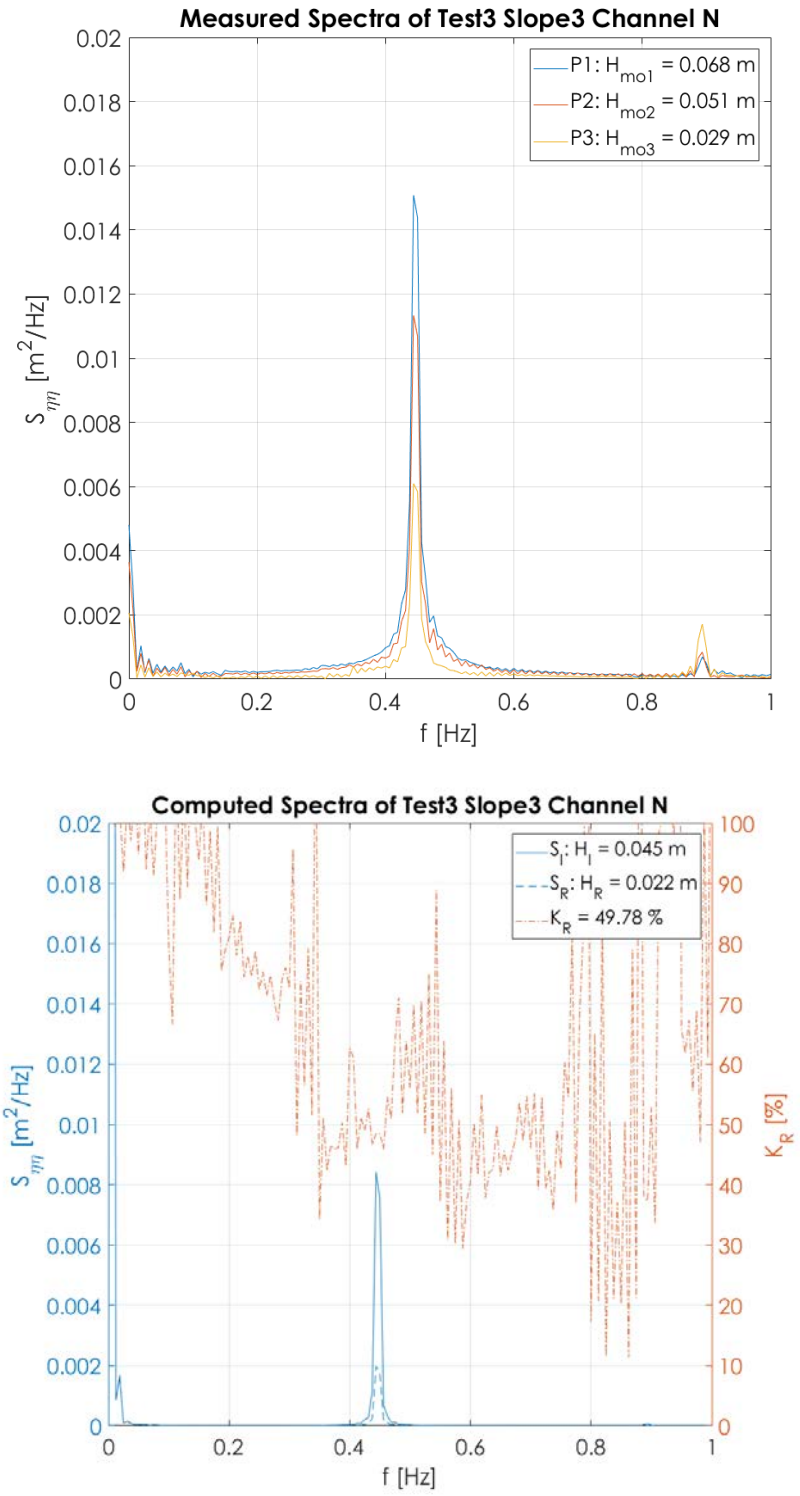

Figure 14. Sample of reflection analysis – measured spectra (top), the spectra of incident wave, reflected wave, and the spectrum of reflection coefficients (bottom).

Figure 14 (top) presents spectra of measured signal from the three wave probes, Figure 14 (bottom) presents spectra of incident and reflect waves and the reflection coefficients that are ratio of reflect over incident wave spectra. The bulk reflection coefficient is 49.84%.

Software comparisons between REFLS and REFANA

Results from this MATLAB-based software are compared with results obtained from GEDAP's REFLM and REFLS. The sampling of surface elevation has a duration of 120 s, and a sampling rate of 25 Hz. Truncation points of time series for reflection analysis are 40 s and 120s. The results are tabulated in Table 24, Table 25, and Table 26, and the corresponding breakwater scenarios for the results are presented in Figure 15, Figure 16, and Figure 17, respectively. The standard deviations of these reflection coefficients under the same test conditions are tabulated in Table 27. The significant wave heights are also computed and compared with input wave heights, which are tabulated in Table 28 and presented in Figure 19.

Table 24. Comparison of reflection coefficients (Slope 1).

Test	North Channel		South Channel		Open Water	
	REFLS	K_R	REFLS	K_R	REFLS	K_R
1	55.00%	55.43%	27.40%	29.90%	17.50%	19.70%
2	55.10%	55.28%	27.50%	30.08%	18.20%	20.15%
3	54.80%	55.03%	27.70%	30.03%	17.80%	19.85%
4	63.20%	64.16%	36.40%	36.79%	8.68%	13.18%
5	63.10%	64.23%	36.50%	36.85%	8.03%	12.85%
6	62.90%	64.26%	36.70%	36.79%	8.45%	13.58%
7	76.70%	78.54%	46.80%	46.72%	14.50%	18.44%
8	76.40%	78.19%	46.60%	46.54%	13.20%	17.84%
9	76.50%	78.37%	46.70%	46.76%	12.20%	16.22%
10	60.60%	61.07%	43.70%	46.17%	7.97%	12.20%
11	60.60%	61.16%	43.60%	46.22%	8.05%	13.28%
12	61.00%	61.41%	44.30%	45.29%	8.81%	12.44%
13	72.20%	71.64%	58.90%	60.41%	25.50%	28.09%
14	70.80%	71.82%	59.30%	60.00%	24.30%	27.29%
15	70.70%	72.00%	59.60%	60.11%	24.10%	27.38%
16	69.80%	70.72%	56.60%	56.18%	13.10%	18.62%
17	69.70%	70.45%	56.10%	56.32%	13.60%	18.71%
18	69.20%	69.52%	56.10%	55.51%	12.00%	19.47%

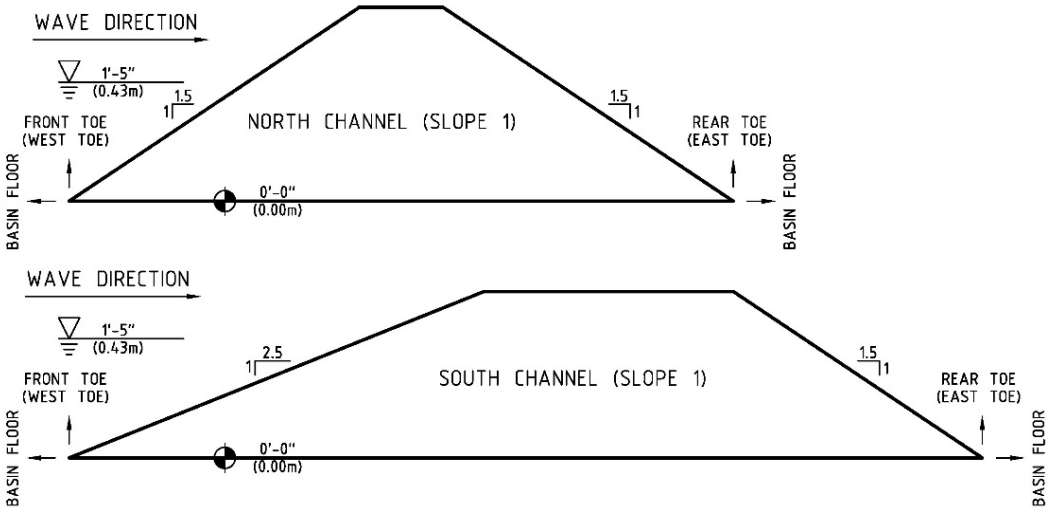

Figure 15. Breakwaters in North Channel (top) and in South Channel in Slope 1

Table 25. Comparison of reflection coefficients (Slope 2).

Test	North Channel		South Channel		Open Water	
	REFLS	K_R	REFLS	K_R	REFLS	K_R
1	29.00%	31.36%	45.10%	46.33%	19.40%	21.99%
2	29.40%	31.75%	44.90%	46.01%	19.00%	20.72%
3	29.20%	31.95%	45.20%	46.17%	18.90%	20.90%
4	45.60%	46.89%	52.60%	53.52%	7.32%	13.00%
5	45.50%	45.89%	52.70%	53.20%	7.41%	10.29%
6	45.40%	46.92%	52.50%	53.68%	7.64%	13.16%
7	60.70%	60.92%	63.50%	64.58%	13.20%	15.47%
8	60.80%	60.21%	63.60%	63.63%	11.30%	13.47%
9	60.90%	61.24%	63.70%	64.80%	11.40%	14.80%
10	52.30%	53.73%	55.10%	55.41%	7.79%	11.47%
11	52.00%	52.65%	55.00%	55.27%	7.62%	11.05%
12	51.90%	53.52%	55.00%	55.90%	7.64%	12.83%
13	61.30%	63.30%	56.80%	58.40%	27.50%	30.55%
14	61.30%	63.95%	56.50%	58.77%	28.30%	32.35%
15	62.00%	63.51%	57.00%	58.62%	28.50%	31.25%
16	66.10%	65.93%	62.30%	62.70%	14.90%	18.88%
17	66.10%	65.74%	62.10%	62.28%	15.00%	20.28%
18	66.00%	66.13%	62.10%	62.64%	14.90%	19.30%

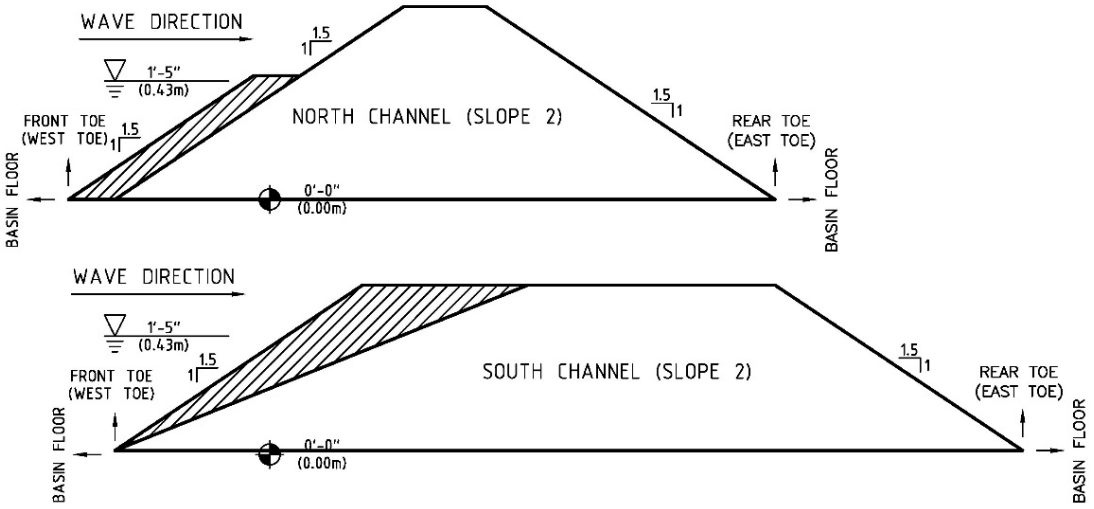

Figure 16. Breakwaters in North Channel (top) and in South Channel in Slope 2

Table 26. Comparison of reflection coefficients (Slope 3).

Test	North Channel		South Channel		Open Water	
	REFLS	K_R	REFLS	K_R	REFLS	K_R
1	48.00%	49.84%	33.60%	35.20%	13.40%	16.54%
2	47.80%	49.41%	33.60%	35.25%	13.80%	17.31%
3	48.00%	49.78%	33.80%	35.40%	12.80%	16.74%
4	53.50%	55.48%	41.10%	41.83%	13.30%	15.06%
5	53.40%	54.86%	40.80%	41.56%	14.00%	15.85%
6	53.70%	55.31%	40.80%	41.45%	14.30%	15.10%
7	64.30%	64.44%	53.70%	54.20%	10.30%	12.81%
8	64.40%	65.40%	54.10%	55.06%	10.30%	14.17%
9	64.60%	65.53%	53.90%	54.68%	10.30%	14.40%
10	57.10%	57.41%	38.90%	39.95%	8.46%	12.71%
11	56.40%	56.78%	38.70%	39.65%	8.56%	12.28%
12	55.80%	56.40%	39.10%	39.78%	8.27%	11.75%
13	63.70%	66.37%	52.00%	52.97%	24.30%	27.15%
14	63.00%	65.97%	51.60%	53.93%	24.10%	35.56%
15	63.00%	65.82%	52.20%	53.99%	23.70%	32.29%
16	66.10%	66.25%	52.90%	53.71%	16.60%	21.19%
17	65.00%	65.63%	52.60%	53.33%	16.60%	20.15%
18	65.00%	65.64%	52.10%	52.22%	16.80%	20.60%

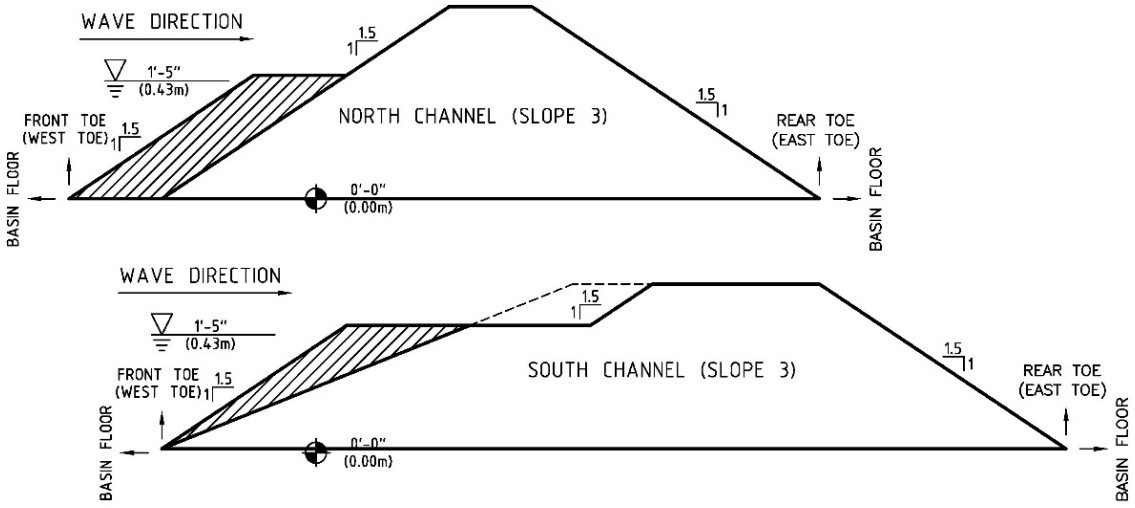

Figure 17. Breakwaters in North Channel (top) and in South Channel in Slope 3

Both computed reflection coefficients have good consistency under the same wave and reflected-object condition with averaged standard deviation under 0.60% and increased proportionally surf similarity parameter ξ (Equation 43), and most of the relatively large values (> 0.40%) occur when $8 < \xi < 12$ (Figure 18, presenting Table 27 graphically in terms of surf similarity parameter). Results computed between these two software reach agreements favorably with average difference of 2.18% and 2.29% for the North and South Channels, respectively, and differences between two sets of results also indicate consistency with standard deviations under 2.2%. For Open Water condition, with much milder sloped rock beach, both software return relatively lower reflection coefficients, and both software present good consistency under the same test condition. Reflection coefficients computed by REFANA are slightly larger on the average than results from REFLS. Tests are repeatable and the average of reflection coefficient for every three repeated tests can present the reflection performance of each scenario.

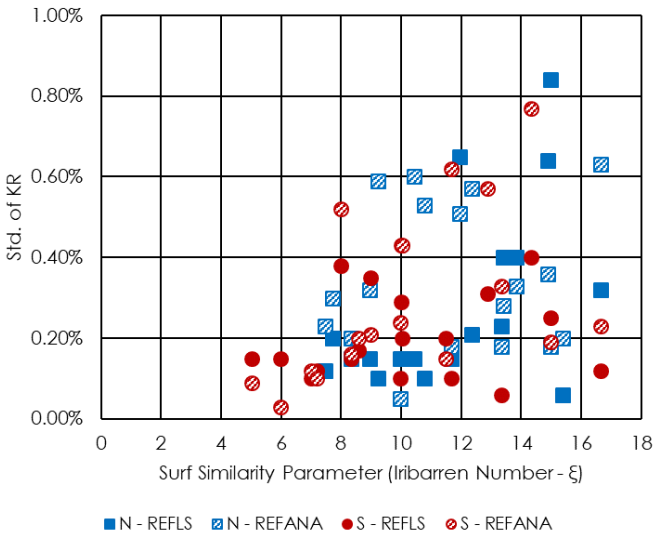

Figure 18. Standard deviation of reflection coefficients versus surf similarity parameter

Table 27. Standard deviation of reflection coefficients.

Scenario	Test	REFLS			REFANA		
		N	S	O	N	S	O
Slope 1	1-3	0.15%	0.15%	0.35%	0.20%	0.09%	0.23%
	4-6	0.15%	0.15%	0.33%	0.05%	0.03%	0.37%
	7-9	0.15%	0.10%	1.15%	0.18%	0.12%	1.15%
	10-12	0.23%	0.38%	0.46%	0.18%	0.52%	0.57%
	13-15	0.84%	0.35%	0.76%	0.18%	0.21%	0.44%
	16-18	0.32%	0.29%	0.82%	0.63%	0.43%	0.47%
Slope 2	1-3	0.20%	0.15%	0.26%	0.30%	0.16%	0.69%
	4-6	0.10%	0.10%	0.17%	0.59%	0.24%	1.61%
	7-9	0.10%	0.10%	1.07%	0.53%	0.62%	1.02%
	10-12	0.21%	0.06%	0.09%	0.57%	0.33%	0.93%
	13-15	0.40%	0.25%	0.53%	0.33%	0.19%	0.91%
	16-18	0.06%	0.12%	0.06%	0.20%	0.23%	0.72%
Slope 3	1-3	0.12%	0.12%	0.50%	0.23%	0.10%	0.40%
	4-6	0.15%	0.17%	0.51%	0.32%	0.20%	0.45%
	7-9	0.15%	0.20%	0.00%	0.60%	0.43%	0.86%
	10-12	0.65%	0.20%	0.15%	0.51%	0.15%	0.48%
	13-15	0.40%	0.31%	0.31%	0.28%	0.57%	4.24%
	16-18	0.64%	0.40%	0.12%	0.36%	0.77%	0.52%
	Ave.	0.28%	0.20%	0.42%	0.35%	0.30%	0.89%

The comparisons between computed incident wave height and input wave height agree well with averaged computed wave heights of 0.053 m, 0.050 m, and 0.045 m in North Channel, South Channel, and Open Water, respectively. The corresponding standard deviations are 0.013 m, 0.009 m and 0.007 m. Accordingly, the estimated incident wave height is ±1cm around the input incident wave height (0.80%~1.20% of the input incident wave height). The comparisons between the computed wave heights and the input wave height are presented in Figure 19 and are tabulated in Table 28.

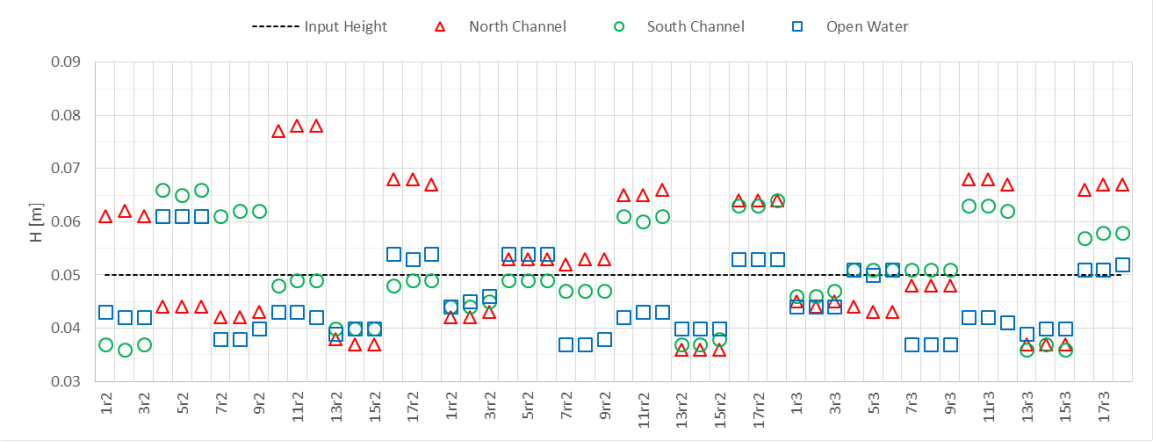

Figure 19. Comparison of computed and input wave heights.

Table 28. Comparison of computed and input wave heights.

Test	Input	Slope 1 (r2)			Slope 2 (rr2)			Slope 3 (r3)		
	H	$(H)_n$	$(H)_s$	$(H)_o$	$(H)_n$	$(H)_s$	$(H)_o$	$(H)_n$	$(H)_s$	$(H)_o$
	[m]	[m]	[m]	[m]	[m]	[m]	[m]	[m]	[m]	[m]
1	0.05	0.061	0.037	0.043	0.042	0.044	0.044	0.045	0.046	0.044
2	0.05	0.062	0.036	0.042	0.042	0.044	0.045	0.044	0.046	0.044
3	0.05	0.061	0.037	0.042	0.043	0.045	0.046	0.045	0.047	0.044
4	0.05	0.044	0.066	0.061	0.053	0.049	0.054	0.044	0.051	0.051
5	0.05	0.044	0.065	0.061	0.053	0.049	0.054	0.043	0.051	0.050
6	0.05	0.044	0.066	0.061	0.053	0.049	0.054	0.043	0.051	0.051
7	0.05	0.042	0.061	0.038	0.052	0.047	0.037	0.048	0.051	0.037
8	0.05	0.042	0.062	0.038	0.053	0.047	0.037	0.048	0.051	0.037
9	0.05	0.043	0.062	0.040	0.053	0.047	0.038	0.048	0.051	0.037
10	0.05	0.077	0.048	0.043	0.065	0.061	0.042	0.068	0.063	0.042
11	0.05	0.078	0.049	0.043	0.065	0.060	0.043	0.068	0.063	0.042
12	0.05	0.078	0.049	0.042	0.066	0.061	0.043	0.067	0.062	0.041
13	0.05	0.038	0.040	0.039	0.036	0.037	0.040	0.037	0.036	0.039
14	0.05	0.037	0.040	0.040	0.036	0.037	0.040	0.037	0.037	0.040
15	0.05	0.037	0.040	0.040	0.036	0.038	0.040	0.037	0.036	0.040
16	0.05	0.068	0.048	0.054	0.064	0.063	0.053	0.066	0.057	0.051
17	0.05	0.068	0.049	0.053	0.064	0.063	0.053	0.067	0.058	0.051
18	0.05	0.067	0.049	0.054	0.064	0.064	0.053	0.067	0.058	0.052
Ave. North:		0.053		Ave. South:		0.050		Ave. Open:		0.045
Std. North:		0.013		Std. South:		0.009		Std. Open:		0.007

Effect of Breakwater Parameters

The effects of breakwater parameters are investigated by varying one parameter while fixing other parameters to evaluate the performance of a breakwater in reducing the reflection in front of itself corresponding to the variation of the parameter and further to obtain the ideal geometric shape of the breakwater that minimizes the reflection, which include the effects of slope change, crest height change, and berm width change. These effects corresponding to the parameter change are plotted on a graph (Figure 20, Figure 21, and Figure 22) of reflection coefficient versus wave period, and the general trend is that reflection coefficients increase proportionally with the wave period and reach maximum at period of 3.13 s, experience a drop at 4.02 s, and then increase again.

Effect of slope change (Figure 20) is investigated by varying the slope and fixing the other parameters, and reflection coefficients for Slope 1 and Slope 2 in South Channel are selected for investigation. It indicates that reflection can be reduced by 10% to 20% using milder slope, and the difference in the reflection coefficient reduction tends to be smaller for the larger wave periods and reaches a minimum at 4.02 s.

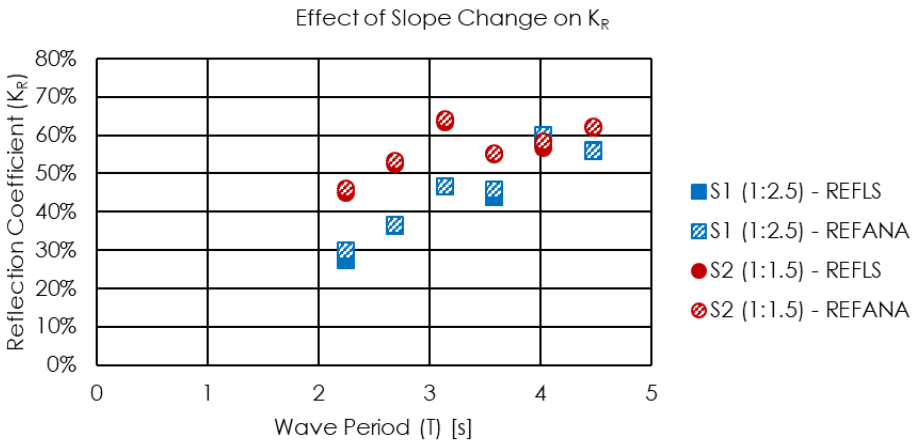

Figure 20. Effect of slope change.

Effect of crest height change (Figure 21) is investigated by varying crest height and fixing other parameters, and reflection coefficients for Slope 2 in South Channel and for Slope 1 in North Channel are selected for investigation. It indicates that reflection can be reduced by 10% to 15% using lower crest height, however investigation on overtopping are needed since the lower crest height may cause more overtopping.

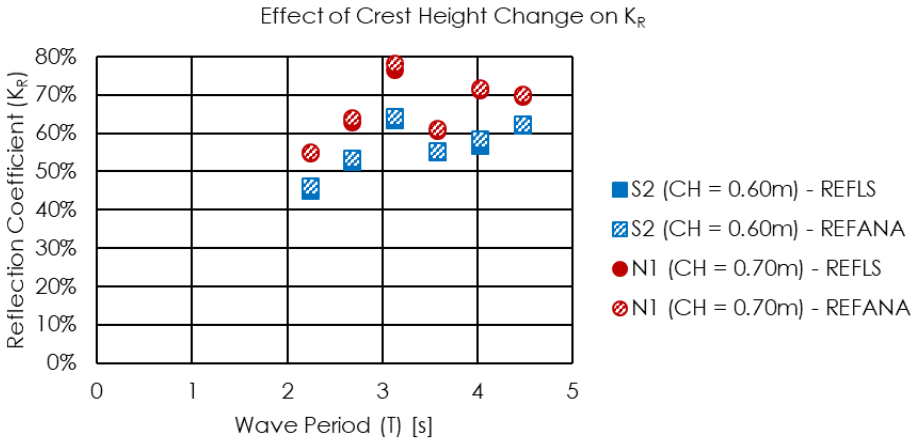

Figure 21. Effect of crest height change.

The effect of berm width change is investigated by varying width of berm and fixing other parameters, and reflection coefficients for Slope 2 in and Slope 3 in South Channel are selected for investigating the effect of existence of berm to the reflection, reflection coefficients for Slope 1, 2, and 3 in North Channel are also selected for investigating the effect of increasing berm width to reduction of reflection coefficients. The existence of berm (Figure 22 and Figure 23) significantly reduces reflection coefficient by 10% to 30%, however the increase in the width of berm may cause higher reflection than a narrower berm (Figure 23).

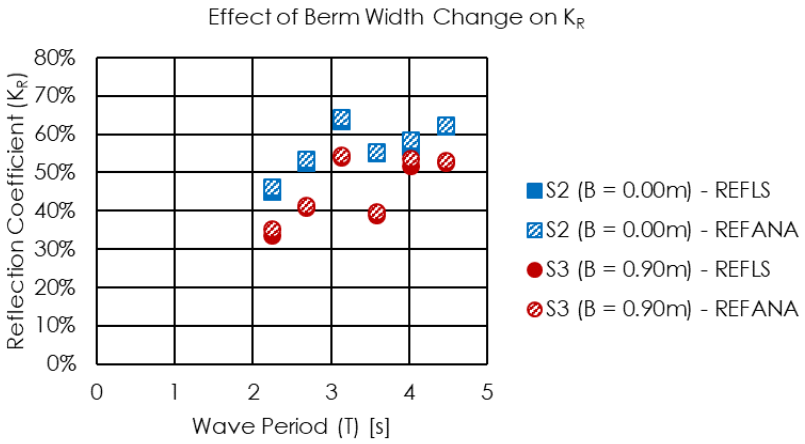

Figure 22. Effect of berm width change – South Channel.

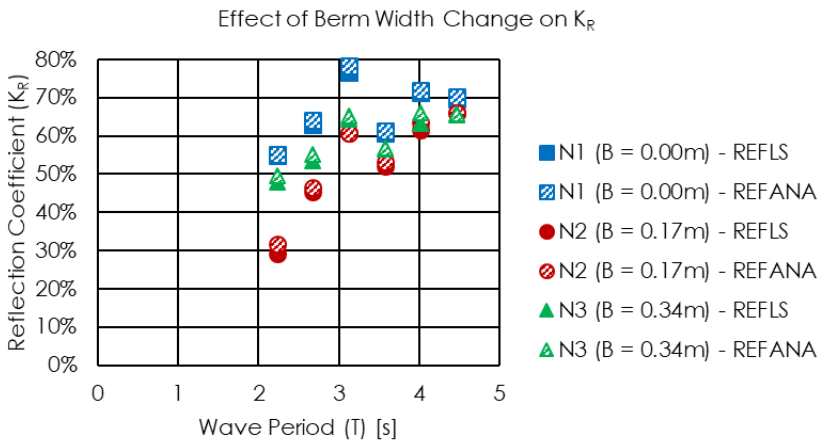

Figure 23. Effect of berm width change – North Channel.

Predicting Reflection Coefficient in Front of a Breakwater

To predict the wave reflection in front of a breakwater without modeling test, one may use an equation empirically relating the reflection coefficient to the function of the parameters, including the geometry shape, roughness, and permeability of breakwater and the wave characters. Overtopping should also be involved into estimating reflection coefficient. For example, the rubble mound breakwaters in the project are rough and permeable structure with either plane slope or berm-width slope. To efficiently estimate the reflection coefficient, the parameters of breakwater and wave may be interpreted as a dimensionless parameter, such as surf similarity number Battjes (1974). Also, the equation shall be effective that approximates the trend of reflection coefficient versus the dimensionless parameter and present the physical bounds, including $K_R = 0$ when absence of breakwater and $K_R \rightarrow 1$ when the breakwater is a vertical, smooth, and impermeable wall.

A review of the empirical equations predicting reflection coefficient in front of breakwater

Miche (1951), Battjes (1974), and Seelig and Ahren (1981) considered that the reflection coefficients are affected by wave transmission and energy dissipation including wave modification due to reflected structure, wave breaking at toe of a structure or in the surf zone, and surface roughness and permeability of structure. Miche (1951) presents that reflection coefficient in front of smooth plane-sloped impermeable breakwater is a function of slope of breakwater θ and the critical steepness, i.e. $(H_o/\lambda_o)_c$, as ratio of deep-water wave height over deep-water wavelength (Equation 87). Additional coefficient may be needed when considering permeability and surface roughness. This equation overestimates the reflections (Ursell et, al, 1960; Seelig and Ahrens, 1981).

$$K_R = \frac{\sqrt{\frac{2\theta}{\pi}\frac{\sin^2\theta}{\pi}}}{(H_o/\lambda_o)} \qquad 87$$

Battjes (1974) present an equation (Equation 88) estimating reflection coefficient as a function of surf similarity number, ξ, a dimensionless parameter presented by Battjes (1974) for plane-sloped breakwater (Equation 89).

$$K_R = 0.1\xi^2 \qquad 88$$

$$\xi = \frac{\tan\theta}{\sqrt{H_i/\lambda_o}} \qquad 89$$

The above equations are mainly used for smooth and impermeable structure. Seelig and Ahrens (1981) later revised the equation proposed by Battjes (1974) and presented several

improved equations considering characters of both breakwater and wave conditions (Equations 90 and 91), which also involve the interpretation of up bound when $K_R \to 1$.

$$K_R = \frac{a\xi^2}{\xi^2 + b} \tag{90}$$

$$K_R = \tanh(0.1\xi^2) \tag{91}$$

Where: a and b are empirical coefficients effected by slope, roughness, permeability, and type of structure. Details of selections of the equations and the corresponding parameters can be found in their report (Seelig and Ahrens 1981). Seelig and Ahrens (1981) suggested that, Equation 90 with $a = 0.6$ and $b = 6.6$ may be used to conservatively estimate reflection coefficient in front of a rubble mounded breakwater. For the same type of breakwater, Zanuttigh and Van der Meer (2006) suggested $a = 0.75$ and $b = 15$ when using Equation 90. Zanuttigh and Van der Meer (2006) also proposed a formula to predict reflection coefficient for plane-sloped breakwater.

$$K_R = \tanh(a\xi^b) \tag{92}$$

Where: the coefficients $a = 0.12$ and $b = 0.87$ are suggested for rock permeable breakwater.

To involve the case of a berm-width breakwater, Zanuttigh and Van der Meer (2007) revised surf similarity parameter as Equation 93 involving the situation of shallow water depth at toe and the deeper cases.

$$\xi = \frac{[\tan\theta_d\,(d - 1.5H_s) + \tan\theta\,(1.5H_s)]}{d\sqrt{H_s/\lambda_o}}, \qquad d > 1.5H_s$$
$$\xi = \frac{\tan\theta}{\sqrt{H_s/\lambda_o}}, \qquad d \le 1.5H_s \tag{93}$$

Where: $\tan\theta$ (= m) is slope (Equation 85) for either plain-sloped breakwater or weighted average slope for berm width breakwater; d is water depth; H is significant wave height; λ_o is deep water wave length. Zanuttigh and Van der Meer (2007) indicates that using the expression of Equation well estimate the situation when the berm is submerged, over-estimates the situation when the berm is emerged, and causes large scatter when the berm is at still water level.

The surf similarity number for the breakwater in the project is presented in Table 29 with subscripts N and S, presenting North Channel and South Channel, respectively.

Table 29. Comparison of computed and input wave heights.

Test	Slope 1		Slope 2		Slope 3	
	ξ_N	ξ_S	ξ_N	ξ_S	ξ_N	ξ_S
1 – 3	8.34	5.01	7.72	8.34	7.47	7.18
4 – 6	9.98	5.99	9.23	9.98	8.94	8.59
7 – 9	11.66	7.00	10.79	11.66	10.44	10.03
10 – 12	13.34	8.00	12.34	13.34	11.94	11.48
13 – 15	14.98	8.99	13.85	14.98	13.40	12.89
16 – 18	16.65	9.99	15.40	16.65	14.90	14.33

Reflection coefficients computed by REFANA and REFLS versus surf similarity number ξ for constant slope (Equation 89) presented by Battjes (1974) and for berm width breakwater (Equation 93) presented by van der Zanuttigh, et al. (2008) are presented and are compared with the estimation curves presented by Seelig and Ahrens (1981), and Zanuttigh and Van der Meer (2008). The prediction curve of Seelig and Ahrens (1981) using coefficients presented by the author with $a = 0.80$ and $b = 50$ according to the measured reflection coefficient are also plotted. The computed reflection coefficient and the estimation curves are represented in the Figure 24.

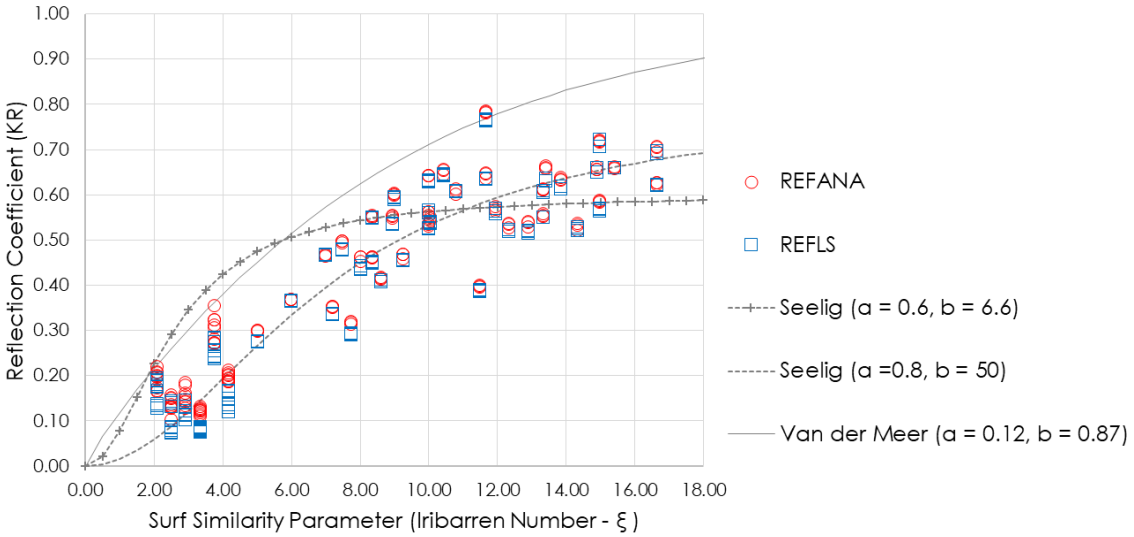

Figure 24. Measured and predicted reflection coefficient for all data.

The curve proposed by Zanuttigh and Van der Meer (2008) using coefficient $a = 0.12$ and $b = 0.87$ conservatively overestimate the reflection coefficient; Seelig and Ahrens (1981) curve using coefficient $a = 0.6$ and $b = 6.6$ over estimate at regions with surf similarity smaller than 8, and estimate the average of the reflection coefficient when surf similarity larger than 8. Using the estimation curve proposed by Seelig and Ahrens (1981) with the coefficients $a = 0.8$ and $b = 50$, the estimation curve passes through the averages of the measured reflection coefficients.

Prediction curve using sigmoid curve

Considering the shape of the curves approximating the reflection coefficients in front of a breakwater versus the surf similarity number, and the physical bounds such that passing zero at zero surf similarity parameter and tend to be one when surf similarity parameter tends to be infinity, formulae in form of sigmoid curve (“S” function) or logistic curve in terms of surf similarity parameter may be used to predict reflection coefficients. Formulae having the shape of

sigmoid function including logistic function (Verhulst 1845), error function, and hyperbolic tangent function, and so on. Using logistic function presented in Equations 94 or error function presented in Equation 95 to estimate the reflection coefficients in terms of surf similarity number.

$$K_R = \frac{2}{1 + e^{-\alpha\xi}} - 1 \qquad 94$$

$$K_R = \text{erf}\left(\frac{\xi^{\beta}}{\gamma}\right) \qquad 95$$

Comparison of the measured reflection coefficients and the predicting curves presented by the author are presented with coefficients of $\alpha = 0.1$, $\beta = 1$, and $\gamma = 20$ are presented in Figure 25, and both of the curves approximate the trend of reflection coefficients relative to the surf similarity numbers.

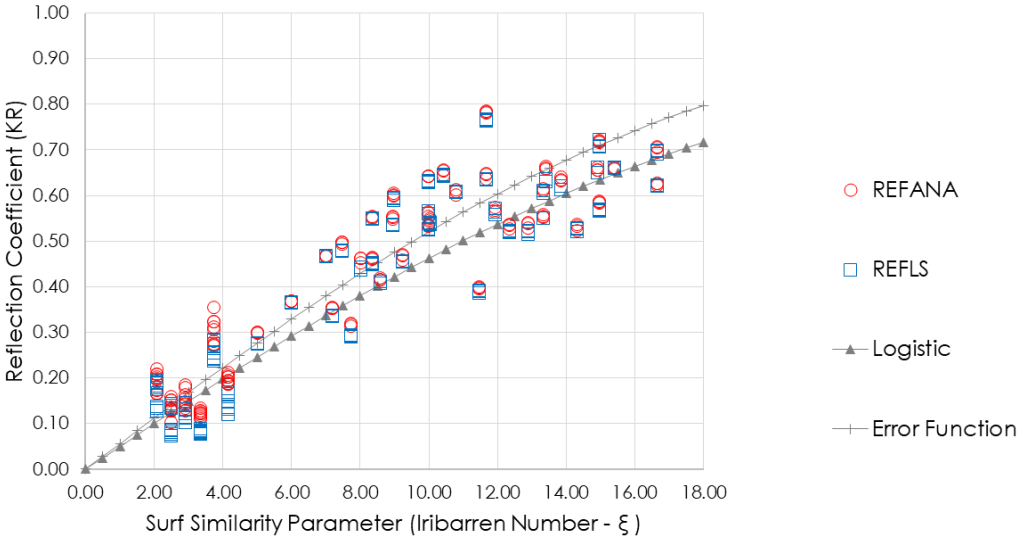

Figure 25. Measured reflection coefficients and the new predicted formulae.

CHAPTER VI

SUMMARY, CONCLUSIONS, AND RECOMMENDATIONS

Summary and Conclusions

An extended least squares method (ELSM) for separating the incident and reflected waves from co-existing wave fields has been developed. A new reflection analysis software, called REFANA is programed based on the least squares method (LSM). The expressions of ELSM indicate that the software can be directly used to compute the reflection coefficients for both normal and oblique long-crested waves, and the software can be further modified to estimate the reflection coefficients for short-crested waves. According to the expression of the spectra of incident and reflected waves and the spectrum of the reflection coefficients, only the positions of the probes along the x-axis affect the results of reflection analysis, and the placement of the probe positions along the y-axis are not necessary.

Using the transfer functions, the expressions of the measured and estimated wave height applied in ELSM indicate that the measurement can be either surface elevation or other wave parameters, such as pressure, velocity, etc. Using the weighting coefficients (Zelt and Sejelbreia 1992), ELSM for reflection analysis can use measurements from an arbitrary number of wave probes.

For long-crested oblique water waves in a laboratory wave basin, the reflection coefficient in front of a model can be corrected by adding the reflected wave component from the basin wave absorber in the expression of the estimated wave before conducting the least squares method. The expressions of the incident and reflected spectra and the spectrum of reflection coefficients with the removal of the basin boundary reflection are developed.

The software REFANA for reflection analysis, based on the ELSM, separates the incident and reflected waves and calculates the reflection coefficients. The separated incident waves approximate the input incident wave and gives a reasonable result of the reflection coefficient in front of the breakwater with known reflection coefficient. The calculated results also agree well with the commercial software REFLS of GEDAP. The average difference is approximately 2%.

The probe spacing algorithm programed in REFANA using 1% margin of probe criteria presented by Mansard and Funke (1980) reduces the total number of the wave probes required for reflection analysis using ELSM when the wave conditions consist of more than one wavelength. The calculation results show that the algorithm automates the arrangement of wave probes, including determining the total number of wave probes, selecting three probes for reflection analysis, and determining the minimum space between the wavemaker and the model reflecting structure.

Three wave probes are necessary when all wavelengths are smaller than 11/9 of the shortest wavelength. Four wave probes are necessary when the wavelengths are categorized into two groups, i.e. $\{\lambda^1, \dots, \lambda^{S_1}\}$ and $\{\lambda^{S_1+1}, \dots, \lambda^M\}$, and the wavelengths of each group is within the interval between 1 and 11/9 of the shortest wavelength of each group, and the longest wave length λ^M is shorter than $100/27\,\lambda^1$. Five wave probes are needed when the wavelengths are categorized into two main groups, i.e. $\{\lambda^1, \dots, \lambda^{M_1}\}$ and $\{\lambda^{M_1+1}, \dots, \lambda^M\}$, with $\lambda^{M_1+1} > 100/27\,\lambda^1$, and the wavelengths of each group are within the interval between 1 and 11/9 of the shortest wavelength of each group. Five probes are also sufficient when the wavelengths categorized into three groups and the longest wavelength λ^M is less than $100/27\,\lambda^1$. More than five probes are needed for other cases.

Two s-shaped sigmoid functions that include a logistic function and an error function are developed by the author to empirically estimate the reflection coefficients in front of a rubble mound breakwater. These empirical equations evaluate the reflection coefficients relative to the surf similarity number and estimate the reflection coefficients in front of a sloped, rough, and permeable rubble mounded breakwater.

Recommendations

The transfer function in this dissertation uses linear wave theory and the linear dispersion relationship. Using the linear assumptions twice may cause more inaccuracy than using the measured surface elevations only, which uses linearity once. Using the transfer function based on measurements enhances the accuracy, but more laboratory data or field data are required to obtain the transfer function based on the measurements.

Procedures to analyze reflection characteristics for directional (short-crested) waves using the method developed from the extended least squares method (ELSM) should be verified by both field and laboratory data in the future and compared with the results using other methods such as maximum likelihood method.

REFERENCES

Barber, N F. 1961. "Directional Resolving Power of an Array of Wave Detectors." *Proceedings of Conference on Ocean Wave Spectra.* 137-150.

Battjes, J A. 1974. "Surf Similarity." *Proceedings of 14th International Conference on Coastal Engineering.* Copenhagen, Denmark: American Society of Civil Engineers. 466-480.

Capon, J, R J Greenfield, and R J Kolker. 1967. "Multidiremensional Maximum Likelihood Processing of a Large Aperture Seismic Array." *Proceeding of IEEE.* 92-211.

Dean, Robert G, and Robert A Dalrymple. 1991. "Partial Standing Waves." In *Water Wave Mechnics for Engineers and Scientists,* by Robert G Dean and Robert A Dalrymple, 90-93. Hackensack, New Jersey: World Scientific Publishing Co. Pte. Ltd.

Eckart, C. 1952. *Propagation of Gravity Waves from Deep to Shallow Water.* Gravity Waves.

Fenton, J D, and McKee. 1990. "On Calculating the Length of Water Waves." *Coastal Engineering* 499-513.

Frigaard, Peter, and Michael Brosen. 1995. "A Time-Domain Method for Separating Incident and Reflected Irregular Waves." *Coastal Engineering* 205-215.

Funke, E R, N L Crookshank, and M Wingham. 1980. *An Introduction to GEDAP - An Integrated Software System for Experimental Control, Data Aquisition and Data Analysis.* Ottawa, Canada: National Research Council of Canada, Hydraulics Laboratory Technical.

Goda, Yoshimi. 1999. "A Comporative Review on the Functional Forms of Directional Wave Spectrum." *Coastal Engineering* 1-20.

Goda, Yoshimi. 1970. "A Synthesis of Breaker Indices." *Transactions of JSCE 2* 227-230.

—. 1985. *Random Seas and Design of Maritime Structure.* Tokyo, Japan: University of Tokyo Press.

Goda, Yoshimi, and Yasumasa Suzuki. 1976. "Estimation of Incident and Reflected Waves in Random Wave Experiments." *Proceedings of the 15th International Conference on Coastal Engineering.* Honolulu, Hawaii: American Society of Civil Engineers. 828-845.

Guza, R T, E B Thornton, and R A Holman. 1984. "Swash on Steep and Shallow Beaches." *Proceedings of the 19th Coastal Engineering Conference.* American Society of Civil Engineers. 708-723.

Hughes, S A. 1993. "Wave Height-to-Stroke Ratio." In *Physical Model and Laboratory Techniques in Coastal Engineering*, by S A Hughes, 345-347. River Edge: World Scientific Publishing Co. Pte. Ltd.

Hughes, Steven A. 1993. "Laboratory Wave Reflection Analysis Using Co-Located Gauges." *Coastal Engineering* 223-247.

Hughes, Steven A. 1993. "Wave Reflection Analysis." In *Physical Models and Laboratory Techniques in Coastal Engineering*, by Steven A Hughes, 502-520. River edge, New Jersey: World Scientific Publishing Co. Pte. Ltd.

Isaacson, Michael. 1991. "Measurement of Regular Wave Reflection." *Journal of Waterway, Port, Coastal, and Ocean Engineering* 553-569.

Isobe, M, and K Kondo. 1984. "Method for Estimating Wave Spectrum in Incident and Reflected Wave field." *Proceeding of 19th Coastal Engineering Conference.* 467-483.

Kamphuis, J W. 2000. "Wave Transformation and Breaking." In *Introduction to Coastal Engineering and Management*, by J W Kamphuis, 160-164. River Edge: World Scientific Publishing Co. Pte. Ltd.

Kamphuis, J. W. 1991. "Alongshore Sediment Transport Rate." *Journal of Waterway, Port, Coastal and Ocean Engineering, Vol. 117* 624-640.

Lin, D Y, and C J Huang. 2004. "Decomposition of Incident and Reflected Higher Harmonic Waves Using Four Wave Gauges." Edited by J M Smith. *Proceedings of the 29th International Conference on Coastal Engineering.* Lisbon, Portugal: International Conference on Coastal Engineering (ICCE). 395-406.

Longuet-Higgins, M S, D E Cartwright, and N D Smith. 1963. "Observation of the directional Spectrum of Sea Waves Using the Motions of a Floating Buoy." *Proceeding of Conference on Ocean Wave Spectra.* Englewood Cliffs, NJ, USA. 111-136.

Mansard, E P D, and E R Funke. 1980. "the Measurement of Incident and relfected Spectra Using a Least Squares Method." *Proceedings of the 17th International Conference on Coastal Engineering.* Sydney, Australia: American Society of Civil Engineers. 154-172.

Mansard, E P D, S E Sand, and E R Funke. 1985. *Reflection Analysis of Non-Linear Regular Waves.* National Research Council of Canada, Hydraulics Laboratory Technical Report, TR-HY-011.

Miche, R. 1951. "Le Pouvoir Reflechissant des Ouvrages Maritimes Exposes a L'action de La Houle." *Ann. Ponts Chaussees* 285-319.

Miche, R. 1944. "Mouvement Ondulatoires de la Mer en Profondeur Constante ou Decroissante." *Annales des Ponts et Chaussees.*

Michell, J. H. 1893. "XLIV. The highest waves in water." *The London, Edinburgh, and Dublin Philosophical Magazine and Journal of Science, Vol. 36* 430-437.

Miles, M D, and E R Funke. 1990. *The GEDAP Software Package for Hydraulics Laboratory Data Analysis.* Ottawa, Canada: National Research Council.

Miles, M. D. 1994. *GEDAP Program REFLS, Version 1.0.* National Research Council Canada (NRC).

Mitsuyasu, H, F Tasai, T Suhara, S Mizuno, M Ohkusu, T Honda, and Rikiishi K. 1975. "Observations of the Dretctional Spectrum of Pcean Waves Using a Cloverleaf Buoy ." *Physics Oceanography* 750-760.

Panicker, N N, and L E Borgman. 1970. "Directional Spectra from Wave-Gauge Arrays." *Coastal Engineering* 117-136.

Panicker, N N, N Narayana, and L Borgman. 1974. "Enchancement of Directional Wave Spectrum Estimates." *Proceeding of 14th Coastal Engineering Conference.* 258-279.

Randall, R E, K Martin, Y Zhi, and R Burke. 2016. *Experimental Measurements of Wave Reflection/Stability/Overtopping for the Rubble Mound Breakwater and Wave Absorber.* College Staion, Texas: Haynes Coastal Engineering Laboratory, Texas A&M University.

Rosas, M D C L. 2007. *Optimal Positioning of Gauges and System Equipment.* College Station, Texas: Haynes Coastal Engineering Laboratory, Texas A&M University.

Seelig, William N, and John P Ahrens. 1981. *Estimation of Wave Relfection and Energy Dissipation Coefficients for Beaches Revetments, and Breakwaters.* Fort Belvoir, Virginia: US Army, Corps of Engineers, Coastal Engineering Research Center.

Sonne, E. 2012. *Helios Data Aquisition Program.* College Station, Texas: Haynes Coastal Engineering Laboratory, Texas A&M University.

Thornton, Edward B, and Ronald J Calhoun. 1972. "Spectral Resolution of Breakwater Reflected Waves." *Waterways, Harbors and Coastal Engineering Division* 443-460.

Ursell, R, R G Dean, and Y S Yu. 1960. "Forced Small-Amplitude Water Waves: A Comparison of Theory and Experiment." *Fluid Mechanics* 33-52.

Varghese, Roobin V, Kiran G Shirlal, Bindiya Hari P, and Sabna Mohanan. 2016. "Review of Developments in Estimation of Wave Reflection from Coastal Structures." (IOSR Journal of Mechanical and Civil Engineering (IOSR-JMCE)).

Verhulst, P -F. 1845. *Recherches mathématiques sur la loi d'accroissement de la population.* Nouv. mém. de l'Academie Royale des Sci. et Belles-Lettres de Bruxelles, 1-41. http://resolver.sub.uni-goettingen.de/purl?PPN129323640_0018.

2016. *WAVELAB - Reflection Analysis.* http://www.hydrosoft.civil.aau.dk/wavelab/reflection/.

Wen, S C, and K J Wu. 1995. "A Proposed Directional Spectrum." *Acta Oceanologica Sinica* 155-166.

Yu, Y, and S Liu. 1994. "Observation and Analyzing Directional Spectrum in the Field Test." *Ocean Engineering (in Chinese)* 1-11.

Yu, Y, and S Liu. 2010. "Wave Reflection." In *Random Wave and Its Applications to Engineering*, by Yuxiu Yu, 302-310. Dalian: Dalian University of Technology Press.

Zanuttigh, B, and J W van der Meer. 2006. "Wave Reflection From Coastal Structures."

Zanuttigh, B, and J W van der Meer. 2007. "Wave Reflection from Composite Slopes."

Zanuttigh, Barbara, and Jentsje W van der Meer. 2008. "Wave Reflection from Coastal Structures in Design Conditions." *Coastal Engineering* 771-779.

Zanuttigh, Barbara, Jentsje W van der Meer, Thomas Lykke Anderson, Javier L Lara, and Inigo J Losada. 2008. "Analysis of Wave Reflection from Structures with Berms through an Extensive Database and 2DV Numerical Modelling." *Proceedings of the 31st Internaitional Conference on Coastal Engineering.* Hamburg, Germany: American Society of Civil Engineers. 3285-3297.

Zelt, J A, and James E Sejelbreia. 1992. "Estimating Incident and Reflected Wave Fields Using an Arbotary Number of Wave Gauges." *Coastal Engineering* 777-789.

APPENDIX I

INSTRUCTION AND CODE FOR CALCULATING BASIN LIMITATION

To use this software:

1. Save wave_itr.m and the software for design curve together
2. Open MATLAB.
3. Run the software for design curve

MATLAB code for wave length iteration:

```
function [ LEN ] = wave_itr( DEP,PRD )
% ************************ INTRO ************************** %
% Inputs:                                                  %
%     DEP = water depth [m];                               %
%     PRD = wave period [s];                               %
% Outputs:                                                 %
%     LEN = wave length [m];                               %
% ******************************************************** %
% initial wavelength for iteration (Fenton & McKee, 1990)
g     = 9.81;            % gravitational acceleration  [m/s^-2]
EPS   = 0.000001;        % step length                       [-]
NMAX  = 10000;           % maximum step                      [-]
Lp    = (g*(PRD^2)/(2*pi))*(tanh((((2*pi/PRD)^2)*DEP/g)^(3/4)))^(2/3);
% derive wavelength by applying iteration
for N = 1:NMAX
    SUM = 0;
    LEN   = (g*(PRD^2)/(2*pi))*tanh((2*pi*DEP)/(Lp));
    DIF = LEN-Lp;
    SUM = SUM+DIF^2;
    RMS = sqrt(SUM/(N));
    Lp  = LEN;
    if RMS < EPS
        break;
    end
end
if (N>0.75*NMAX)
    disp('Convergence does not achieved');
end
```

MATLAB code for design curve:

```
% Initialize
clear all; clc;
% Inputs
% Wave characteristics
DEP = linspace(0.1,1,10);       % water depth                    [m]
```

```
PRD = linspace(0.0625,10,160);  % wave period                    [m]
SGM = 2*pi./PRD;                % circular frequency         [rad/s]
GRV = 9.81;                     % gravitational acceleration [m/s^2]
% Piston characteristics
STK = 0.494;                    % stroke amplitude               [m]

% Iteration to find wave length
for j = 1:length(DEP);
    for i = 1:length(PRD);
        [ LEN(i,j) ] = wave_itr( DEP(j),PRD(i));
        % Wave number k [rad/m]
        KWN(i,j)     = 2*pi/LEN(i,j);

        % Height to stroke ratio (HSR) [-]
        HSR(i,j)     = 2*(cosh(2*KWN(i,j)*DEP(j))-1)/...
                       (sinh(2*KWN(i,j)*DEP(j))+2*KWN(i,j)*DEP(j));
        % Wave height from HSR [m]
        HWM(i,j)     = 2*STK*HSR(i,j);
        % Wave height limitation for piston type wave maker [m]
        HPT(i,j)     = HWM(i,j);

        % Breaking criterion (Stokes, 1880)
        % Deep and intermediate water depth (Michell, 1893 and Miche, 1944)
        if KWN(i,j)*DEP(j) >= pi/10;
            HST(i,j) = min(0.78*DEP(j),(LEN(i,j)/7)*tanh(KWN(i,j)*DEP(j)));
            if HST(i,j) > HPT(i,j);
                HBKST(i,j) = HPT(i,j);
            else
                HBKST(i,j) = HST(i,j);
            end
        % Shallow water depth (McCowan, 1891)
        elseif KWN(i,j)*DEP(j) < pi/10;
            HST(i,j) = 0.78*DEP(j);
            if HST(i,j) > HPT(i,j);
                HBKST(i,j) = HPT(i,j);
            else
                HBKST(i,j) = HST(i,j);
            end
        end

        % Breaking criterion (Goda, 1970)
        HGD(i,j)     = 0.17*LEN(i,j)*...
                       (1-1/exp(1.5*pi*DEP(j)/LEN(i,j)));
        % Scope determination (/bounding)
        if HGD(i,j) > HPT(i,j);
            HBKGD(i,j) = HPT(i,j);
        else
            HBKGD(i,j) = HGD(i,j);
        end

        % Breaking criterion (Kamphuis, 1990a)
        % Deep and intermediate water depth
        if KWN(i,j)*DEP(j) >= pi/10;
            HKP(i,j) = min(0.56*DEP(j),...
```

```
                        (0.095*LEN(i,j))*tanh(KWN(i,j)*DEP(j)));
            if HKP(i,j) > HPT(i,j);
                HBKKP(i,j) = HPT(i,j);
            else
                HBKKP(i,j) = HKP(i,j);
            end
        % Shallow water depth
        elseif KWN(i,j)*DEP(j) < pi/10;
            HKP(i,j) = 0.56*DEP(j);
            if HKP(i,j) > HPT(i,j);
                HBKKP(i,j) = HPT(i,j);
            else
                HBKKP(i,j) = HKP(i,j);
            end
        end
    end
end

% Plots
% Ledgend lables
LL = {'d = 0.1 m','d = 0.2 m','d = 0.3 m','d = 0.4 m','d = 0.5 m',...
      'd = 0.6 m','d = 0.7 m','d = 0.8 m','d = 0.9 m','d = 1.0 m'};
% Plot dispersion relationship and wave length
figure(1)
% Plot dispersion relationship
subplot(1,2,1);
SIG = sort(SGM,'descend');
for j = 1:10;
    loglog(SIG.^2,KWN(:,j));
    hold on
    xlabel('\sigma^{2} (rad^2)');
    ylabel('k (rad/m)');
    title('Dispersion Relationship');
    grid on
    axis square
end
legend(LL);
% Plot wave length
subplot(1,2,2);
for j = 1:10;
    plot(PRD,LEN(:,j));
    hold on
    xlabel('T (s)');
    ylabel('\lambda (m)');
    title('Wave Length from Dispersion Relation');
    grid on
    axis square
end
legend(LL);
% Plot breaking criteria
figure(2)
for i = 1:3;
    for j = 1:10;
        subplot(1,3,i);
        if i == 1;
```

```
            plot(PRD,HST(:,j));
            title('Breaking Wave Height (Stokes, 1880)');
        elseif i == 2;
            plot(PRD,HGD(:,j));
            title('Breaking Wave Height (Goda, 1970)');
        elseif i == 3;
            plot(PRD,HKP(:,j));
            title('Breaking Wave Height (Kamphuis, 1990a)');
        end
        hold on
        xlabel('T (s)');
        ylabel('H_{b} (m)');
        ylim([0,1]);
        grid on
        axis square
    end
    legend(LL);
end
% Plot wave height from height-to-stroke ratio
figure(3)
for j = 1:10;
    plot(PRD,HPT(:,j));
    hold on
    xlabel('T (s)');
    ylabel('H_{max} (m)');
    title('Wave Height from Height-to-stroke Ratio');
    grid on
end
legend(LL);
% Plot breaking wave design curve
figure(4)
for i = 1:3;
    for j = 1:10;
        subplot(1,3,i);
        if i == 1;
            plot(PRD,HBKST(:,j));
            title('Design Curve (Stokes, 1880)');
        elseif i == 2;
            plot(PRD,HBKGD(:,j));
            title('Design Curve (Goda, 1970)');
        elseif i == 3;
            plot(PRD,HBKKP(:,j));
            title('Design Curve (Kamphuis, 1990a)');
        end
        hold on
        xlabel('T (s)');
        ylabel('H_{max} (m)');
        ylim([0,1]);
        grid on
        axis square
    end
    legend(LL);
end
```

APPENDIX II

INSTRUCTION AND CODE FOR REFLECTION ANALYSIS SOFTWARE

The software REFANA for reflection analysis, i.e. refana_ref.m, is programmed using MATLAB based on least squares method (LSM) applying the measurements from three wave probes positioned perpendicular to the wavemaker. This software is applicable for separating the co-existing waves for long-crested wave propagating either normally or obliquely. The software refana_ref.m uses functions of autospec.m and crosspec.m to compute auto- and cross- spectra, respectively and these files shall be saved together with the data file.

The data file is usually in the format of ".txt" and the sample file has the file name in the format of "Name of the project prefix" + "Test index and scenario" + ".format", which is specified using the code "load measured signal", such that

```
% Load measured signal
INDX = 3; % Test index
CHAN = 1;  % Channel index (1=north,4=south,7=open)
TEST = ['Test',num2str(INDX),' ','Slope3']; % Test index and scenario
PROJ = 'CalData_SG_'; % Name of the project (prefix)
FMAT = '.txt'; % Format of the data file
FILE = [PROJ,TEST,FMAT];
FILE = char(FILE); % Name of the data file
WAVE = load(FILE);
```

The above code is an example to load data file "CalData_SG_Test3 Slope3.txt", and the information is used later for the titles of the graphs. The variable "CHAN" is the channel index specifying Channel North, Channel South, or Open Water, and the datafile contains the columns of time steps (the first column, in second, every 0.04 s for 25 Hz capturing rate) and the corresponding surface elevations (in meter) for each time step.

The information of each test can be either manually specified or using function "testinfo.m" to extract information consisting of probe spacings, water depth, wave period, wavelength, circular frequency, and incident wave amplitude, such that

```
% Test information
[ X1P,D,TP,AI ] = testinfo( INDX );
% X1P = Distance between the probe P and 1        [m]
% D   = Water depth                               [m]
% TP  = Wave period                               [s]
% AI  = Incident wave amplitude                   [m]
X1  = 9.73;      % Distance between P1 and WM     [m]
X1R = 12.16;     % Distance between P1 and object [m]
L   = wave_itr( D,TP );           % Wavelength    [m]
W   = 2*pi/TP;           % Circular frequency [rad/s]
```

To use the software:

1. Save the data file together with "refana_ref.m", "autospec.m", and "crosspec.m".
2. Modify the name of the data file according to the format in "Load measured signal", e.g. "CalData_SG_Test3 Slope3.txt".
3. Open MATLAB.
4. Modify test index, i.e. the variable "INDX", for example Test 3 INDX = 3.
5. Modify channel index, i.e. "CHAN", for example Channel North CHAN = 1. This variable is used to select the column of the data according to the three probes used for reflection analysis.
6. Modify the test scenario, such as "Slope1", "Slope2", and "Slope3"
7. Modify the variable "X1P" by modifying the variable in "testinfo.m". If the test information is manually presented, delete "Test information", otherwise, using "testinfo.m" and the test information in "testinfo.m" need to be specified (see code of "Inputting information of the tests for breakwater project"). For example, Test 3, the indx

= 3, hence the d, Tp, and AI shall be under the scenario T1-T3. To use “testinfo.m” the function “wave_itr” to compute wavelength should be saved together.

8. Specify the start point for time series, i.e. “TS”, to make sure that the wave field is fully developed, which excludes the ramping up time (for wave maker) and includes the reflected waves for all wave gauges.
9. Run the software and save the results

The test results are presented in a two-panel figures (measured and computed spectra) with one of the plots of the spectra of measured surface elevations from three wave probes and the corresponding zero moment wave heights; the other plot illustrates the separated spectra of the incident wave and the reflected wave and the spectrum of the reflection coefficient and the incident H_I and the reflected wave H_R heights and the reflection coefficient K_R.

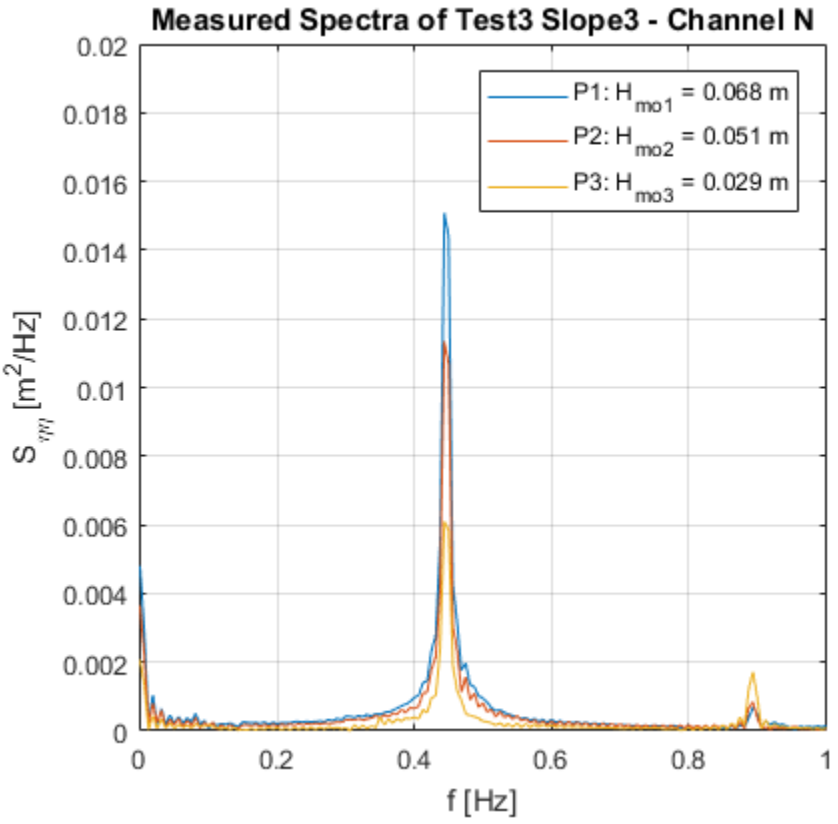

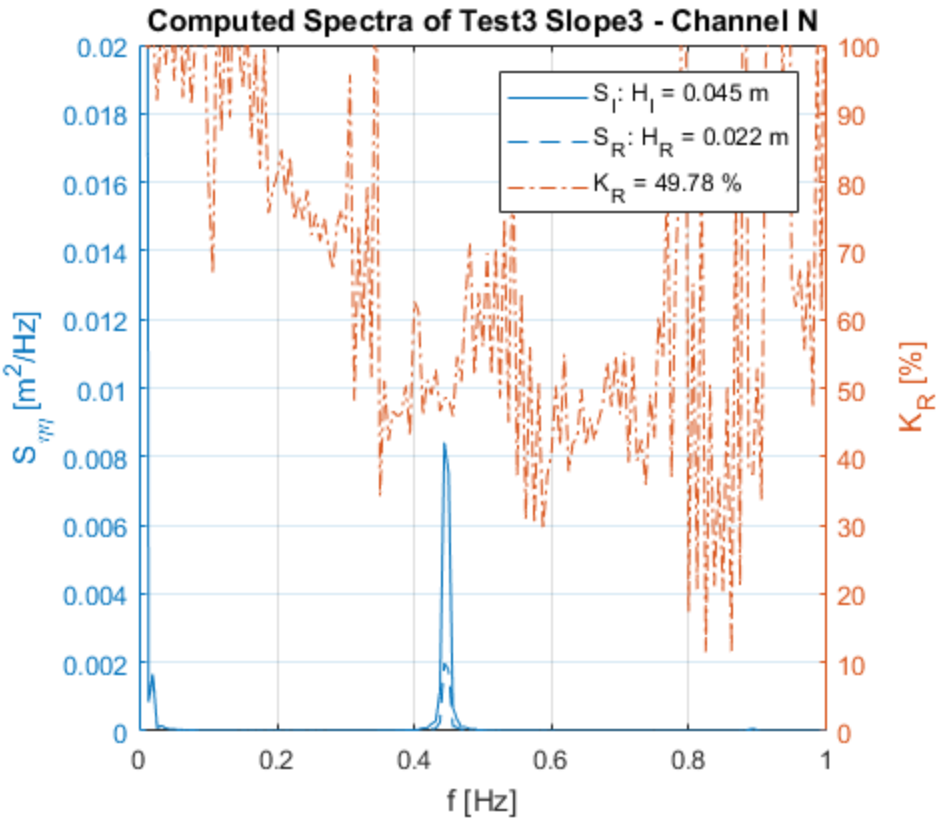


```
% Code for refana_ref
% Initialization
clc; clear all;

% Load measured signal
INDX = 3; % Test index
CHAN = 1;  % Channel index (1=north,4=south,7=open)
TEST = ['Test',num2str(INDX),' ','Slope3']; % Test index and scenario
PROJ = 'CalData_SG_'; % Name of the project prefix
FMAT = '.txt'; % Format of the data file
FILE = [PROJ,TEST,FMAT];
FILE = char(FILE); % Name of the data file
WAVE = load(FILE);

% Test information
[ X1P,D,TP,AI ] = testinfo( INDX );
% X1P = Distance between the probe P and 1        [m]
% D   = Water depth                               [m]
% TP  = Wave period                               [s]
% AI  = Incident wave amplitude                   [m]
X1  = 9.73;      % Distance between P1 and WM     [m]
X1R = 12.16;     % Distance between P1 and object [m]
L   = wave_itr( D,TP );           % Wavelength    [m]
W   = 2*pi/TP;           % Circular frequency [rad/s]
```

```
% Total time vector
TIME = WAVE(:,1);
% Parameter for time domain
DT   = TIME(2)-TIME(1);     % Sampling rate      [s]
FS   = 1/DT;                % Sampling frequency [Hz]
% Wave elevation (total co-existing elevation)
ELEV = zeros(length(TIME),3);
for j = 1:3
    ELEV(1:length(WAVE(:,j+CHAN)),j) = WAVE(:,j+CHAN);
    ELEV(:,j) = (ELEV(:,j)-mean(ELEV(1:5*25,j)))/1000; % z-cross
end

% Extract compsite wave (co-wave)
% TS = Start point of co-wave (re-reflection reach P3)
TS = 40;

% Co-waves (COWV)
for j = 1:3
    COWV(:,j) = ELEV(ceil(TS*FS):end,j);
end
TC = TIME(ceil(TS*FS):end); % time vector (co-wave)
T  = TC-TC(1);              % time vector (common)

% Spectra analysis
% Auto spectra
for j = 1:3
    [ AXX(:,j),SXX(:,j),APH(:,j),FA(:,j),HMO(j) ]...
        = autospec( T,COWV(:,j) );
end
for j = 1:3
    [ AXY(:,j),SXY(:,j),XPH(:,j),FX(:,j) ]...
        = crosspec( T,COWV(:,1),COWV(:,j) );
end

for j = 1:length(FA(:,1))
    [ LN(j) ] = wave_itr( D,1/FA(j,1) );
end
LN = LN';
KN = 2*pi./LN;

% Least square method for reflection
for j = 1:3
    O1(:,j) = exp(2i*KN*X1P(:,j));
    O2(:,j) = exp(-2i*KN*X1P(:,j));
    O3(:,j) = AXX(:,j).*exp(1i*(XPH(:,j)+KN*X1P(:,j)));
    O4(:,j) = AXX(:,j).*exp(1i*(XPH(:,j)-KN*X1P(:,j)));
end
% Parameterizing
O1 = O1(:,1)+O1(:,2)+O1(:,3);
O2 = O2(:,1)+O2(:,2)+O2(:,3);
O3 = O3(:,1)+O3(:,2)+O3(:,3);
O4 = O4(:,1)+O4(:,2)+O4(:,3);
% Amplitude spectra of incident and reflect wave
NAI = abs((O2.*O3-3*O4)./(O1.*O2-9));
```

```
NAR = abs((O1.*O4-3*O3)./(O1.*O2-9));
% Spetra densities of incident and reflect wave
DF  = FA(2,1)-FA(1,1);
NSI = (NAI.^2)/(2*DF);
NSR = (NAR.^2)/(2*DF);
% Spectrum of reflection coefficients
KRN = NAR./NAI;
% Incident and reflect wave height
NS = 16;
HI = 4*sqrt(sum(NSI(NS:end))*DF);
HR = 4*sqrt(sum(NSR(NS:end))*DF);
% Coherency factor
CF12 = SXY(:,2)./sqrt(SXX(:,1).*SXX(:,2));
CF13 = SXY(:,3)./sqrt(SXX(:,1).*SXX(:,3));

% Display of reflection analysis
if CHAN == 1
    CNUM = ' - Channel N';
elseif CHAN == 4
    CNUM = ' - Channel S';
elseif CHAN == 7
    CNUM = ' - Open Water';
end
% Titles of the plots
TT1 = ['Measured Spectra of ',num2str(TEST),num2str(CNUM)];
TT2 = ['Computed Spectra of ',num2str(TEST),num2str(CNUM)];
% Lables of the Hmo
ML1 = ['P1: H_{mo1} = ',num2str(round(HMO(1)*1000)/1000),' m'];
ML2 = ['P2: H_{mo2} = ',num2str(round(HMO(2)*1000)/1000),' m'];
ML3 = ['P3: H_{mo3} = ',num2str(round(HMO(3)*1000)/1000),' m'];
% Lables of HI, HR, and KR
MLI = ['S_I: H_{I} = ',num2str(round(HI*1000)/1000),' m'];
MLR = ['S_R: H_{R} = ',num2str(round(HR*1000)/1000),' m'];
MLKR = ['K_R = ',num2str(round(HR/HI*10000)/100),' %'];

% Plot 1: Measured spectra
figure (1)
for j = 1:3
    plot(FA(:,j),AXX(:,j));
    hold on
end
xlim([0,1]);
ylim([0,0.02]);
xlabel('f [Hz]');
ylabel('S_{\eta\eta} [m^2/Hz]');
legend(num2str(ML1),num2str(ML2),num2str(ML3));
title(num2str(TT1));
hold off
grid on
pbaspect([1 1 1]) % Equal axis lengths in all directions

% Plot 2: Computed spectra
figure(2)
% Spectra of HI and HR
```

```
yyaxis left % y-axis of HI and HR
title(num2str(TT2));
plot(FA(:,1),NSI(:,1));
hold on
plot(FA(:,1),NSR(:,1));
xlim([0,1]);
ylim([0,0.02]);
xlabel('f [Hz]');
ylabel('S_{\eta\eta} [m^2/Hz]');
% Spectrum of KR
yyaxis right % y-axis of KR
plot(FA(:,1),KRN*100,'-.');
xlim([0,1]);
ylim([0,100]);
ylabel('K_R [%]');
legend(num2str(MLI),num2str(MLR),num2str(MLKR));
hold off
grid on
pbaspect([1 1 1]) % Equal axis lengths in all directions
```

Inputting information of the tests for breakwater project

```
function [ x1p,d,Tp,AI ] = testinfo( indx )
% Information of input signal
% Input
% indx = indices of test
% Output
% x1p = relative probe positions
% d   = input water depth
% Tp  = input peak period
% AI  = input incident amplitude

% T1-T6
if indx >= 1 && indx <= 6;
    x1p = [0,0.480,1.170];
    if indx >= 1 && indx <= 3; % T1-T3
        d  = 0.43;
        Tp = 2.24;
        AI = 0.025;
    elseif indx >= 4 && indx <= 6; %T4-T6
        d  = 0.43;
        Tp = 2.68;
        AI = 0.025;
    end
% T7-T12
elseif indx >= 7 && indx <= 12;
    x1p = [0,0.670,1.670];
    if indx >= 7 && indx <= 9; % T7-T9
        d  = 0.43;
        Tp = 3.13;
        AI = 0.025;
    elseif indx >= 10 && indx <= 12; % T10-T12
        d  = 0.43;
        Tp = 3.58;
        AI = 0.025;
    end
% T13-T18
elseif indx >= 13 && indx <= 18;
    x1p = [0,0.905,2.263];
    if indx >= 13 && indx <= 15; % T13-T15
        d  = 0.43;
        Tp = 4.02;
        AI = 0.025;
    elseif indx >= 16 && indx <= 18; % T16-T18
        d  = 0.43;
        Tp = 4.47;
        AI = 0.025;
    end
end
end
```

Function computing the auto-spectra

```
function [ Axx,Sxx,Phi,f,Hmo ] = autospec( t,eta )
% Generating single-sided auto amplitude and power spectra
% Input:
% t   = time vector
% eta = time series of signal
% Output:
% Axx = 1-sided amplitude spectrum
% Sxx = 1-sided power spectrum
% Phi = phase angle
% f   = frequency vector
% Hmo = significant wave height

% Parameters for frequency domains
nfft = 2*length(t)-1;             % Length of signal
dt   = t(2)-t(1);                 % Sampling rate        [s]
fs   = 1/dt;                      % Sampling frequency   [Hz]
fN   = fs/2;                      % Nyquist frequency    [Hz]
fo   = 1/(nfft*dt);               % Fundmental frequency [Hz]
f    = fo*(0:(nfft+1)/2-1)';      % Frequency vector     [Hz]

% Auto spectra (Axx and Sxx)
Axx2 = fft(eta,nfft)/nfft;        % 2-sided Axx(f) (complex)
Axx  = 2*abs(Axx2(1:(nfft+1)/2)); % 1-sided Axx(f) (real)
Sxx  = Axx.^2/(2*fo);             % 1-sided Sxx(f)
Phi  = angle(Axx2(1:(nfft+1)/2)); % Phase angle
Hmo  = 4*sqrt(sum(Sxx*fo));       % Hmo

end
```

Function computing the cross-spectra

```
function [ Axy,Sxy,XPh,f ] = crosspec( t,eta1,eta2 )
% Generating single-sided cross spectra
% Input:
% t    = time vector
% eta1 = time series of signal1
% eta2 = time series of signal2
% Output:
% Axy = 1-sided amplitude cross spectrum
% Sxy = 1-sided power cross spectrum
% XPh = phase shift
% f   = frequency vector

% Parameters for frequency domains
nfft = 2*length(t)-1;             % Length of signal
dt   = t(2)-t(1);                 % Sampling rate        [s]
fs   = 1/dt;                      % Sampling frequency   [Hz]
fN   = fs/2;                      % Nyquist frequency    [Hz]
fo   = 1/(nfft*dt);               % Fundmental frequency [Hz]
f    = fo*(0:(nfft+1)/2-1)';      % Frequency vector     [Hz]

% Auto spectra (Axx and Sxx)
Axx1 = fft(eta1,nfft)/nfft;       % 2-sided Axx(f) for eta1 (complex)
Axx2 = fft(eta2,nfft)/nfft;       % 2-sided Axx(f) for eta2 (complex)
Axy2 = sqrt(Axx1.*conj(Axx2));    % 2-sided Axy(f)
Axy  = 2*abs(Axy2(1:(nfft+1)/2)); % 1-sided Axy(f) (real)
Sxy  = Axy.^2/(2*fo);             % 1-sided Sxy(f)
XPh  = angle(Axx1(1:(nfft+1)/2)./Axx2(1:(nfft+1)/2)); % Phase shift

end
```

Function to iterate the wavelength

```
function [ LEN ] = wave_itr( DEP,PRD )
% ************************ INTRO *************************** %
% Inputs:                                                   %
%     DEP = water depth [m];                                %
%     PRD = wave period [s];                                %
% Outputs:                                                  %
%     LEN = wave length [m];                                %
% ************************************************************ %
% initial wavelength for iteration (Eckhart, 1951)
g     = 9.81;            % gravitational acceleration  [m/s^-2]
EPS   = 0.000001;        % step length                       [-]
NMAX  = 100000;          % maximum step                      [-]
Lp    = (g*(PRD^2)/(2*pi))*(tanh((((2*pi/PRD)^2)*DEP/g)^(3/4)))^(2/3);
% derive wavelength by applying iteration
for N = 1:NMAX
    SUM = 0;
    LEN   = (g*(PRD^2)/(2*pi))*tanh((2*pi*DEP)/(Lp));
    DIF = LEN-Lp;
    SUM = SUM+DIF^2;
    RMS = sqrt(SUM/(N));
    Lp  = LEN;
    if RMS < EPS
        break;
    end
end
if (N>NMAX)
    disp('Convergence does not achieved');
end
```

APPENDIX III

INSTRUCTIONS AND CODE FOR PROBE ARRANGEMENT SOFTWARE

To use this software:

1. Open MATLAB.
2. Run “refana_probe.m”
3. Input the wavelengths in a format of linear array, e.g. [4.33,5.29,6.24,7.18,8.12,9.05]

Sample result

```
Array of Wave Lengths [L1,L2,...,Ln] = [4.33,5.29,6.24,7.18,8.12,9.05]
    Name      L       XAB      XAC      PA     PB     PC
    _____    _____    _____    _____    __     __     __

    "L1"     4.33     0.48     1.13     1      2      4
    "L2"     5.29     0.48     1.13     1      2      4
    "L3"     6.24     0.67     1.13     1      3      4
    "L4"     7.18     0.67     1.13     1      3      4
    "L5"     8.12     1.13     2.11     1      4      5
    "L6"     9.05     1.13     2.11     1      4      5

    Name      X1P
    _____    ____

    "X12"    0.48
    "X13"    0.67
    "X14"    1.13
    "X15"    2.11

Probe Numer = 5
Total Distance = 20.21m
```

```
% Initialization
clc;clear all;

% Input wavelengths and sort ascend
L = input('Array of Wave Lengths [L1,L2,...,Ln] = ');
L = sort(L,'ascend');

% Probe spacing criteria
PC = [9/100,11/100,100/600,100/300];

% Empty matrix for writting in the results
XAB = zeros(length(L),1);
XAC = zeros(length(L),1);
PPA = ones(length(L),1);
PPB = zeros(length(L),1);
PPC = zeros(length(L),1);

% Group the wavelengths (MG):
di = 0;
for i = 1:length(L)
    if di+1 <= length(L)
        MI(i) = find(L(:) < (PC(4)/PC(1))*L(di+1), 1, 'last' );
        di = MI(i);
    else
        break
    end
end

MG = zeros(length(MI),2);
for i = 1:length(MI)
    if i == 1
        MG(i,:) = [1,MI(i)];
    else
        MG(i,:) = [MI(i-1)+1,MI(i)];
    end
end

% Catogorise the wavelengths of each group (SG)
SG = zeros(4,max(MG(:,2)-MG(:,1))+1,size(MG,1));
for i = 1:size(SG,3)
    SG1 = intersect(find(L(MG(i,1):MG(i,2))>0),...
        find(L(MG(i,1):MG(i,2))<...
        (PC(2)/PC(1))*L(MG(i,1))));
    SG2 = intersect(find(L(MG(i,1):MG(i,2))>...
        (PC(2)/PC(1))*L(MG(i,1))),...
        find(L(MG(i,1):MG(i,2))<...
        (PC(3)/PC(1))*L(MG(i,1))));
    SG3 = intersect(find(L(MG(i,1):MG(i,2))>...
        (PC(3)/PC(1))*L(MG(i,1))),...
        find(L(MG(i,1):MG(i,2))<...
        ((PC(2)/PC(1))*(PC(3)/PC(1)))*L(MG(i,1))));
    SG4 = intersect(find(L(MG(i,1):MG(i,2))>...
        ((PC(2)/PC(1))*(PC(3)/PC(1)))*L(MG(i,1))),...
```

```
        find(L(MG(i,1):MG(i,2))<...
        (PC(4)/PC(1))*L(MG(i,1))));
    if i == 1
        SG1 = SG1+0; SG2 = SG2+0; SG3 = SG3+0; SG4 = SG4+0;
    else
        SG1 = SG1+MG(i-1,2); SG2 = SG2+MG(i-1,2); SG3 = SG3+MG(i-1,2);
        SG4 = SG4+MG(i-1,2);
    end
    if isempty(SG1) == 1
        SG(1,:,i) = zeros(1,size(SG,2));
    elseif isempty(SG1) == 0
        SG(1,1:length(SG1),i) = SG1;
    end
    if isempty(SG2) == 1
        SG(2,:,i) = zeros(1,size(SG,2));
    elseif isempty(SG2) == 0
        SG(2,1:length(SG2),i) = SG2;
    end
    if isempty(SG3) == 1
        SG(3,:,i) = zeros(1,size(SG,2));
    elseif isempty(SG3) == 0
        SG(3,1:length(SG3),i) = SG3;
    end
    if isempty(SG4) == 1
        SG(4,:,i) = zeros(1,size(SG,2));
    elseif isempty(SG4) == 0
        SG(4,1:length(SG4),i) = SG4;
    end
end

SGL = L(nonzeros(SG));

% For the singularity values
SSI = find(not(ismember(L,SGL)));
if isempty(SSI) == 0
    XAB_S = zeros(1,length(SSI));
    XAC_S = zeros(1,length(SSI));
    for i = 1:length(SSI)
        XAB_S(i) = L(SSI(i))/10;
        XAC_S(i) = L(SSI(i))/4;
    end
elseif isempty(SSI) == 1
    XAB_S = [];
    XAC_S = [];
end
XAB(SSI,1) = XAB_S;
XAC(SSI,1) = XAC_S;

% For the non-sigularity values
PP = zeros(size(SG,1)*size(SG,2),1,size(SG,3));
for i = 1:size(SG,3)
    N1 = length(nonzeros(SG(1,:,i))); % Length of nonzero SG1
    N2 = length(nonzeros(SG(2,:,i))); % Length of nonzero SG2
    N3 = length(nonzeros(SG(3,:,i))); % Length of nonzero SG3
```

```
N4 = length(nonzeros(SG(4,:,i))); % Length of nonzero SG4
% Catagories of SG2 to further merge XABs
if isempty(nonzeros(SG(2,:,i))) == 0
    d2j = 0;
    for j = 1:N2
        if d2j+1 <= N2
            MN2(j) = find(L(nonzeros(SG(2,:,i))) <...
                (PC(2)/PC(1))*L(nonzeros(SG(2,d2j+1,i))), 1, 'last' );
            d2j = MN2(j);
        else
            break
        end
    end
    MG2 = zeros(length(MN2),2);
    for j = 1:length(MN2)
        if j == 1
            MG2(j,:) = [1,MN2(j)];
        else
            MG2(j,:) = [MN2(j-1)+1,MN2(j)];
        end
    end
    NN2 = 1:size(MG2,1);
end
% Catagories of SG4 to further merge XABs
if isempty(nonzeros(SG(4,:,i))) == 0
    d4j = 0;
    for j = 1:N4
        if d4j+1 <= N4
            MN4(j) = find(L(nonzeros(SG(4,:,i))) <...
                (PC(2)/PC(1))*L(nonzeros(SG(4,d4j+1,i))), 1, 'last' );
            d4j = MN4(j);
        else
            break
        end
    end
    for j = 1:length(MN4)
        if j == 1
            MG4(j,:) = [1,MN4(j)];
        else
            MG4(j,:) = [MN4(j-1)+1,MN4(j)];
        end
    end
    NN4 = 1:size(MG4,1);
end

% CASE 1: SG1 <> 0 and SG2,SG3,SG4 = 0
if isempty(nonzeros(SG(1,:,i))) == 0 &&...
        isempty(nonzeros(SG(2:4,:,i))) == 1
    PP(1,1,i) = mean((1/10)*L(nonzeros(SG(1,:,i))));
    PP(2,1,i) =...
        (PC(3)*max(L(nonzeros(SG(1,:,i))))...
        +PC(4)*min(L(nonzeros(SG(1,:,i)))))/2;
    % Write into result
    XAB(nonzeros(SG(1,:,i)),1) =...
        round(ones(length(nonzeros(SG(1,:,i))),1)*PP(1,1,i),2);
```

```
    XAC(nonzeros(SG(1,:,i)),1) =...
        round(ones(length(nonzeros(SG(1,:,i))),1)*PP(2,1,i),2);

% CASE 2: SG1,SG2 <> 0 and SG3,SG4 = 0
elseif isempty(nonzeros(SG(1,:,i))) == 0 &&...
        isempty(nonzeros(SG(2,:,i))) == 0 &&...
        isempty(nonzeros(SG(3:4,:,i))) == 1
    PP(1,1,i) = mean((1/10)*L(nonzeros(SG(1,:,i))));
    % Write into result
    XAB(nonzeros(SG(1,:,i)),1) =...
        round(ones(length(nonzeros(SG(1,:,i))),1)*PP(1,1,i),2);
    for j = 1:length(NN2)
        PP(1+NN2(j),1,i) =...
            mean((1/10)*L(nonzeros(SG(2,MG2(j,1):MG2(j,2),i))));
        % Write into result
        XAB(SG(2,MG2(j,1):MG2(j,2),i),1) =...
            round(ones(length(SG(2,MG2(j,1):MG2(j,2),i)),1)*...
            PP(1+NN2(j),1,i),2);
    end
    PP(1+NN2(end)+1,1,i) =...
        (PC(3)*max(L(nonzeros(SG(2,:,i))))...
        +PC(4)*min(L(nonzeros(SG(1,:,i)))))/2;
    % Write into result
    XAC(nonzeros(SG(1:2,:,i)),1) =...
        round(ones(length(nonzeros(SG(1:2,:,i))),1)*...
        PP(1+NN2(end)+1,1,i),2);

% CASE 3: SG1,SG3 <> 0 and SG2,SG4 = 0
elseif isempty(nonzeros(SG(1,:,i))) == 0 &&...
        isempty(nonzeros(SG(3,:,i))) == 0 &&...
        isempty(nonzeros(SG(2,:,i))) == 1 &&...
        isempty(nonzeros(SG(4,:,i))) == 1
    PP(1,1,i) = mean((1/10)*L(nonzeros(SG(1,:,i))));
    PP(2,1,i) =...
        (PC(1)*max(L(nonzeros(SG(3,:,i))))...
        +PC(4)*min(L(nonzeros(SG(1,:,i)))))/2;
    PP(3,1,i) =...
        (PC(3)*max(L(nonzeros(SG(3,:,i))))...
        +PC(4)*min(L(nonzeros(SG(3,:,i)))))/2;
    % Write into result
    XAB(nonzeros(SG(1,:,i)),1) =...
        round(ones(length(nonzeros(SG(1,:,i))),1)*PP(1,1,i),2);
    XAC(nonzeros(SG(1,:,i))) =...
        round(ones(length(nonzeros(SG(1,:,i))),1)*PP(2,1,i),2);
    XAB(nonzeros(SG(3,:,i))) =...
        round(ones(length(nonzeros(SG(3,:,i))),1)*PP(2,1,i),2);
    XAC(nonzeros(SG(3,:,i))) =...
        round(ones(length(nonzeros(SG(3,:,i))),1)*PP(3,1,i),2);

% CASE 4: SG1,SG4 <> 0 and SG2,SG3 = 0
elseif isempty(nonzeros(SG(1,:,i))) == 0 &&...
        isempty(nonzeros(SG(4,:,i))) == 0 &&...
        isempty(nonzeros(SG(2,:,i))) == 1 &&...
        isempty(nonzeros(SG(3,:,i))) == 1
```

```
PP(1,1,i) = mean((1/10)*L(nonzeros(SG(1,:,i))));
% Write into result
XAB(nonzeros(SG(1,:,i)),1) =...
    round(ones(length(nonzeros(SG(1,:,i))),1)*PP(1,1,i),2);
if length(nonzeros(SG(4,:,i))) == 1
    PP(2,1,i) =...
        (PC(1)*L(nonzeros(SG(4,:,i)))...
        +PC(4)*min(L(nonzeros(SG(1,:,i)))))/2;
    PP(3,1,i) = (1/4)*L(nonzeros(SG(4,:,i)));
    % Write into result
    XAC(nonzeros(SG(1,:,i))) =...
        round(ones(length(nonzeros(SG(1,:,i))),1)*PP(2,1,i),2);
    XAB(nonzeros(SG(4,:,i))) =...
        round(ones(length(nonzeros(SG(4,:,i))),1)*PP(2,1,i),2);
    XAC(nonzeros(SG(4,:,i))) =...
        round(ones(length(nonzeros(SG(4,:,i))),1)*PP(3,1,i),2);
elseif length(nonzeros(SG(4,:,i))) > 1
    PP(2,1,i) =...
        (PC(1)*min(L(nonzeros(SG(4,:,i))))...
        +PC(4)*min(L(nonzeros(SG(1,:,i)))))/2;
    % Write into result
    XAC(nonzeros(SG(1,:,i))) =...
        round(ones(length(nonzeros(SG(1,:,i))),1)*PP(2,1,i),2);
    XAB(nonzeros(SG(4,1,i))) =...
        round(ones(length(nonzeros(SG(4,1,i))),1)*PP(2,1,i),2);
    if size(MG4,1) == 1
        PP(1+NN4(end),1,i) =...
            mean((1/10)*L(nonzeros(SG(4,2:end,i))));
        PP(1+NN4(end)+1,1,i) =...
            (PC(3)*max(L(nonzeros(SG(4,:,i))))...
            +PC(4)*min(L(nonzeros(SG(4,:,i)))))/2;
        % Write into result
        XAB(nonzeros(SG(4,2:end,i))) =...
            round(ones(length(nonzeros(SG(4,2:end,i))),1)*...
            PP(1+NN4(end),1,i),2);
        XAC(nonzeros(SG(4,:,i))) =...
            round(ones(length(nonzeros(SG(4,:,i))),1)*...
            PP(1+NN4(end)+1,1,i),2);
    elseif size(MG4,1) > 1 % Re-define NN4
        for j = 1:N4-1
            if d4j+1 <= N4-1
                MN4(j) = find(L(nonzeros(SG(4,2:end,i))) <...
                    (PC(2)/PC(1))*...
                    L(nonzeros(SG(4,d4j+1,i))), 1, 'last' );
                d4j = MN4(j);
            else
                break
            end
        end
        for j = 1:length(MN4)
            if j == 1
                MG4(j,:) = [2,MN4(j)+1];
            else
                MG4(j,:) = [MN4(j-1)+2,MN4(j)+1];
            end
```

```
                PP(1+NN4(j),1,i) =...
                    mean((1/10)*...
                    L(nonzeros(SG(4,MG4(j,1):MG4(j,2),i))));
                % Write into result
                XAB(SG(4,MG4(j,1):MG4(j,2),i),1) =...
                    round(ones(length(SG(4,MG4(j,1):MG4(j,2),i)),1)*...
                    PP(1+NN4(j),1,i),2);
            end
            NN4 = 1:size(MG4,1);
            PP(1+NN4(end)+1,1,i) =...
                (PC(3)*max(L(nonzeros(SG(4,:,i))))...
                +PC(4)*min(L(nonzeros(SG(4,:,i)))))/2;
            % Write into result
            XAC(nonzeros(SG(4,:,i))) =...
                round(ones(length(nonzeros(SG(4,:,i))),1)*...
                PP(1+NN4(end)+1,1,i),2);
        end
    end

% CASE 5: SG1,SG2,SG3 <> 0 and SG4 = 0
elseif isempty(nonzeros(SG(1,:,i))) == 0 &&...
        isempty(nonzeros(SG(2,:,i))) == 0 &&...
        isempty(nonzeros(SG(3,:,i))) == 0 &&...
        isempty(nonzeros(SG(4,:,i))) == 1
    PP(1,1,i) = mean((1/10)*L(nonzeros(SG(1,:,i))));
    % Write into result
    XAB(nonzeros(SG(1,:,i)),1) =...
        round(ones(length(nonzeros(SG(1,:,i))),1)*PP(1,1,i),2);
    for j = 1:length(NN2)
        PP(1+NN2(j),1,i) =...
            mean((1/10)*L(nonzeros(SG(2,MG2(j,1):MG2(j,2),i))));
        % Write into result
        XAB(SG(2,MG2(j,:),i),1) =...
            round(ones(length(SG(2,MG2(j,:),i)),1)*PP(1+NN2(j),1,i),2);
    end
    PP(1+NN2(end)+1,1,i) =...
        (PC(1)*max(L(nonzeros(SG(3,:,i))))...
        +PC(4)*min(L(nonzeros(SG(1:2,:,i)))))/2;
    PP(1+NN2(end)+2,1,i) =...
        (PC(3)*max(L(nonzeros(SG(3,:,i))))...
        +PC(4)*min(L(nonzeros(SG(3,:,i)))))/2;
    % Write into result
    XAC(nonzeros(SG(1:2,:,i))) =...
        round(ones(length(nonzeros(SG(1:2,:,i))),1)*...
        PP(1+NN2(end)+1,1,i),2);
    XAB(nonzeros(SG(3,:,i))) =...
        round(ones(length(nonzeros(SG(3,:,i))),1)*...
        PP(1+NN2(end)+1,1,i),2);
    XAC(nonzeros(SG(3,:,i))) =...
        round(ones(length(nonzeros(SG(3,:,i))),1)*...
        PP(1+NN2(end)+2,1,i),2);

% CASE 6: SG1,SG2,SG4 <> 0 and SG3 = 0
elseif isempty(nonzeros(SG(1,:,i))) == 0 &&...
        isempty(nonzeros(SG(2,:,i))) == 0 &&...
```

```
    isempty(nonzeros(SG(4,:,i))) == 0 &&...
    isempty(nonzeros(SG(3,:,i))) == 1
PP(1,1,i) = mean((1/10)*L(nonzeros(SG(1,:,i))));
% Write into result
XAB(nonzeros(SG(1,:,i)),1) =...
    round(ones(length(nonzeros(SG(1,:,i))),1)*PP(1,1,i),2);
for j = 1:length(NN2)
    PP(1+NN2(j),1,i) =...
        mean((1/10)*L(nonzeros(SG(2,MG2(j,1):MG2(j,2),i))));
    % Write into result
    XAB(SG(2,MG2(j,1):MG2(j,2),i),1) =...
        round(ones(length(SG(2,MG2(j,1):MG2(j,2),i)),1)*...
        PP(1+NN2(j),1,i),2);
end
if length(nonzeros(SG(4,:,i))) == 1
    PP(1+NN2(end)+1,1,i) =...
        (PC(1)*L(nonzeros(SG(4,:,i)))...
        +PC(4)*min(L(nonzeros(SG(1:2,:,i)))))/2;
    PP(1+NN2(end)+2,1,i) = (1/4)*L(nonzeros(SG(4,:,i)));
    % Write into result
    XAC(nonzeros(SG(1:2,:,i))) =...
        round(ones(length(nonzeros(SG(1,:,i))),1)*...
        PP(1+NN2(end)+1,1,i),2);
    XAB(nonzeros(SG(4,:,i))) =...
        round(ones(length(nonzeros(SG(4,:,i))),1)*...
        PP(1+NN2(end)+1,1,i),2);
    XAC(nonzeros(SG(4,:,i))) =...
        round(ones(length(nonzeros(SG(4,:,i))),1)*...
        PP(1+NN2(end)+2,1,i),2);
elseif length(nonzeros(SG(4,:,i))) > 1
    PP(1+NN2(end)+1,1,i) =...
        (PC(1)*L(nonzeros(SG(4,:,i)))...
        +PC(4)*min(L(nonzeros(SG(1:2,:,i)))))/2;
    % Write into result
    XAC(nonzeros(SG(1:2,:,i))) =...
        round(ones(length(nonzeros(SG(1,:,i))),1)*...
        PP(1+NN2(end)+1,1,i),2);
    XAB(nonzeros(SG(4,1,i))) =...
        round(ones(length(nonzeros(SG(4,1,i))),1)*...
        PP(1+NN2(end)+1,1,i),2);
    if size(MG4,1) == 1
        PP(1+NN2(end)+NN4(end)+1,1,i) =...
            mean((1/10)*L(nonzeros(SG(4,2:end,i))));
        PP(1+NN2(end)+NN4(end)+2,1,i) =...
            (PC(3)*max(L(nonzeros(SG(4,:,i))))...
            +PC(4)*min(L(nonzeros(SG(4,:,i)))))/2;
        % Write into result
        XAB(nonzeros(SG(4,2:end,i))) =...
            round(ones(length(nonzeros(SG(4,2:end,i))),1)*...
            PP(1+NN2(end)+NN4(end)+1,1,i),2);
        XAC(nonzeros(SG(4,:,i))) =...
            round(ones(length(nonzeros(SG(4,:,i))),1)*...
            PP(1+NN2(end)+NN4(end)+2,1,i),2);
    elseif size(MG4,1) > 1 % Re-define NN4
        for j = 1:N4-1
```

```
                if d4j+1 <= N4-1
                    MN4(j) = find(L(nonzeros(SG(4,2:end,i))) <...
                        (PC(2)/PC(1))*...
                        L(nonzeros(SG(4,d4j+1,i))), 1, 'last' );
                    d4j = MN4(j);
                else
                    break
                end
            end
            for j = 1:length(MN4)
                if j == 1
                    MG4(j,:) = [2,MN4(j)+1];
                else
                    MG4(j,:) = [MN4(j-1)+2,MN4(j)+1];
                end
                PP(1+NN2(end)+NN4(j)+1,1,i) =...
                    mean((1/10)*...
                    L(nonzeros(SG(4,MG4(j,1):MG4(j,2),i))));
                % Write into result
                XAB(SG(4,MG4(j,1):MG4(j,2),i),1) =...
                    round(ones(length(SG(4,MG4(j,1):MG4(j,2),i)),1)*...
                    PP(1+NN2(end)+NN4(j)+1,1,i),2);
            end
            NN4 = 1:size(MG4,1);
            PP(1+NN2(end)+NN4(end)+2,1,i) =...
                (PC(3)*max(L(nonzeros(SG(4,:,i))))...
                +PC(4)*min(L(nonzeros(SG(4,:,i)))))/2;
            % Write into result
            XAC(nonzeros(SG(4,:,i))) =...
                round(ones(length(nonzeros(SG(4,:,i))),1)*...
                PP(1+NN2(end)+NN4(end)+2,1,i),2);
        end
    end

% CASE 7: SG1,SG3,SG4 <> 0 and SG2 = 0
elseif isempty(nonzeros(SG(1,:,i))) == 0 &&...
        isempty(nonzeros(SG(3,:,i))) == 0 &&...
        isempty(nonzeros(SG(4,:,i))) == 0 &&...
        isempty(nonzeros(SG(2,:,i))) == 1
    PP(1,1,i) = mean((1/10)*L(nonzeros(SG(1,:,i))));
    PP(2,1,i) =...
        (PC(1)*max(L(nonzeros(SG(3,:,i))))...
        +PC(4)*min(L(nonzeros(SG(1,:,i)))))/2;
    % Write into result
    XAB(nonzeros(SG(1,:,i)),1) =...
        round(ones(length(nonzeros(SG(1,:,i))),1)*PP(1,1,i),2);
    XAC(nonzeros(SG(1:3,:,i))) =...
        round(ones(length(nonzeros(SG(1:3,:,i))),1)*PP(2,1,i),2);
    XAB(nonzeros(SG(3,:,i))) =...
        round(ones(length(nonzeros(SG(3,:,i))),1)*PP(2,1,i),2);
    for j = 1:length(NN4)
        PP(2+NN4(j),1,i) =...
            mean((1/10)*L(nonzeros(SG(4,MG4(j,1):MG4(j,2),i))));
        % Write into result
        XAB(SG(4,MG4(j,1):MG4(j,2),i),1) =...
```

```
                round(ones(length(SG(4,MG4(j,1):MG4(j,2),i)),1)*...
                PP(2+NN4(j),1,i),2);
        end
        PP(2+NN4(end)+1,1,i) =...
            (PC(3)*max(L(nonzeros(SG(3:4,:,i))))...
            +PC(4)*min(L(nonzeros(SG(3:4,:,i)))))/2;
        % Write into result
        XAC(nonzeros(SG(3:4,:,i))) =...
            round(ones(length(nonzeros(SG(3:4,:,i))),1)*...
            PP(2+NN4(end)+1,1,i),2);

    % CASE 8: SG1,SG2,SG3,SG4 <> 0 = 0
    elseif isempty(nonzeros(SG(1,:,i))) == 0 &&...
            isempty(nonzeros(SG(3,:,i))) == 0 &&...
            isempty(nonzeros(SG(4,:,i))) == 0 &&...
            isempty(nonzeros(SG(2,:,i))) == 0
        PP(1,1,i) = mean((1/10)*L(nonzeros(SG(1,:,i))));
         % Write into result
        XAB(nonzeros(SG(1,:,i)),1) =...
            round(ones(length(nonzeros(SG(1,:,i))),1)*PP(1,1,i),2);
        for j = 1:length(NN2)
            PP(1+NN2(j),1,i) =...
                mean((1/10)*L(nonzeros(SG(2,MG2(j,1):MG2(j,2),i))));
            % Write into result
            XAB(SG(2,MG2(j,1):MG2(j,2),i),1) =...
                round(ones(length(SG(2,MG2(j,1):MG2(j,2),i)),1)*...
                PP(1+NN2(j),1,i),2);
        end
        PP(1+NN2(end)+1,1,i) =...
            (PC(1)*max(L(nonzeros(SG(3,:,i))))...
            +PC(4)*min(L(nonzeros(SG(1:2,:,i)))))/2;
        % Write into result
        XAC(nonzeros(SG(1:2,:,i))) =...
            round(ones(length(nonzeros(SG(1:2,:,i))),1)*...
            PP(1+NN2(end)+1,1,i),2);
        XAB(nonzeros(SG(3,:,i))) =...
            round(ones(length(nonzeros(SG(3,:,i))),1)*...
            PP(1+NN2(end)+1,1,i),2);
        for j = 1:length(NN4)
            PP(1+NN2(end)+NN4(j)+1,1,i) =...
                mean((1/10)*L(nonzeros(SG(4,MG4(j,1):MG4(j,2),i))));
            % Write into result
            XAB(SG(4,MG4(j,1):MG4(j,2),i),1) =...
                round(ones(length(SG(4,MG4(j,1):MG4(j,2),i)),1)*...
                PP(1+NN2(end)+NN4(j)+1,1,i),2);
        end
        PP(1+NN2(end)+NN4(end)+2,1,i) =...
            (PC(3)*max(L(nonzeros(SG(4,:,i))))...
            +PC(4)*min(L(nonzeros(SG(4,:,i)))))/2;
        % Write into result
        XAC(nonzeros(SG(3:4,:,i))) =...
            round(ones(length(nonzeros(SG(3:4,:,i))),1)*...
            PP(1+NN2(end)+NN4(end)+2,1,i),2);
    end
end
```

```
if isempty(XAB_S) == 1 && isempty(XAC_S) == 1
    Probe = sort(nonzeros(PP),'ascend');
elseif isempty(XAB_S) == 0 && isempty(XAC_S) == 0
    Probe = sort([nonzeros(PP);XAB_S';XAC_S'],'ascend');
    Probe = unique(Probe);
end
% Minimum required number of wave probes
ProbeNumber   = length(Probe)+1;
% Minimum required distance between wave maker and structure
TotalDistance = 2*max(L)+max(Probe);

% Probe for each wavelength
Result1 = [XAB,XAC];
Result2 = round(Probe,2);
for i = 1:length(L)
    [liaB,B] = ismember(Result1(i,1),Result2);
    [liaC,C] = ismember(Result1(i,2),Result2);
    PPB(i) = B+1;
    PPC(i) = C+1;
end

% Results
Name1 = strings(length(L),1);
for i = 1:length(L)
    Name1(i,1) = ['L',num2str(i)];
end
Name2 = strings(length(Probe),1);
for i = 1:length(Probe)
    Name2(i,1) = ['X1',num2str(i+1)];
end
TAB1 = table((Name1),L',XAB,XAC,PPA,PPB,PPC);
TAB1.Properties.VariableNames = {'Name' 'L' 'XAB' 'XAC' 'PA' 'PB' 'PC'};
TAB2 = table((Name2),round(Probe,2));
TAB2.Properties.VariableNames = {'Name' 'X1P'};
disp(TAB1)
disp(TAB2)
disp(['Probe Numer = ',num2str(ProbeNumber)])
disp(['Total Distance = ',num2str(round(TotalDistance,2)),'m'])
```